CHALMERS
UNIVERSITY OF TECHNOLOGY

Dynamics of CO_2 Capture Integrated in a Steel Mill

Master's thesis of the Joint Nordic Programme "Innovative and Sustainable Energy Engineering" within the Heat and Power Track

GUILLERMO JUAN MARTINEZ CASTILLA

Department of Energy and Environment
Division of Energy Technology
Chalmers University of Technology
Gothenburg, Sweden 2018

Master's thesis 2018

Dynamics of CO_2 Capture Integrated in a Steel Mill

Guillermo Juan Martinez Castilla

CHALMERS
UNIVERSITY OF TECHNOLOGY

Department of Energy and Environment Division of Energy Technology
Combustion and Carbon Capturing Technologies Chalmers University of Technology Gothenburg, Sweden 2018

Dynamics of CO_2 Capture Integrated in a Steel Mill

GUILLERMO JUAN MARTINEZ CASTILLA

© GUILLERMO JUAN MARTINEZ CASTILLA, 2018.

Supervisor: Dr. Rubén Mocholí Montañés (Chalmers)

Max Biermann (Chalmers)

Dr. Hafþór Ægir Sigurjónsson (Háskóli Íslands)

Examiner: Associate Professor Dr. Fredrik Normann

Master's Thesis 2018
Department of Energy and Environment
Division of Energy Technology
Combustion and Carbon Capturing Technologies
Chalmers University of Technology
SE-412 96 Gothenburg
Telephone +46 31 772 1000

Cover: Abandoned steel mill in Bethlehem, PA, USA.

Printed by Reproservice
Gothenburg, Sweden 2018

Abstract

Anthropogenic CO_2 emissions are recognized to be the main factor contributing to climate change. Steel production accounts for 10% of the total CO_2 emissions from fossil fuels worldwide, with especially high levels of emissions coming from the blast furnace processing due to the use of coke and coal as reducing agent and energy supply. Ongoing research and policy plans are trying to reduce such a large carbon footprint, with Carbon Capture and Storage (CCS) in the forefront of the possible solutions.

Steel mills inherently operate with a surplus of energy, as the required reducing potential in the blast furnace generates an off-gas with a high heating value. This energy is often utilized in an integrated combined heat and power (CHP) plant, providing the energy required for the steel processing, power for the grid, and heat to local district heating networks. Due to the variations in the steel-making process and the integrated the CHP plant, a dynamic analysis is required for a successful implementation of CO_2 capture and to evaluate the plant behavior, potential and controllability.

This work analyzes the hourly transient events of an integrated steel mill during an entire year, performing its analysis and discretization while creating two scenarios: variations in available heat for the capture unit, and variations in the blast furnace gas flow to be treated in the capture unit. In addition, a dynamic model of the post-combustion capture plant is built, where the two scenarios are simulated. Three cases are considered for each scenario, based on the amount of heat available for the capture plant, i.e., the season of the year. The dynamic response of the process is studied and a control strategy is designed in order to optimize the performance towards maximum CO_2 capture. A comparison between the dynamic and steady-state performance of the plant is also carried out.

The data analysis shows the large amount of variations that the steel mill experiences: most of them related to the flared gas, available excess steam and blast furnace gas flow. Their magnitude and frequency reflects the importance of considering these disturbances. The amount of heat available for CCS can be doubled (in case of low heat available it can raise from 30 to 60 MW for some hours), or the blast furnace gas flow can drop to zero for periods of two to twelve hours, among other events.

The simulation results show how the plant reacts to the disturbances found, and how different the responses are for each variable and case considered. The same variable can stabilize five times faster in summer (large amount of heat available) than in winter. Results also show that in the periods when there is no gas entering the absorber, the stripper keeps producing CO_2 for eight to ten hours, due to the high loading of the solvent in steady-state conditions. The CO_2 produced in the stripper is increased after implementing the control strategy, and the plant stabilizes several minutes faster. This thesis shows that the capture unit can handle the disturbances caused by the steel mill, even showing a potential increase in CO_2 captured compared to the steady-state case.

This work shows the large amount of hourly variations occurring within a steel plant and its integrated power plant, and how important is to take them into account when designing the capture plant. It also helps understanding the implications of the disturbances and how a dynamic model differs from off-design steady-state models.

Keywords: steel production, post-combustion, dynamic modelling, transient data analysis, process control

Acknowledgements

First of all, I want to express all my gratitude to my supervisor Rubén Mocholí Montañés, who has been guiding and helping me throughout all this thesis. His office has always been open for me, and his knowledge and enthusiasm about the dynamic modelling field has been crucial for the development of this work.

I am also extremely thankful for the support given by Max Biermann. One more time, his door has been open day after day, providing me with light in everything related to the steelworks, as well as brilliant ideas of how to enhance this report.

Thanks to Fredrik Normann, my examiner, for the weekly discussions and inspiration. His knowledge within the CO_2 capture is fascinating, and it has been an honor to receive his guidance. I am really grateful as well for all the opportunities he has given me, allowing me to present my thesis in several occasions and attending meetings which will be highly valuable for my future career.

Thanks to Háskóli Íslands for everything it taught me. It was an amazing year full of learning in all different aspects of my life. Special thanks to Hafþór Ægir Sigurjónsson for accepting to be the supervisor of this thesis from the distance.

I also want to mention Marino Lindgren from Lulekraft and Leif Nilson from SSAB for providing useful data for this work, as well as David Bellqvist from SSAB for valuable comments on this thesis.

Finally, I would like to thanks my MSc partners Tim, Felicia and Charlene, for the wonderful adventure we have had in the past two years. Thanks to Stefanía, for walking next to me through all this work, and infinite thanks to my parents, for making all this possible.

Guillermo Juan Martinez Castilla, Göteborg, June 2018

CONTENTS

NOMENCLATURE

ABBREVIATIONS

AP	Absolute Percentage
BF	Blas Furnace
BFG	Blast Furnace Gas
BFW	Boiler Feed Water
BOF	Basic Oxygen Furnace
BOFG	Basic Oxygen Furnace Gas
CCS	Carbon Capture and Storage
CHP	Combined Heat and Power
COG	Coke Oven Gas
CV	Controlled Variable
CW	Cooling Water
DH	District Heating
EAF	Electric Arc Furnace
FB	Feedback
FC	Flow Controller
FF	Feedforward
FT	Flow Transmitter
GHG	Greenhouse Gases
GLC	Gas Liquid Contactors
HE	Heat Exchanger
HPT	High Pressure Turbine
IPT	Intermediate Pressure Turbine
LC	Level Controller
LPT	Low Pressure Turbine
LT	Level Transmitter
MEA	Monoethanolamine
MV	Manipulated Variable
PCC	Post-Combustion Capture
PID	Proportional Integrative Derivative
RC	Relative Change
TC	Temperature Controller
TCM	Technology Center Mongstad
TT	Temperature Transmitter

SYMBOLS		**UNIT**
$A_{i,f}$	Contact Area	m^2
C_{abs}	Capture Rate at the absorber	%
c_{ef}	Correction Factor	-
$c_{i,b}$	Molar concentrations in the bulk phase	mol/m^3
$c_{i,if}$	Molar concentrations in the interphase	mol/m^3
c_{MEA}	Molar free-MEA Concentration	mol/m^3
D_{CO2}	Diffusivity of CO_2 in water	m^2/s
E	Enhancement Factor	-
He_i	Henry´s Constant	$mol/(m^3Pa)$

k	Gain	-
k_{CO2}	Overall Reaction Constant for CO_2	kg/s
k_i	Mass transfer Coefficient	m/s
L_{abs}	Lean Concentration at Absorber inlet	mol/mol
$m_{CO2\text{-}in}$	Mass flow of CO_2 entering the absorber	kg/s
$m_{CO2\text{-}out}$	Mass flow of CO_2 leaving the absorber	kg/s
$n_{i,L}$	Molar flow rate of the liquid	mol/s
$n_{i,v}$	Molar flow rate of the gas	mol/s
Θ	Dead Time	s
P	Pressure	Pa
P_{CO2}	Production of CO_2	kg/s
P_{el}	Electrical Power	MW
$p_{i,b}$	Partial Pressures in the bulk phase	mol/mol
$p_{i,if}$	Partial Pressures in the interphase	mol/mol
Q_b	Heat generated in the Boiler	MW
Q_{CCS}	Heat used for CCS	MW
Q_{DH}	Heat used for District Heating	MW
Q_f	Heat provided by the Fuel	MW
Q_{OF}	Heat sent to Other Facilities	MW
Q_{SM}	Heat sent to the Steel Mill	MW
R	Ideal Gas Constant	J/(mol ·K)
R_{str}	Rich Concentration at Stripper inlet	mol/mol
T	Temperature	°C / K
Td	Derivative Time Constant	s
Ti	Integral Time Constant	s
t_s	10% Stabilization Time	s
t_{sta}	Total stabilization Time	s
T_{str}	Temperature at Stripper bottom	°C / K
U	Heat Transfer Coefficient	$W/(m^2K)$
x_{dm}	Value in the Dynamic Model	-
x_{sm}	Value in the Steady-State Model	-
y_0	Initial Value	-
y_∞	Final Value	-
γ_i	Activity Coefficients	-
Δy	Change in process variable value	-
η	Total Efficiency	-
η'	Total Efficiency with CCS	-

LIST OF FIGURES

LIST OF TABLES

1. INTRODUCTION

This thesis evaluates the dynamic behavior of a carbon dioxide absorption unit integrated into a steel mill, including an analysis of the transient events related to the operation of the steel mill and their effect on the performance of the capture plant. The work is part of the CO2stCap project, which focuses on cost reduction of carbon capture and storage in process industry by applying partial capture. Here, the concept of partial capture is investigated as the capture rate is varied dependent on season and the operation of the steel mill. This chapter provides an introduction to the thesis, places it in context and defines the aim and scope of it, along with its limitations.

1.1. BACKGROUND

Carbon dioxide emissions related to human activity is the main cause of climate change [1]. Ambitious goals have been set in the recent years, aiming to limit the global temperature rise to below 2°C. This will require large actions within a wide spectrum of fields – industry is by far one of the biggest actors.

Steel processing accounts for 10% of CO_2 emissions from fossil fuel use in the entire world [2], what can also be read as the 5% of the total worldwide GHG emissions. Particularly, due to the use of a powerful reducing agent like coke, the Blast Furnace and Basic Oxygen Furnace production path represents the biggest responsible of this issue (with a share of 60% in global steel production according to WorldSteel Association [3], emitting up to 1.8 ton of CO_2 per ton of steel [4] in case of the European production). As a pathway to reduce these emissions and enhance the steel production footprint, the ULCOS program[5] was released in 2004 with the aim of heavily cut the CO_2 emissions by suggesting new processing routes. Out of the four technologies eventually suggested, Carbon Capture and Storage (CCS) was present in three of them.

Post-combustion CO_2 capture is a proven technology that has been demonstrated at full scale for coal fired power plants, with around 15 projects worldwide [6] and with several research articles published regarding its performance and application to not only power plants but also integrated steel mills, see e.g. [7]. Some studies have also been made regarding the dynamic simulation of chemical absorption integrated in power plants, see e.g. [8]. However, the interaction of the dynamic performance of post-combustion capture and a steel mill are not investigated.

Steel mills experience notable transient behavior related to its integrated CHP plant as well as large variations over time on its available excess heat, and flaring is a common procedure to handle excess blast furnace gas that the system cannot take care of. Furthermore, there is an increasing demand on load flexibility and flexible control strategies in power generation. Modern power plants need to be flexible due to daily and seasonal variations as well as changes in fuel composition [9] as the capacity of renewable intermittent energy is increased, due to reasons related to market conditions, regulations, power system operation, hardware, among others [10]. Dynamic operation and suitable control strategies of the capturing process may, thus, be a powerful tool to handle these variations.

1.2. AIM AND SCOPE

The main goal of this thesis is to determine the effect that the inherent variations of the steel mill at different time scales have over the capture plant and its performance, as well as the design of an optimal control strategy capable to handle these transient events as good as possible and reduce the energy penalty during dynamic conditions. By carrying out dynamic process simulations, the transient behavior of the process will be compared with the base case analysis, where the steel plant is running steadily. The main variables of the process will be tracked against time under different disturbances, so a general understanding of the dynamic performance will be given.

More specifically, the analysis will focus on real transient data provided by SSAB from its integrated steel mill in Luleå, Sweden. The disturbances and variations that will be included in the study are short time transients, i.e. changes that occur within hours. The definition and selection of these variations is a key aspect of the thesis, since they will define the boundaries and scope of the analysis.

As main limitations of the analysis, the large long-term transient events remain out of the scope of the study, i.e., variations occurring in periods longer than two weeks. Seasonal variations during winter and summer are quite large in the steel mill (since the district heating gets extremely reduced during summer time), producing enormous variations of performance and profitability of the CO_2 capture plant. However, this study will focus in the hourly variations instead. Important also to specify that the dynamic modeling and simulation are developed and performed only for the chemical absorption process. The integration with the steel mill is implemented based on boundary conditions. Another limitation of the present study is the detailed design of the absorption process. Since the analysis will focus on its dynamic performance, the size and other design parameters of the process will be taken as outputs from existing models. The fact that the process is still under development and research also contribute to this limitation. Process modifications such as intercooling or rich splitting are left outside of the scope, since the optimization of the capture process is not part of the scope.

2. STEEL MANUFACTURING

A background of the steelmaking process is given in this chapter. Starting from general statistics and data regarding global and European production, the chapter will focus on the manufacturing process as well as the current environmental concerns and emissions related to the steelmaking industry. Also in this chapter, a brief description of the planned measures, policies and technologies to tackle the environmental issues is given. At the end of the section, a description of the reference steel mill included in this study is given.

2.1. STEEL FROM A GLOBAL PERSPECTIVE

Iron and steel have been two crucial actors in the development of human civilization through several millennia, with uses and applications in all kind of fields such as agriculture, generation and distribution of power, construction and medicine, among others [4]. Nowadays, strength, formability and versatility are the most attractive properties of steel. Figure 1 shows the steel consumption by sector in 2010, with data taken from [11]:

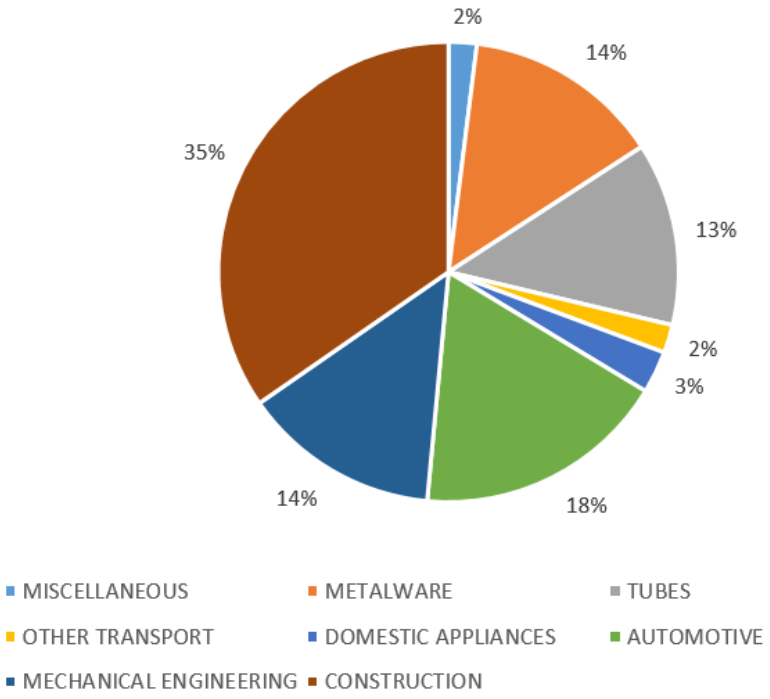

Figure 1. Steel consumption by sector in 2010 [12].

The world steel production has largely increased over history, especially after 2000, exceeding 1000 million tonnes (Mt) for the first time in 2004 [4] and reaching 1520 Mt in 2012, with the 11% of it being manufactured in the EU27 [11] . The development of China is one of the main reasons behind this large increase, which has multiplied its steel production by a factor of four in the past decades [4]. On top of these numbers, global steel production is forecast to raise by 70% before 2050 [13]. Figure 2 shows the share of steel production increase between 2001 and 2011 [3] [11].

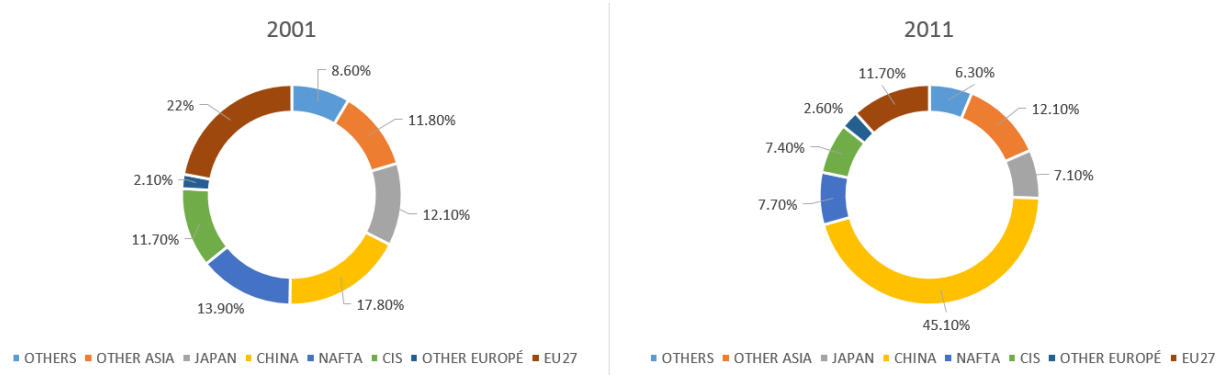

Figure 2. Worldwide Evolution in Steel Production from 2001 to 2011 divided by Production Areas

The European steel industry is located in 23 EU Member States [11], and produces around 170 million tonnes of crude steel per year, which accounts for 1.4% of the EU´s GDP [12].

2.2. STEEL TECHNOLOGY PATHWAYS

Four production routes are currently used for the manufacturing of steel: the blast furnace route, the direct melting of scrap (electric arc furnace), the smelting reduction and the direct reduction. However, the direct reduction route accounts for approximately 0.2% of the European steel production [11], while the smelting reduction is not present in the European steel production mix. Therefore, this section will focus on the two main production pathways present in Europe: the blast furnace and the electric arc furnace routes.

2.2.1. Blast Furnace Route

This route represents the most complex process of the four listed above, taking place in large industrial complexes known as integrated steel plants. A more detailed description of the process can be found in [11]. The main unit of the process is the blast furnace (it might be more than one in the plant), where the iron ores get reduced to liquid iron (called hot metal) through the addition of reducing agents. The inputs into the blast furnace are therefore two: the iron ore after preparation and the reducing agent.

The iron ore is physically and metallurgically prepared in sinter or pelletization plants, that can be located either on-site or in external sites. Regarding the reducing agents, pulverized coal, coke or oil are the most common ones, forming carbon monoxide and hydrogen that reduce the iron oxides. A hot blast of air (previously formed in the hot stoves unit) is used to generate the carbon monoxide needed for the reduction.

The hot metal leaving the blast furnace is converted into steel in a basic oxygen furnace, where oxygen is injected. This is a highly exothermic process that needs to be cooled down, so scrap, iron ore and other coolants are also fed into the furnace. After the basic oxygen furnace unit, the liquid steel is cast in metallurgical treatment. Figure 3 shows a schematic diagram of the blast furnace route.

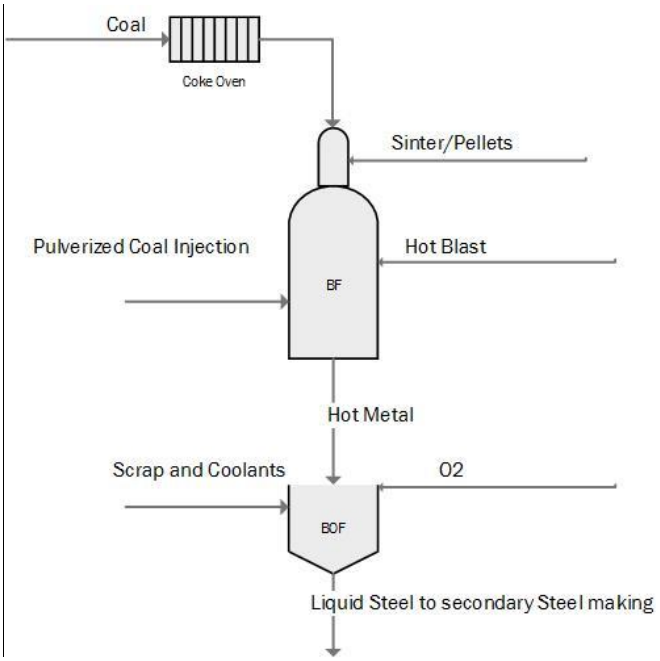

Figure 3. Simplified schematic graph of the Blast Furnace Production Route [11].

Integrated steel mills import relatively small amounts of energy for utilities [11], since most of the energy requirements of the process are satisfied by the combustion of the waste gases formed during the process.

2.2.2. Electric Arc Furnace Route

The Electric Arc Furnace (EAF) route is a secondary steelmaking process because its major feedstock is ferrous scrap. This scrap can come from the steel mill (home scrap), from steel consumer industries (pre-consumer scrap) or from steel products after utilization (obsolete scrap). Alternative feedstocks such as cast iron can also be fed into the EAF [11].

Compared to the BF route presented in section 2.2.1, the EAF route is presents less process steps since scrap metal is already reduced and only requires re-smelting and refining to obtain the desired steel product. The main operational unit is the EAF where the scrap is converted into steel by using electricity as main energy source (other energy sources can rarely be used such as natural gas or coal). Secondary streams going into the unit are fluxes and oxygen. Likewise the BF route, the liquid steel leaving the furnace is sent into metallurgical treatment before being cast. Figure 4 shows a schematic process diagram of the EAF route.

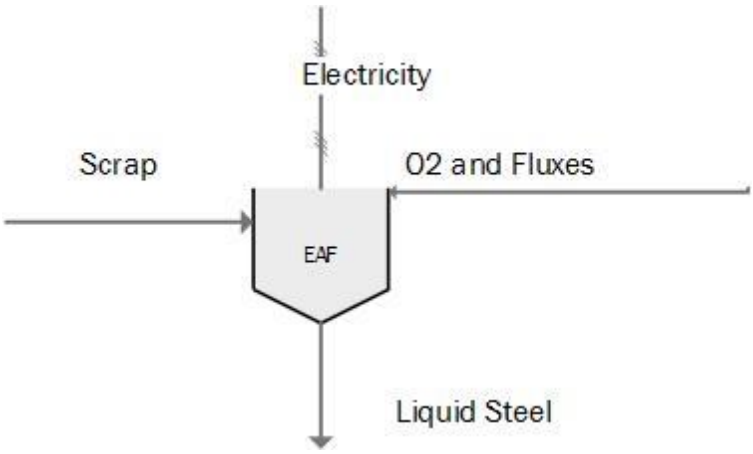

Figure 4. Schematic Graph of the Electric Arc Production Route. Line with crossed lines represent electricity [11].

It is important to mention that this route adds impurities to the steel product due to the use of scrap instead of raw ferrous material. Therefore the electric arc furnace route tends to be used to produce steel that is going to be used in products that are less sensitive to impurities [11].

2.3. MAIN ENVIRONMENTAL ISSUES

The steel industry is highly intensive in materials and energy. Literature shows that roughly half of the inputs ends up as residues [4]: either as off-gases, solid wastes or process gases. The blast furnace process is the one with highest emissions to all media (soil, water and air) because of the large use of reducing agents (mainly coal and coke) as well as its high energy consumption. The main environmental issues in a blast furnace plant are dust, waste water, SO_2 and H_2S emissions as well as CO_2 emissions, which will be covered in detail in section 2.4. This section focuses on the emissions to air of the blast furnace route.

The four main pollutants present in the exhaust flue gases of an integrated steelworks are (excluding carbon dioxide): dust, SO_2, CO and NOx. Table 1 shows the achieved emission values averaged for 20 different power plants burning steel process gases [12] (important to mention that there are other stacks (coking plant, lime kiln, hot stoves, etc.) which may have different pollution values than the ones shown in Table 1):

Table 1. Achieved emissions values averaged for 20 different power plants burning steel process gases [12].

Mg/Nm³	**Annual Averages**			
	NOx	**SO_2**	**CO**	**Dust**
Mean	87.9	97.7	7.7	6.4
Max	190	305	33	31
Min	14	1.1	0.8	0.8

Different abatement techniques are currently installed in order to achieve allowable emission levels. In case of dust, the process gases are dedusted before being combusted. The same occurs for the Sulphur dioxide: the process gases containing H_2S (precursor of SO_2) need to be desulphurised in wet scrubbers (generating the waste water mentioned above). Regarding carbon monoxide, most of it disappears when the carrying gas is burned, so no further measure is needed. Finally, the nitrogen

oxides strongly depend on the efficiency of the plant, nitrogen content of the fuel as well as the related oxygen content in the waste gas [4]. In integrated steelworks, the NOx are formed only in some specific process gases (coke oven gas mostly) [4], which are mixed with other low-NOx streams, leading to low total emission concentrations without the need of any further abatement measure to meet pollution requirements..

2.4. STEEL AS CO_2 MITIGATION ENABLER

Steel industry is a large releaser of CO_2 into the atmosphere, either directly (generated in-situ during the steel manufacturing) or indirectly (i.e. the pollutant is formed when the electricity needed for the process is generated). There are several sources of CO_2 in the iron and steel processes, caused mainly by the following three causes: a) providing the high temperatures required to carry out the chemical and physical processes needed, b) providing the reductant (usually CO) to reduce the iron oxide and c) providing the power and steam needed in the system.

The CO_2 intensity of the blast furnace route is around 1.89 tonnes/tonne of steel, while for the electric arc furnace route is roughly 0.455 tonnes/tonne of steel [11], although it highly depends on the procured electricity used in the steel mill. The mentioned numbers point out that the EAF route has by far the lowest CO_2 intensity. However, as it was stated in section 2.2, the share of EAF steel is constrained by the availability of scrap as well as the quality requirements of certain applications [11].

In order to mitigate Climate Change down to a manageable threat (which is defined as a maximum increase of 2°C by 2050 compared to pre-industrial levels), a massive reduction in GHG emissions is needed. According to literature [11], spreading the use of the cleanest technologies and implementing large energy savings is not enough. In the case of some industrial processes such as the steel manufacturing, this is even truer, mainly affected by the steep increase in demand of steel that is forecast. Therefore, action plans containing breakthrough technologies are necessary. In particular related to the steel industry, the largest and most ambitious European program is called ULCOS (Ultra Low CO_2 Steel Making).

ULCOS is a consortium of 48 European companies and organizations working cooperatively in a R&D initiative to achieve a drastic reduction in carbon dioxide emissions related to steel production. More specifically, ULCOS aims to identify steel production routes that reduce CO_2 emissions in more than 50% per tonne of steel. Three main concepts are being explored [4]: a) capturing and sequestering CO_2, b) use of energy and reducing agents not based on carbon and c) use of sustainable biomass.

After analyzing, benchmarking, modeling and pilot testing over 80 different pathways, 4 routes were finally selected: a) Blast Furnace with Top Gas Recycling (ULCOS-BF), b) Bath smelting (Hlsarna), c) Direct Reduction (ULCORED) and d) Electrolysis (ULCOWIN). Three of them keep using carbon agents such as coal, coke or natural gas, so they rely on the use of Carbon Capture and Storage (CCS), while the fourth one uses electricity directly. Based on these results, it can be seen that CCS acquires a big role in the emissions reduction of steel manufacturing. Section 3 covers the different carbon capture technologies available today, focusing on its applications, advantages and disadvantages.

2.5. DESCRIPTION OF THE REFERENCE CASE

The current study is based on the SSAB Integrated Steel Mill placed in Luleå, Sweden [14]. The integrated steel mill in Luleå follows the blast furnace route, being one of the most efficient blast

furnace operations in the world [15]. The plant also uses the excess energy of its process gases to supply heat for district heating network for the nearby locations as well as electricity, being the two latest outputs produced in Lulekraft [16], a combined heat and power plant adjacent to the steel site. Due to the large variations in district heating demand due to the seasonal variations, the potential to use this heat to run a carbon dioxide capture units is high. In addition, all the gases that the power plant cannot digest (due to limitation of boiler/power plant capacity and disturbances) are sent to flaring, where more excess heat is currently being wasted.

The steel mill produces CO_2 emissions in many different parts of the process, being the main emission sources the Blast Furnace, the Basic Oxygen Furnace and the Cooking Plant [17]. The current numbers say that the mean CO_2 emissions of the integrated plant are 3120 ktonne/yr [17], which correspond to 1.66 tonne/tonne of steel product.

In Figure 5 a schematic process diagram of the integrated steel mill is shown. The green arrows show the material flow, from the coke plant to the ladle and post-processing, while the orange arrows indicate the process gas flows. The bold numbers around the diagram refer to the share of total CO_2 site emissions, so the distribution along the different units and stacks is shown. A detailed description of the process is presented in section 2.2:

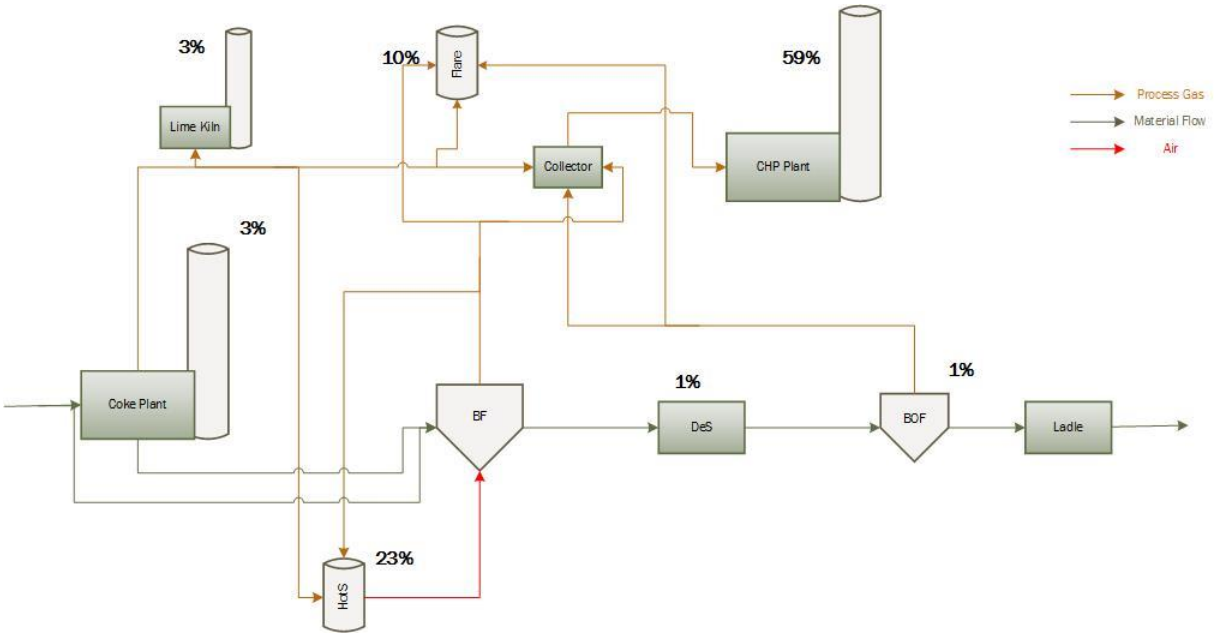

Figure 5. Simplified Process Diagram of SSAB steel mill in Luleå. Green arrows indicate material flows, orange ones refer to process gases and red is air. Percentages show the share of total CO_2 site emissions. HotS: Hot Stoves. BF: Blast Furnace. DeS: De-shulpurization. BOF: Basic Oxygen Furnace. Some of the raw materials (fluxes, iron ore) goes to BF directly, skipping the Coke Oven. Figure based on [18].

2.5.1. The Power Plant

An important part of the SSAB´s Luleå plant is the CHP plant, Lulekraft [16], where excess process gases coming from the steel mill are combusted to generate district heating and electricity. Whenever the steel mill cannot provide enough gases to run the boiler at the desired capacity, auxiliary oil is burnt. The power cycle consists of a steam cycle running a turbine train where electricity is generated and connected to the Swedish electricity national grid. Some steam bleeds are sent to the steel process or other nearby industrial facilities, while the two main bleedings from the turbine are condensed in

district heating heaters, where the return water coming from the network is heated up again. The condensate mixes with the condensate from the main condenser, and the boiler feed water returns to the boiler. A schematic diagram of the process is shown in Figure 6.

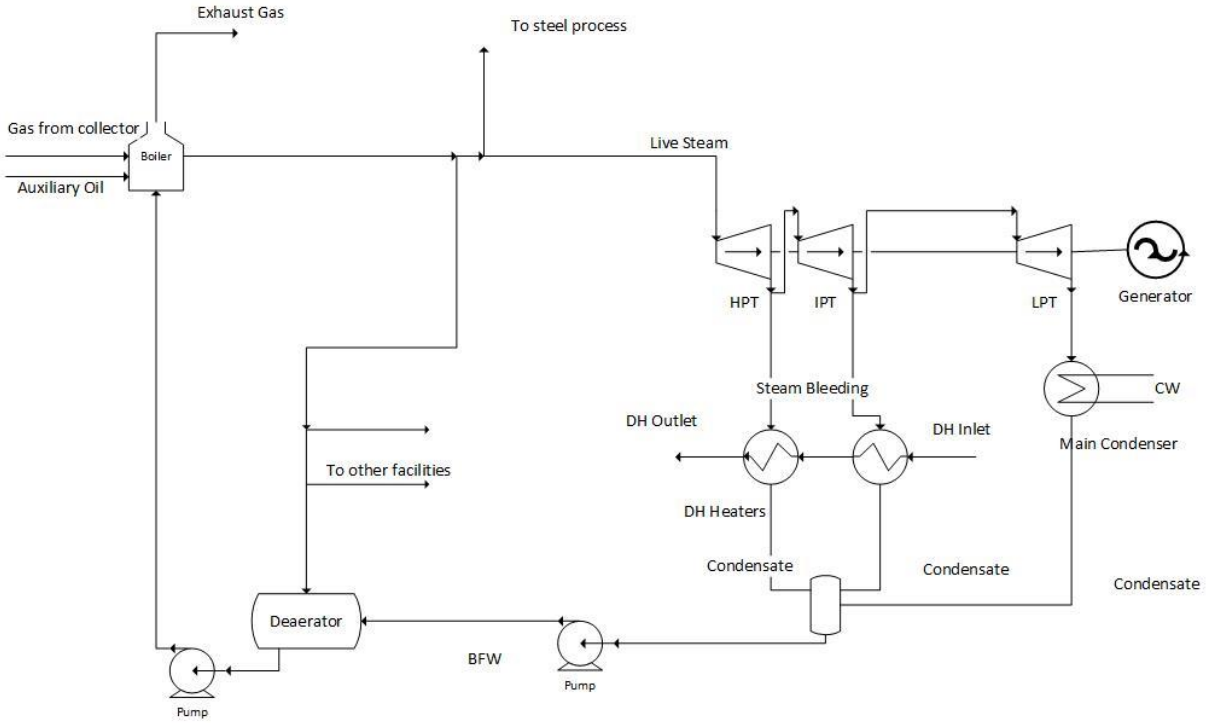

Figure 6. Schematic process diagram of the steam cycle in Lulekraft. HPT: High pressure turbine, IPT: Intermediate pressure turbine, LPT: Low pressure Turbine, CW: Cooling water, BFW: Boiler feed water, DH: District heating.

The steam boiler remains at full capacity throughout the entire year, at an average of 290 MW. This heat is distributed between the steam sent to the steel mill and the neighbor facilities (remains also constant through the year and accounts for 16 MW), the district heating and the electricity. It is important to define an efficiency in order to measure how the heat generated in the boiler is distributed through the cycle. Equation 1 shows how the total efficiency of the plant has been defined, where Q_{SM} is the heat sent to the steel mill, Q_{OF} is the heat sold to other facilities, P_{el} is the electricity production, Q_{DH} is the district heating production and Q_f is the heat input to the boiler:

$$\eta = \frac{Q_{SM} + Q_{OF} + P_{el} + Q_{DH}}{Q_f} \qquad (1)$$

The district heating produced varies along the year, going from 150-200 MW in winter down to 30 MW in summer. It is a function of the outdoor temperature, and it has to match the demand of the nearby municipalities.

Regarding the electricity production, the steel mill consumes 60 MW steadily through the year, while the power plant requires around 6 MW for own electricity equipment (mostly pumps and compressors). The excess electricity produced is put into the Swedish national grid and sold into the spot market of NordPool [19]. The electricity production increases during summer, but not as much as the district heating production decreases. This means that the power plant total efficiency defined in Equation 2 experiences a large drop, presenting a high potential gap for CCS, shown in Figure 7. This is based on the fact that the heat used to run the capture unit represents an "useful" output, contributing positively to the power plant efficiency. Equation 2 shows the total efficiency η' taking the heat used

for the capture into account (Q_{CCS}), while Figure 7 shows the efficiency gap defined in Equation 2 for the considered year in Lulekraft.

$$\eta' = \frac{Q_{SP} + Q_{OF} + P_{el} + Q_{DH} + Q_{CCS}}{Q_f} \qquad (2)$$

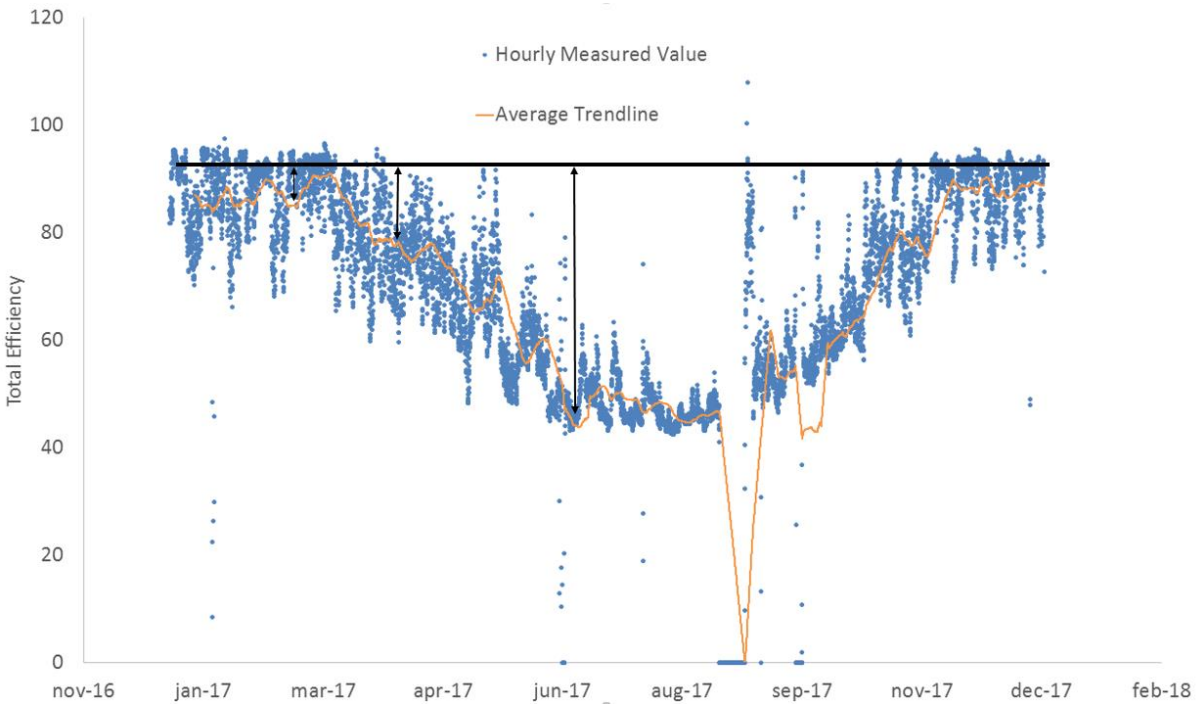

Figure 7. Lulekraft total efficiency and potential for CCS in 2017. The horizontal line shows the maximum efficiency that the plant is capable to perform while the vertical arrows show the potential for CCS at different times of the year. The drop during August/September represents the outage due to maintenance.

3. CARBON CAPTURE AND STORAGE

This chapter covers the theory background of the carbon capture process, focusing on the chemical absorption process. A brief explanation of the partial capture concept is given due to the importance for this work, as well as a review of the theory behind the dynamic modelling of these type of units.

3.1. CO_2 CAPTURE TECHNOLOGIES

Several technologies have been developed for the purpose of capturing CO_2 from different types of streams and processes, being the most common classification as post-, pre- and oxy-fuel combustion technologies [20]. In order to select one of the technologies for a particular purpose, the benefits and drawbacks of each of them must be analyzed accurately. Post-combustion captures the pollutant from a flue gas, which means that can be retrofitted to an existing plant relatively easily [20]. This represents the main reason behind the selection of this type of CCS technology for the steel manufacturing industry.

Within the post-combustion technology, several techniques can be found in literature [20]. In this thesis the chemical absorption with aqueous MEA 30wt% is the one applied, being a technology broadly studied and tested as potential CCS technology for large industrial plants. A simplified process scheme of the chemical absorption process with MEA is shown in Figure 8. The flue gas containing CO_2 enters the absorber at the bottom, meeting the solvent entering in the upper part of the column. The CO_2 gets absorbed by the solvent by intensive liquid-gas contacting, which leaves the absorber through the bottom and is pumped to the stripper. In this second column, the solvent rich in CO_2 is heated up in the reboiler up to the stripping temperature, breaking the chemical bounds [20] and releasing the CO_2 through the top of the column . After being cooled down in order to condensate the water present in the gas stream, the almost pure CO_2 is sent to compression. The regenerated solvent is pumped back to the absorber, being cooled in a heat exchanger with the rich stream in order to improve the energy efficiency of the process.

The capture efficiency of the process, also called capture rate, is defined as the amount of CO_2 absorbed by the solvent compared to the amount of CO_2 entering the process, as can be seen in Equation 3, where C_{abs} is the capture efficiency, $m_{CO2\text{-}in}$ is the CO_2 entering the process and $m_{CO2\text{-}out}$ the CO_2 leaving the absorber in the clean gas.

$$C_{abs} = \frac{m_{CO2-in} - m_{CO2-out}}{m_{CO2-in}} * 100 \qquad (3)$$

The absorption takes place at around 40-60°C, temperature at which the reaction kinetics are maximized [20] and therefore external cooling for the lean stream is needed. The main heat consumption of the process, and therefore the energy penalty for the emitting plant takes place in the reboiler, with a heat demand of 3.5 to 5 MJ/kg CO_2 captured [21]. On the other hand, the capture efficiency can be really high, reaching values up to 95% [22].

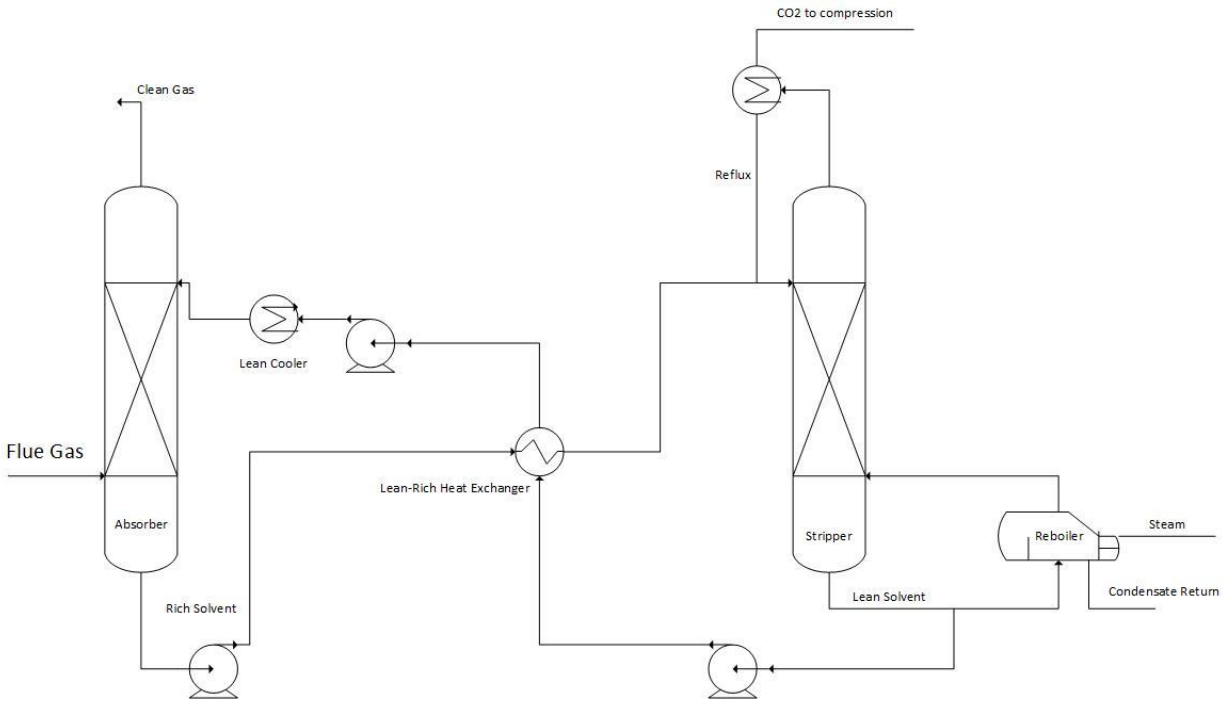

Figure 8. Simplified process of a generic MEA absorption process.

3.2. PARTIAL CAPTURE

Even though climate change is globally accepted and proved by the scientific community, and big plans are being carried out in order to reduce CO_2 emissions, the implementation and commercialization of CCS is not happening yet. The analysis of the reasons behind this is a very complex task, but some of the main reasons are the high cost, both capital and operational, and the lack of regulations regarding carbon emissions. In other words, CCS has shown to be too expensive to experience a broad implementation with the current market conditions [15]. In order to reduce this cost the concept of partial capture has been introduced.

Partial capture is defined as a process that for economic reasons is deliberately designed to capture only some parts of the CO_2 produced [15], instead of the traditional idea of capturing as much as possible. There are several cases that present favorable conditions for partial capture, such as plants with several stacks, with access to low-cost heat or plants that must reach certain emission performance standards [15]. Partial capture can also be feasible for industrial facilities that can adapt their product portfolio flexibly when market conditions are favorable, e.g. capturing CO_2 discontinuously or at different load without the need of reaching high capture efficiencies constantly.

In those plants with several stacks such as steel mills, partial capture can be implemented under two different approaches: capture a relatively low fraction of CO_2 in all the sources, or capturing a high fraction in one or a few of the sources, being the last one the most favorable in terms of retrofitting and increasing the capture efficiency in case of needed [23].

3.3. DYNAMIC MODELLING OF POST-COMBUSTION UNITS

The chemical absorption process consists of the absorption of CO_2 into the solvent through two different ways: chemical reactions and mass transfer. Two main approaches are found in literature to model the dynamics of the two columns: equilibrium-based and rate-based [20]. Both approaches divide the absorber and stripper into several stages connected through mass and energy balance equations [24]. The equilibrium-based approach considers the gas and liquid phases to reach thermodynamic equilibrium at each stage, which is not always true. On the other hand, the rate-based approach considers the rate of mass transfer, being therefore more accurate and complex than the equilibrium one. A summary of the different types of models is shown in Figure 9, where the mass transfer complexity is measured in the Y-axis while the chemical reactions complexity in the X-axis. The lower row shows the equilibrium based models (model 1 and 2), i.e., not considering the rate of mass transfer. Model 2 considers the kinetics of the reactions. In the upper row the three rate-based model possibilities are shown. Mass transfer is included into the models through the two-film theory, which assumes the liquid and gas phases to have bulk and film regions with an interphase between the two phases where the mass transfer occurs. The complexity of the models increases gradually, since Model 3 does not consider reaction kinetics, Model 4 includes them in the bulk, using an enhancement factor to describe the influence of the mass transfer in the kinetics, and Model 5 takes into account mass transfer resistances, electrolyte calculations and the reaction system in both the film and the bulk [20]. In this work, the Aspen model explained in section 4.3 follows the approach 2, while the dynamic process model presented in section 5 uses approach 4.

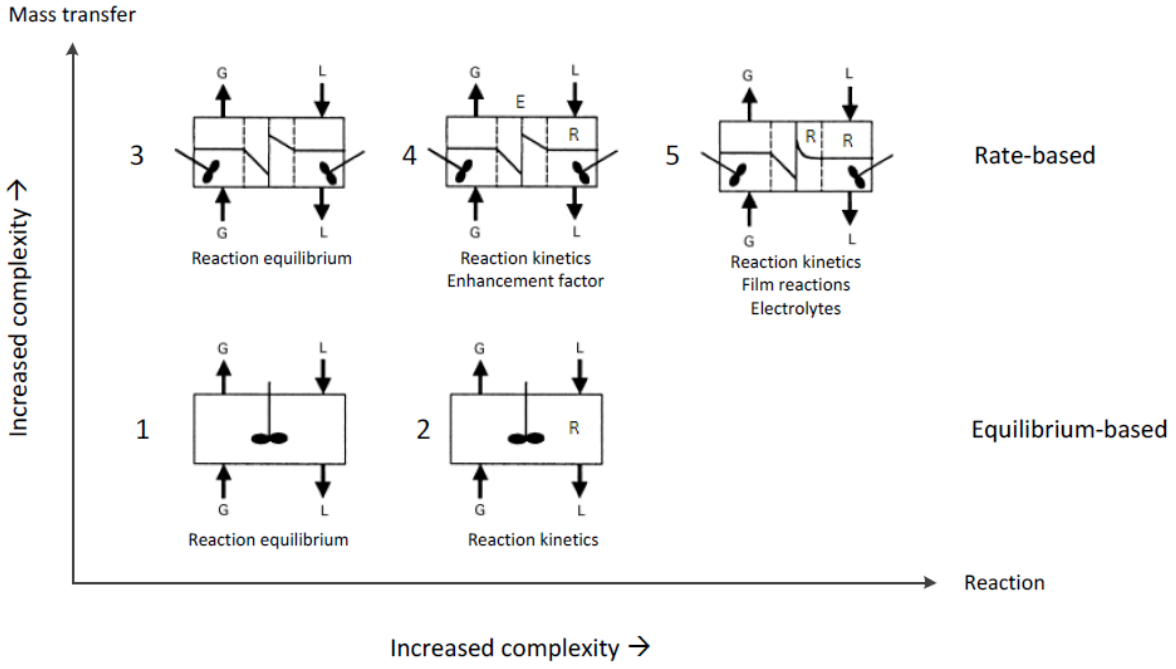

Figure 9. Different approaches for modelling chemical absorption processes [25]

4. METHOD

This chapter presents the methodology used. The second section describes the processes and their interaction. The third section covers the treatment of the steel mill transient data as well as the definition of scenarios to run in the model. The forth section covers the details regarding the simulation and how the analysis is going to be performed, while the fifth section of the chapter focuses on the method behind the regulatory control implemented in the process. The last subsection describes the tools used to develop the model where the simulations will be run.

4.1. GENERAL PROCEDURE

Figure 10 shows the workflow of the developed tasks. This work is based on plant data from the steel mill described in Section 2.5 collected for an entire year (2017). The plant data is used 1) to the design the process model of the capture unit and the heat integration into the steel mill, and 2) to obtain the transient boundary conditions for the CO_2 source to be treated as well as the heat available for solvent regeneration. Based on this, a transient events analysis of the most relevant variables was performed for the capture unit.

In order to build the dynamic model of the capture unit, the capture plant had to be sized and designed for the reference case included in this work. In order to do so, a model developed in Aspen Plus has been used to generate all the design and steady-state performance data needed to be included in the dynamic model, and it is described in section 4.3. The dynamic model has been built by using Modelica language with Dymola software and the Gas Liquid Contactors (GLC) library [26] developed by Modelon [27], and a further explanation is given in section 4.7 and chapter 5. The final dynamic model was validated with the steady-state model developed in Aspen Plus. Results of the validation are shown in chapter 6. A regulatory control layer was implemented into the model, which is described in section 4.6. Simulations of the different scenarios were run after the validation according the methodology described in section 4.4.

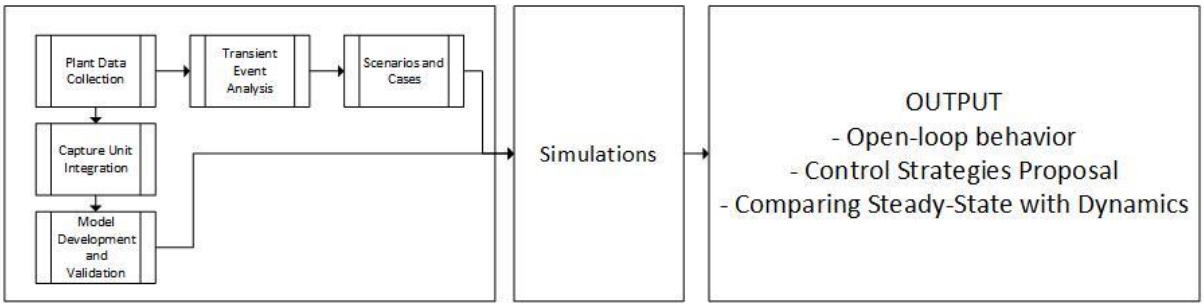

Figure 10. Workflow of the activities carried out during this thesis.

4.2. INTEGRATION OF THE CAPTURE UNIT INTO THE REFERENCE PLANT

This section describes how the capture unit has been placed and sized according to the reference steel mill requirements. The section starts with a description of the power plant integrated in the steel mill, followed by the selection of CO_2 source to treat as well as the sizing based on process boundaries.

Most of the study is based on current operational conditions, while some of it is based on hypothetical situations, as it will be explained further on this section.

4.2.1. Selection of CO_2 Source

As it was shown in Figure 5, the collector (also called gas holder) is a tank where the three main process gases are blended together before being sent to the power plant: Blast Furnace Gas (BFG), Coke Oven Gas (COG) and Basic Oxygen Furnace Gas (BOFG). In case that the flow exceeds the amount of gas that the power plant can burn, the process gases are alternatively sent to the flare. Other reasons for flaring can be quality of the gas or disturbances in the power plant, among others. In Table 2 the composition of the three main process gases is shown, as well as the volumetric flow:

Table 2. COG, BFG and BOFG molar composition and volumetric flow [28]

	Unit	**COG**	**BFG**	**BOFG**
CO_2	(mol/mol)%	1.5	24.6	16.3
N_2	(mol/mol)%	5.9	49.6	15.6
O_2	(mol/mol)%	0.2	0	0
H_2O	(mol/mol)%	2.3	2.2	1.1
CO	(mol/mol)%	5.7	20.4	64.1
CH_4	(mol/mol)%	21.5	0	0
$C_2.5H_5$	(mol/mol)%	2.6	0	0
H_2	(mol/mol)%	60.4	3.2	3
Flow	(kNm^3/h)	37.3	352.5	24.2

The study made by Skagestad et al.[15] suggested four different capture cases: two of them focused on capturing the CO_2 after the CHP plant (pure post-combustion CO_2 capture) while the two others were placed before the combustion of the gases. The study also suggested the added value of capturing before the combustion of the gases due to the related increase of heating value of the gases, improving the efficiency of the combustion.

Arasto et al. [7] discussed the importance of treating the Blast Furnace Gas from the perspective of the steel manufacturing and how the other process gasses (COG and BOFG) become negligible compared to the large volume flow of the stream of BFG (see Table 2).

Since BFG represents the largest fuel gas stream of the SSAB´s Luleå steel mill (in volumetric flow), and based on the two studies mentioned above, it is decided to place the capture plant for this study before the gas holder in order to treat only blast furnace gas. In addition to, the BFG stream has a large volumetric flow of CO_2, i.e., larger partial pressure, which is highly beneficial for gas separation.

4.2.2. Heat Boundaries

In the present study the heat available in the reboiler is considered an input given by the steel mill plant. The approach followed in this work is to design the carbon capture plant in order to be able to run with the maximum amount of heat available in the steel mill, and study its performance with

smaller amounts of heat. Therefore this subsection focuses on defining the maximum and minimum amount of heat that can be used for the absorption process.

Heat integration opportunities for CO_2 capture require analysis of heat levels, heat sources and sinks, and pinch analysis, among others [7]. The integration of the capture plant within other processes has been widely discussed [29][30][31], and it has been shown that the most efficient method of providing the heat required by the capture process is condensing steam [32]. For this study, only two sources of heat are going to be considered: the available excess heat in the power plant and the heat available in the flaring. Regarding the later, it was assumed that there is a way of recovering the heat present in the flaring gas, i.e. a steam boiler. Under this hypothesis, the heating value of the flare gas can be analyzed and converted into useful heat. The average heat available in the flare that can be considered in the analysis is 10 MW. However, the amount of gas sent to flaring changes drastically every hour, as it is discussed in section 4.4. Peaks of up to 30 MW on top of the average happen regularly, having a total of 40 MW available to be used at times.

Regarding the heat available in the steam cycle, it is important to mention that the boiler capacity remains constant over the year (data is given in Appendix A), averaging 290 MW. Considering all the heat flows within the power plant (shown in Figure 6), the simplified power balance of the steam cycle is computed as shown in Equation 4 (where minor losses have been left out of the system), with Q_b being the power in the boiler transferred to the steam, Q_{DH} the power transferred to the district heating network in the district heating heaters, P_{el} the gross electric power generated and Q_{OF} and Q_{SM} the steam sent to other facilities and the steel mill, respectively:

$$Q_b = Q_{condenser} + Q_{DH} + P_{el} + Q_{OF} + Q_{SM} \quad (4)$$

All of the power (both heat and electricity) consumers of the process are assumed constant in this study. This means that it is assumed that the only unit from which the heat can be extracted for the capture unit is the cold condenser. Computing this value, it can be extracted that a large amount of heat is available in summer (110 MW of average and peaks up to 125 MW). An important aspect to mention is the quality of the heat (temperature and pressure of the steam), which in this work has not been analyzed in detail. It is assumed that the steam can be extracted from the cycle with pressure and temperature enough to run the reboiler.

According to the two variations observed in the heat sources available to run the capture plant, it is concluded that the maximum heat available is 155 MW: 125 MW corresponds to the steam cycle and 30 MW to the flare gas.

It is important to define the opposite scenario of minimum amount of heat available as well. By looking at the two heat sources, it can be extracted that theoretically having 0 MW available could happen. However, this would mean that the power plant cycle is utilizing the entire steam capacity to the production of both electricity and district heating, at the same time that the flaring gas drops to 0. Due to the rarity of such conditions, this option is discarded, taking a value of 30 MW as minimum heat boundary.

4.3. Description of the Post-Combustion Capture Plant

The carbon capture plant considered in this study consists of a post-combustion unit with 30% wt MEA as chemical solvent. The capture unit has been designed by the commercial software Aspen Plus [33]. The configuration considered contains two columns: one absorber that includes a washing section on the upper part and one stripper. Modified process configurations presented in other works [34], such

as intercooling or rich splitting are not considered in this work, since the optimization of the capture plant performance is not among the aims of this thesis. Regarding the dynamic process models in GLC library, it has been discussed and explained in detail in other works [35], so only an overview of it will be given.

As it was stated in section 4.2, the design point chosen for the design of the capture unit is to treat the stream of blast furnace gas (60 m3/s) with a maximum available heat in the reboiler of 155 MW. Receiving this maximum amount of heat, the plant is designed in order to capture 90% of the CO2 present in the BFG. The lean solvent feed into the absorber is cooled down to 40°C in a water cooler before entering the column. Mellapack 250Y is chosen as the structured packing in both columns. The diameter of the columns is calculated by Aspen after defining a flooding limit of 85% in both absorber and stripper. In order to maximize the efficiency of the plant, a lean loading of 0.32 is fixed in all design cases as the most optimum point for partial capture, based on [36]. Important to point out that the absorber is pressurized, since the blast furnace gas enters the absorber with a pressure of almost 2 bar, which leads the rich loading to be higher than in conventional capture units, as it was experimentally shown by Dreillard et.al [37] A schematic diagram of the carbon capture unit is shown in Figure 13. Relevant input and output data of the steady-state simulations is shown in Table 3.

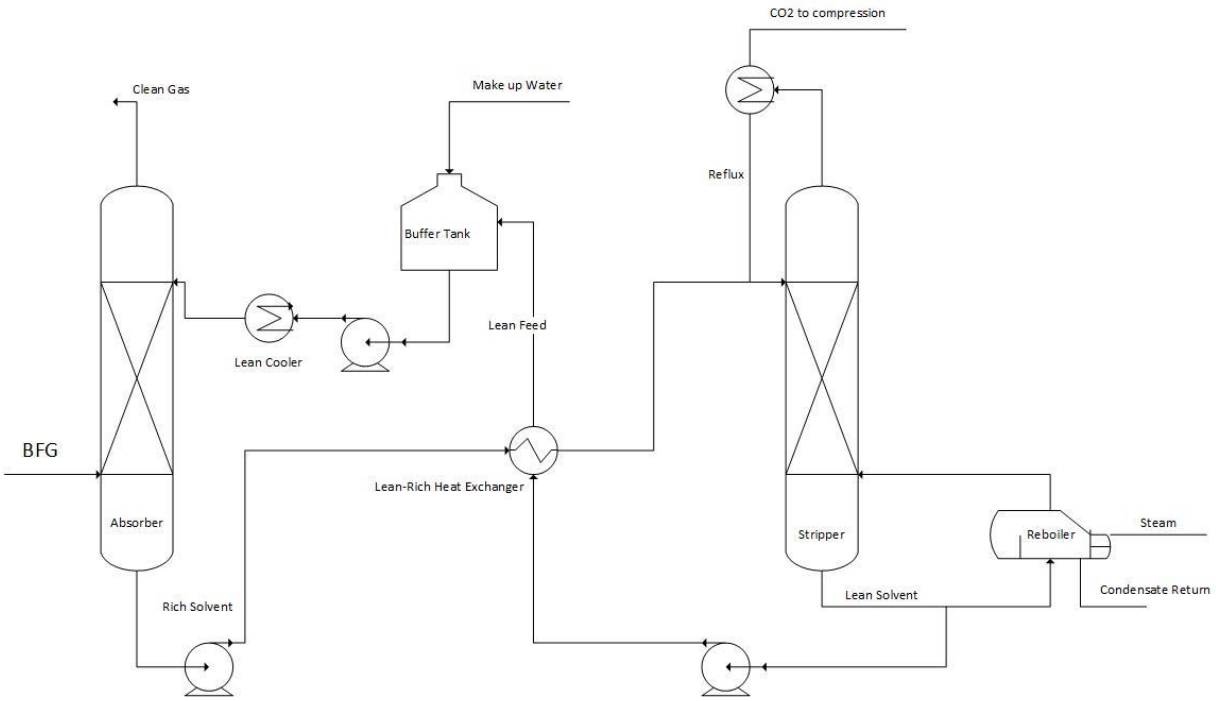

Figure 11. Schematic process diagram of the capture unit to study in this work treating Blast Furnace Gas (BFG).

Table 3. Design and geometry values of the main units of the PCC unit: Absorber, Washer, Stripper and Heat Exchanger. Values taken from a Steady-State Model developed with Aspen Plus.

Absorber	Washer	Stripper	Heat Exchanger
Stages - 30	Height – 1.5m (2.1 total)	Stages - 20	Average U – 1.5 kW/m^{2}K
Height – 25m (35.6 total)		Height – 15m (21.4 total)	
Diameter – 8.42m	Diameter – 8.42m	Diameter – 6.89m	
Lean Loading – 0.32		Lean Loading – 0.32	Lean-rich temperature approach – 10K
Rich Loading – 0.54		Rich Loading – 0.54	
Lean Solvent Temp – 40 °C		Lean Solvent Temp – 120 °C	
Pressure – 1.81 bar		Pressure – 2 bar	HE Area – 8281 m^2

4.3.1. Plant Performance under different Operation Conditions.

Since the capture plant is designed and sized for 155 MW, it is important to analyze its performance under different heat loads, since it will be operating with less than 155 MW for most part of the year. In order to find new operation parameters such as stripper temperature or lean and rich loading, an optimization study has been performed.

Since in this case the heat in the reboiler is treated as a boundary condition that experiences disturbances, instead of something that can be manipulated, the only free variable remaining to be changed is the circulating solvent flow rate (important to point out that the entire blast furnace gas flow goes through the absorber, so it cannot be a manipulated variable). Several simulations have been run in the dynamic model changing the solvent flow rate to maximize capture rate, taking into account operation constraints that cannot be violated, such as the temperature in the reboiler. This approach is a common procedure to find optimum operation points in actual pilot plants such as the optimum specific reboiler duty for given capture rates [36].

4.4. Transient Events and Scenarios

As it is explained in sections 4.2 and 4.3, the integration of the carbon capture unit within the steel mill happens mainly in two different parts of the process: the gas entering the absorber and the steam going into the reboiler. This means that the steel mill variations that can affect the capture unit generating disturbances are the ones related to the blast furnace gas and the steam going into the reboiler. Therefore, the transient events analysis is divided into three independent parts: variations in the blast furnace gas, variations in the available heat in the steam cycle and variations in the heat available in the flaring.

4.4.1. Analysis of Variations

Section 4.2 discusses how the capture unit is connected to the steel mill and the adjacent power plant in terms of heat and gas entering the absorber. There are three variables whose variations will

represent disturbances for the capture plant: BFG flow, heat available in the flare gases and excess heat available for CCS in the steam cycle. Figure 12 shows a simplified block diagram of how the capture plant is connected to the steel mill and the CHP plant. This section explains how the analysis of these three variables has been carried out.

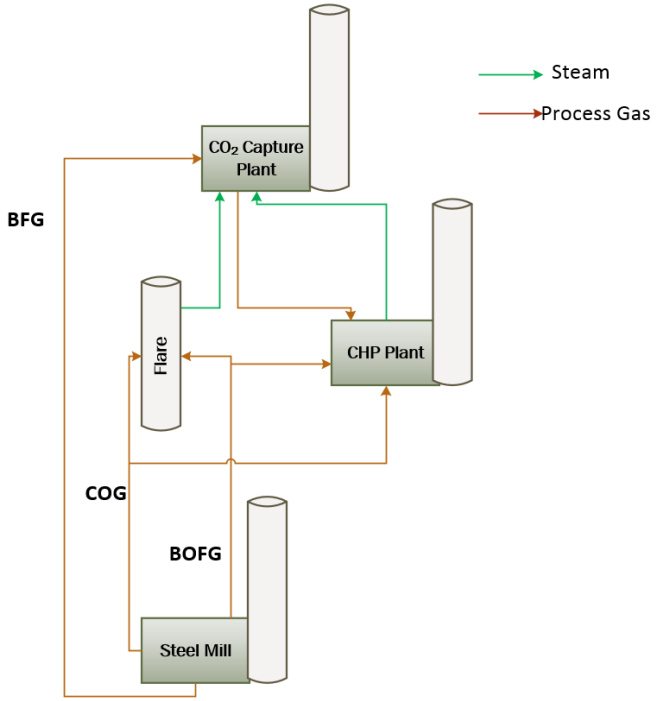

Figure 12. Capture plant integrated in the steel mill and CHP plant. Green arrows represent heat and orange arrows process gases.

The available heat for CCS in the steam cycle was defined in section 4.2.2. Therefore, by analyzing the variations in heat in the condenser, the variations in available heat for CCS are also analyzed. In order to do so, the analysis has focused in two times of the year, where the average computed available heat flattens out: the period with maximum district heating demand, with an available heat average of 0 MW, and the period with minimum district heating demand, with an average available heat of 110 MW. A Matlab [37] code has been developed in order to compute the variations in time (the code is shown in Appendix B). The output of the code is for how many straight hours the objective variable (in this case the available heat) remains above or below a particular value, and with what frequency, i.e. the number of such events. Variations in the excess heat may for example represent variations in electricity generation or in district heating loading due to outdoor temperatures and weather conditions.

Regarding the flaring, it has been already pointed out that the average heat available in the flare gases is 10 MW. Therefore, the variations with respect to this load are analyzed. The yearly data is again evaluated in two different periods, corresponding to: a) before the shutdown of the power plant (4769h) and b) after shutdown (3236h). The procedure followed for the variations analysis is the same than the explained for the excess heat, i.e., using the Matlab algorithm available in Appendix B. Flare gas variations imply more heat available temporarily in the reboiler or a decrease on the available heat for a certain amount of hours.

Finally, in section 4.2.1 the blast furnace gas to be treated was presented. It goes first into a gas holder, where it is mixed with the basic oxygen furnace gas and the coke oven gas forming the mixed gas. The

latter is burnt in the power plant, while everything that exceeds the power plant boiler capacity is flared. The blast furnace gas stream accounts for 75% of the total volume flow of the mix gas. It is assumed that this proportion is constant through the year. The nominal flow of blast furnace gas that the capture unit treats is 60 Nm^3/s, while the average volumetric flow of gas mix entering the CHP plant is 80 Nm^3/s. By analyzing the variations of the mix gas entering the power plant the variations of blast furnace gas can be computed assuming that it represents a 75% v/v of the mix. It is also important to mention that it has been assumed that a drop in flow in the mix gas implies a drop in the process gases flow. In other words, a decrease in flow of the mix gas is not caused by an increase in flaring (would not make economic sense to flare the process gases if they can be burnt in the power plant). The analysis has been separated into three different types of variations: a) 10% drop, b) 20% drop and c) drop to 0 cubic meters of flow (100% drop), while the year has been divided into two parts: before and after the power plant shutdown. The way of performing the analysis has been one more time with the algorithm shown in Appendix B.

4.4.2. Scenarios

Two scenarios are defined based on the analysis of the plant operation to set the boundary conditions for the transient events in the simulations:

- Scenario 1: gas flow variations from the blast furnace of 10% drop, 20% drop and 100% drop.
- Scenario 2: reboiler duty variations (based on the available heat in flaring or power plant steam) of ±10 MW, ±20 MW and ±30 MW.

The scenarios depend on the steady state conditions from which they are initiated, i.e. the same variations will have different effect on the plant if they happen at maximum reboiler duty, or at minimum. Therefore, each scenario will contain 3 cases: A) the plant is running at maximum heat (155 MW), B) minimum heat (30 MW) and C) intermedium heat (100 MW) corresponding to the different seasons, summer, winter, and spring/fall, respectively. Case A is thus only including a decrease of heat while case B only includes an increase, since the plant is operating at maximum and minimum conditions, respectively.

4.5. SIMULATIONS

In this section, the procedure followed for the simulations is explained, which is similar than the ones carried out in [8] and [38]. The simulations consisted of step changes of the magnitudes described above. For both scenario 1 and scenario 2 the step is considered a valid assumption, since it is known that both variations occur very quickly. The step changes were applied while keeping the remaining process variables constant and tracking the output of the main process variables in open-loop response, i.e. with no control structure implemented more than the regulatory control layer described in section 4.5.

The variables recorded are listed below:

- Solvent lean CO2 loading at absorber inlet L_{abs}.
- Solvent rich CO_2 loading and stripper inlet R_{str}.
- Temperature at stripper column bottom T_{str}.
- CO_2 capture rate at absorber outlet C_{abs}.

- CO_2 product mass flow at stripper condenser outlet P_{CO2}.

In order to measure the dynamics of the listed variables under the studied disturbances, dead times and 10% settling times were calculated, as well as other parameters described below [8]:

- The dead time Θ represents the delay time. In other words, how long it takes to the process variable to start responding to a change in a process input. It is considered that the beginning of the response occurs when the trajectory of the process variable moves out of the initial steady-state towards the final steady-state.
- The 10% settling time t_s is computed as the time it takes from the moment the process variable begins to respond to a change until it remains within an error band defined by the final steady-state and 10% of the change in the process variable, as expressed in Equation 5.
- The total stabilization time t_{sta} is computed as the sum of the dead time and the 10% settling time.
- The relative change RC of the process variable is calculated according to Equation 6, where y_0 is the initial steady-state and y_∞ is the new steady-state.

$$y_\infty - 0.1\Delta y < y_\infty < y_\infty + 0.1\Delta y \quad (5)$$

$$RC(\%) = 100 \cdot \frac{y_\infty - y_0}{y_0} \quad (6)$$

4.6. Regulatory Control

The next step of the work is to choose, implement and tune a consistent inventory control strategy. In order to design such a regulatory control layer, the paper published by Aske and Skogestad [39] has been followed. The first important decision to make when it comes to design a consistent regulatory control layer is where to place the throughput manipulator for the solvent mass flow circulating through absorber and stripper [32] .In the present work it has been decided to locate it in the absorber inlet, i.e., at the outlet of the buffer tank. The main variables that need to be controlled for a consistent and stable operation are listed below:

- Lean solvent temperature at inlet of the absorber.
- Absorber and stripper sump levels.
- Stripper pressure.
- Stripper condenser temperature.
- Make-up water.

The water side level of the reboiler should have been included in the listed variables, but since the reboiler has been modeled as a heat input for the model it has been left out of the regulatory control as well (see section 5.1). The list below shows the manipulated variables utilized to control the listed process variables, what can also be seen in Figure 13:

- Pump speeds to control absorber and stripper sump levels.
- Control valve to control stripper pressure.
- Flow of cold water to control temperatures of lean solvent and condenser in the stripper.
- The make-up water flow is added in order to have a MEA concentration of 30% w/w (in real life is measured with periodic samples while in the model it is a real time mass balance of water what is determining the water addition).

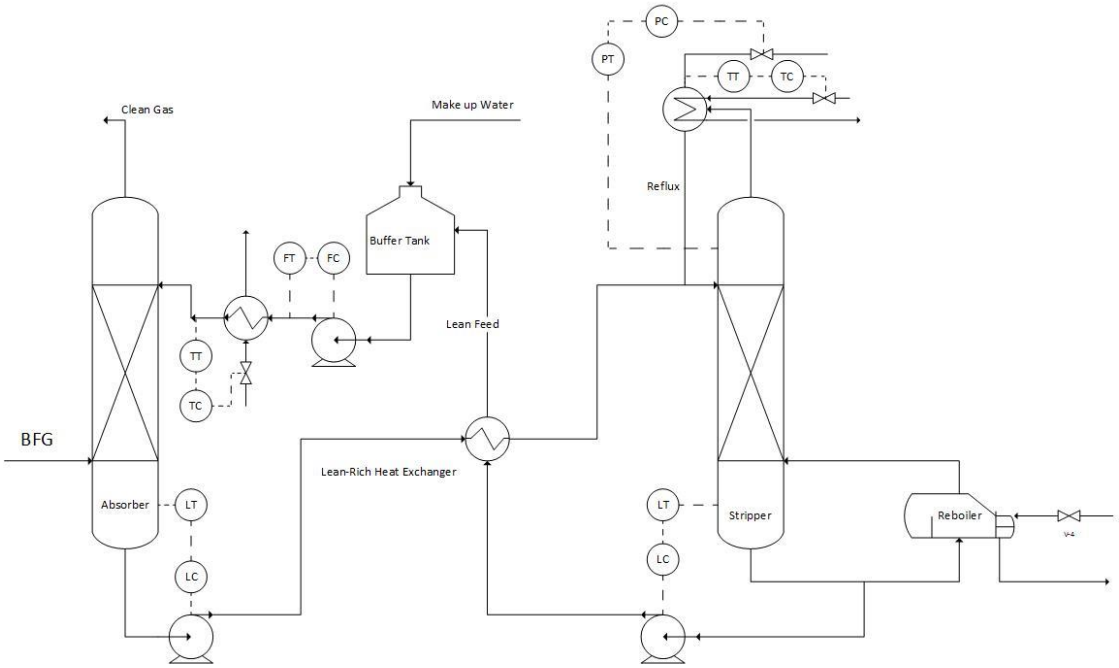

Figure 13. Regulatory control layer implemented in the capture unit. The first letter of the control icons represent the controlled variable. L: Level, T: Temperature, P: Pressure, F: Flow. The second letter represents the type of unit. T: Transmitter, C: Controller.

Once the regulatory control loops have been placed they need to be tuned. Such tuning has been developed based on the simplified internal model control (SIMC) method for smooth PID controller tuning developed by Skogestad and Grimholt [40]. Table 4 summarizes the tuning values for the different controllers:

Table 4. Tuning Values of the different controllers of the regulatory control layer. Table shows the controller type and the parameters. k = gain, Ti = integral time, Td = derivative time

Variable	Controller Type	Parameters
Absorber Sump Level	PI	k=-4.655 Ti = 480s
Stripper Sump Level	PI	k=-1.57 Ti = 480s
Lean Solvent Temperature	PID	k=0.1366 Ti = 480s Td = 100s
Condenser Temperature	PID	k=0.054 Ti = 480s Td = 100s
Stripper Pressure	PI	k=0.6475 Ti = 480s

The process supervisory control layer has one degree of freedom, which can also be extracted from Figure 13: the flow rate of the lean solvent entering the absorber, since the reboiler duty (mass flow rate of steam entering the reboiler) cannot be manipulated. Therefore, the solvent flow rate will be

used further on the study to control different process variables depending on the control strategies that will be analyzed later on.

4.7. MODELING TOOLS

The main tool used to develop the dynamic model of the process has been Dymola [24], a software based on Modelica language. An overview of both tools is given in this section, as well as a brief explanation about the specific library used.

Modelica is a modeling language created by Modelica Association [41], focused on modeling complex physical systems and used in industry since year 2000. It is object oriented and uses differential, algebraic and discrete equations to solve the models, but no partial differential equations like FEM and CFD methods do. There are several Modelica simulation Environments [41]. The one that is going to be used in this study is Dymola (standing for Dynamic Modeling Laboratory) [24]. This software allows the user to both model and simulate utilizing a very intuitive interface for the different components (of all kind of applications: thermal, electric or fluids, among others). The combination of Modelica /Dymola is the perfect tool to develop the objective model of the present study, not only due to its powerful dynamic simulation language but also because it allows the user to have a deep understanding of how the modeling carried out works, something really useful in academic approaches.

Finally, it is important to mention that Modelica covers a wide range of engineering fields. Libraries are built from models developed by different users, representing a domain of physical systems. The main library to be used in the present study is the Gas Liquid Contractors (GLC) library [26], developed by Modelon AB [27]. Into this library, different dynamic models of the main equipment of the process can be found, such as packed absorption columns, sumps, reboiler, condensers, water washers and valves among others. The validation of these process models have already been validated for an absorption process with MEA with steady-state and transient plant data by Montañés et al. [42] [38].

5. THE MODEL

In this section a detailed description of the dynamic model of the process is given. As it will be explained later, the model is based on the model presented by Akeson et al. in [43]. This chapter comprises two different subsections: first of all the development of the dynamic model is covered, followed by the results of the verification carried out with the steady-state model.

5.1. DYNAMIC MODEL DEVELOPMENT

5.1.1. Model Review

As it was presented in section 4.4, the dynamic process model was developed by using the physical modeling language Modelica [41] through the library called Gas Liquid Contactors [26] and Dymola [24]. The model was developed by parametrizing and modifying the different models provided in the library, so a detailed explanation of the different tuning parameters, sizes, geometry and materials is given in this section. The dynamic models found in the GLC library have been deeply explained in other articles [9] [38] ,so in this work only an overview of them will be given. In order to follow a methodic model development the model was built in 3 different parts (absorber, lean-rich heat exchanger and stripper with reboiler) before placing them all together.

The model considers five main reactions between the CO_2, MEA and water, listed below [43]:

$$2H_2O \leftrightarrow H_3O^+ + OH^-$$

$$CO_2 + 2H_2O \leftrightarrow H_3O^+ + HCO_3^-$$

$$HCO_3^- + H_2O \leftrightarrow H_3O^+ + CO_3^{2-}$$

$$MEAH^+ + H_2O \leftrightarrow H_3O^+ + MEA$$

$$MEACOO^- + H_2O \leftrightarrow MEA + HCO_3^-$$

All the above reactions are assumed to occur in the liquid phase and the interphase as well as assumed to be in chemical equilibrium [43]. This means that reaction kinetics are left out of the model, due to the lack of reliable data [43]. This assumption is justified at high temperatures (stripper). However it is also used in the absorber since the reaction between CO_2 and MEA is considered to be fast [44] and therefore the assumption is acceptable. The chemical equilibrium constants are taken from Böttinger [45] while the Van´t Hoff equation is used to calculate the heat of reaction from the chemical equilibrium constant [43].

The models of the two columns (absorber and stripper) are built based on the two-film theory, so thermodynamic equilibrium is assumed at the phase interphase. According to the classification given in section 2.3, the mass transfer is modeled following a rate-based approach, where an Enhancement factor is included describing the impact of chemical reactions on the mass transfer. Concentrations and pressure gradients are used to calculate the mass transfer for both the liquid and gas phase respectively ($n_{i,L}$ and $n_{i,V}$), as can be seen in Equations 7 and 8 [43], where A_{if} is the contact area, E the enhancement factor mentioned above, k_i the mass transfer coefficients by Onda [46], $c_{i,b}$ and $c_{i,if}$ the

molar concentrations at liquid bulk and interface, $p_{i,b}$ and $p_{i,if}$ the partial pressures in the gas phase and T is the temperature in the bulk phase:

$$n_{i,L} = A_{if} k_{i,L} E\left(c_{i,b} - c_{i,if}\right) \quad i = CO_2 \qquad (7)$$

$$n_{i,V} = \frac{A_{if} k_{i,V} E(p_{i,b} - p_{i,if})}{RT} \quad i = CO_2, H_2O \qquad (8)$$

The enhancement factor definition can be seen in Equation 9, where C_{ef} is a correction factor, c_{MEA} is the molar free MEA-concentration taken from [47], k_{CO2} is the overall reaction constant for CO_2 [47] and D_{CO2} is the diffusivity of CO_2 in water taken from [48]. It is also important to mention that mass and energy storage are only present in the bulk flows [43].

$$E = C_{ef} \frac{\sqrt{c_{MEA} k_{CO2} D_{CO2}}}{k_{i,l}} \quad i = CO_2 \qquad (9)$$

Regarding phase equilibrium at the gas-liquid interface for both water and carbon dioxide, Equations 10 and 11 are used, where the solubility in water of CO_2 is considered by Henry´s law with He_i from [48] and γ_i are activity coefficients from [45]:

$$y_i P = \gamma_i x_i He_i \quad i = CO_2 \qquad (10)$$

$$y_i P = \gamma_i x_i p_{i,sat}(T) \quad i = H_2O \qquad (11)$$

The columns are modeled as several packed volumes with a sump at the bottom assumed to be ideally mixed. Each packed volume contains packing material whose function is to increase the contact area between the two phases. The packing characteristics of Mellapak 250Y [51] have been considered in the model, with a surface area of 256 m^2/m^3 and a void fraction of 0.987. Within each packed volume there are both liquid and gas flows modeled as separate media with different thermodynamic properties: the ideal gas law applies in the gas phase to calculate densities and pressures while a constant density is used for the liquid. Regarding the pressure in both columns is determined by the gas pressure, while the pressure drop is implemented as an input. The number of packed volumes to include in each column and its discretization defines the accuracy of the calculations. However, increased discretization results in longer simulation times. It has been included a total of 4 packed segments in the absorber and 2 in the stripper, while the discretization has been made in order to match the number of theoretical stages calculated by Aspen and shown in Table 3. The main size and design values of the different components of the model have been taken from the steady-state model developed in Aspen Plus [33]. They can be found in section 4.3, in Table 3.

Some other assumptions have been considered in the model, and can be found listed below [38] [43]:

- MEA is considered nonvolatile and therefore no make-up is needed.
- The reboiler is modeled as an equilibrium flash stage.
- Mass and heat transfer are restricted to packed section.
- Negligible temperature difference between the liquid bulk and interface to gas phase.
- All liquid from the packing bottom in the stripper is fed to the reboiler with a constant liquid level.

Regarding the lean-rich heat exchanger between the absorber and stripper, a model of a static heat exchanger is implemented, which uses the ε-NTU approach. Values of heat transfer area and heat transfer coefficients are taken from the steady-state model as Table 3 shows. The pressure drop is computed through a simple linear loss model.

It is also important to mention that the absorber includes a model of a washer placed on top of the column, consisting of a volume with phase saturation and a temperature controller that sets the temperature such that the gas is saturated with water. A solvent buffer tank is added before the absorber, where a make-up stream of water is added to account for the H_2O losses of the system.

An important aspect in the dynamic process model is the solvent inventory at the different equipment of the plant [40]. In order to implement a realistic volume distribution in each equipment as well as residence times as realistic as possible, values from the Tiller CO2 capture test facility have been taken [52]. The reason of choosing Tiller facility is that is a pilot plant designed in order to have residence times as close as industrial plants. Therefore, by taking the residence times from literature and scaling them up to the sizes found in Table 3, the solvent hold-up in each equipment is calculated, and can be seen in Table 5. However, several exceptions have been made, listed below along other related comments:

- For the stripper sump a residence time from TCM (Technology Centre Mongstad) pilot plant has been taken, since the value of Tiller plant was extremely high and did not match the rest of the values.
- The hold-up of the absorber and stripper packing calculated from the pilot plant data does not match with the calculated in the Aspen steady-state model. It is decided to take the values from Aspen since the liquid to gas ratio of the process is considerably higher than in a conventional plant, which highly affects the residence time and therefore the relationship between hold-up and volume flow (which does not change linearly as shown in literature [49], also explained in detail in appendix XX). The packing hold-up has been implemented into the model as a constant value defined by the parameter epsilon, considered to be the ratio between the liquid volume and the total volume into the packed section.
- The residence time in the buffer tank before the absorber has been chosen in order to be the highest of the plant based on [38].
- The solvent inventory related to the cross heat exchanger and piping between the two columns has been implemented in the model with the component “TransportDelayPipe” from the Modelon library TPL [27], which allows the user to add a volume with its correspondent delay into the model, as suggested in [38].

Table 5. Averaged solvent inventory values (in m^3) of the different equipment of the PCC unit. Table also shows the reference pilot plant where the residence time values have been taken from.

MAIN EQUIPMENT	SOLVENT INVENTORY (M^3)	REFERENCE PILOT PLANT
ABSORBER SUMP	264	Tiller
ABSORBER PACKING	111.9	Calculated in Aspen
STRIPPER SUMP	249.8	TCM
STRIPPER PACKING	47.2	Calculated in Aspen
REBOILER	5	TCM
BUFFER TANK	503	Tiller
CROSS HEAT EXCHANGER AND PIPING	1080	Tiller

To provide a deeper understanding of the solvent inventory and residence times over the system, Figure 14 shows the circulation time of the solvent over the different volumes of the process, for each one of the cases studied, developed using a similar approach than in [50].

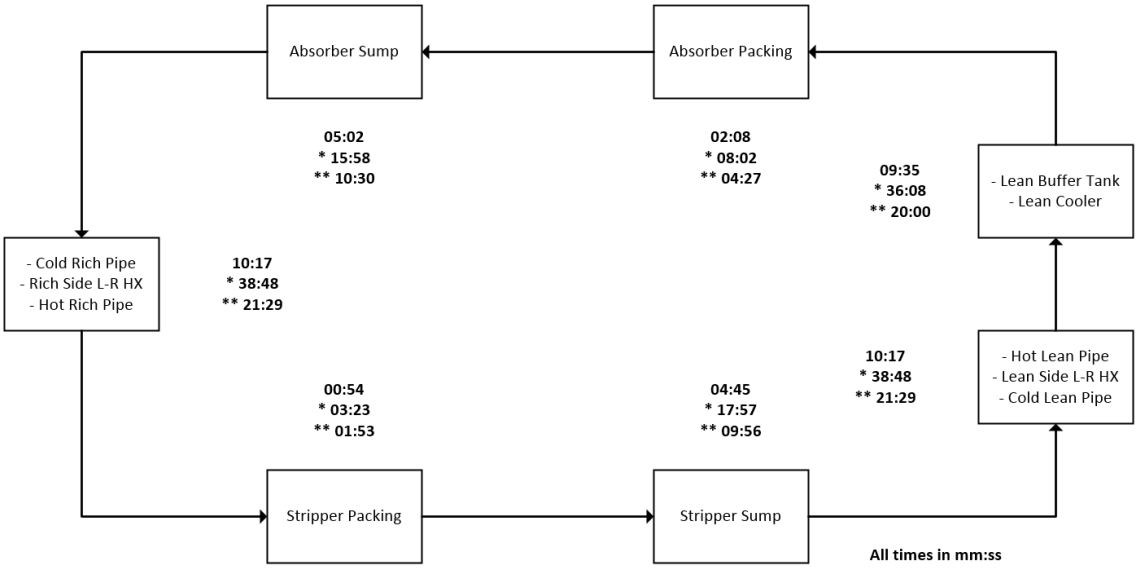

*Figure 14. Circulation Times over all the volumes of the process. The first number refers to solvent flow rate in Case A, * refers to Case B and ** to Case C*

Adding up all the circulation times for each case, the total circulation time for the flow network can be calculated, resulting in 42:18 for Case A, 02:39:04 for Case B and 01:29:44 for Case C.

To conclude, it is important to add that a regulatory control layer was implemented in the model according to the methodology explained in section 4.6.

5.1.2. Boundary Conditions and Parameters Tuning

The model has been developed only for the chemical absorption process. This means that its integration within the steel mill is included in the model as boundary conditions. Also, the model has been tuned in order to reach 90% capture for the maximum heat available in the steel mill. Hence, this section covers how the model has been adapted to the particular case study.

The flue gas model present in Dymola contains only four components: the four main species typically found in coal and natural gas combustion flue gas. However, as it could be seen in Table 2, the blast furnace gas to be modeled contains carbon monoxide, so some assumptions were taken in order to model the flue gas.

It is known that the CO remains inert in the chemical absorption process [51]. In addition, it has the same molecular weight than the other inert gas, nitrogen (both having 28 g/mol). Therefore, it was assumed that all the CO present in the stream is going to behave as nitrogen. In order to check the assumption, the properties of the stream are calculated in Aspen and the columns are re-sized after the assumption. The results can be found in Table 6 and Table 7.

Table 6. BFG properties comparison with and without assumption, i.e. modeling the CO as N_2.

With Assumption		Without Assumption	
Total Flow (kmol/s)	4.36	Total Flow (kmol/s)	4.36
Total Flow (kg/s)	138.44	Total Flow (kg/s)	134.80
Total Flow (m^3/s)	60.42	Total Flow (m^3/s)	60.42
Temperature (K)	302.15	Temperature (K)	302.15
Pressure (bar)	1.8	Pressure (bar)	1.8
Enthalpy (J/kmol)	-1E+08	Enthalpy (J/kmol)	-1.24E+8
Enthalpy (J/kg)	-3215400	Enthalpy (J/kg)	-4031900
Enthalpy (Watt)	-4.5E+08	Enthalpy (Watt)	-5E+8
Density (kmol/ m^3)	0.07	Density (kmol/ m^3)	0.07
Density (kg/ m^3)	2.29	Density (kg/ m^3)	2.23
Average Heat (MW)	31.73	Average Heat (MW)	30.90

Table 7. Capture Unit plant re-sized after assumption, i.e. after modeling the CO present in the BFG stream as N2. Results compared with the size before the assumption

With Assumption		Without Assumption	
Column diameter (m)	8.46	Column diameter (m)	8.42
Lean Loading (mol/mol)	0.32	Lean Loading (mol/mol)	0.32
Rich Loading (mol/mol)	0.55	Rich Loading (mol/mol)	0.55
Specific Reboiler Duty (MW/kg)	3.65	Specific Reboiler Duty (MW/kg)	3.65

It can be seen that the density of the streams barely changes, so the change in mass flow is considered relatively small (from 134 to 138 kg/s) and therefore the column diameters as well as lean and rich loading and reboiler duty. Hence, the CO present in the BFG is modeled as nitrogen, and the assumption is considered valid for the purpose of the application.

The list of boundary conditions are defined in Table 8 shown below:

Table 8. Boundary Conditions implemented in the Dynamic Model

Boundary	Properties	Comments
Source of BFG	T = 29 C P = 1.8 bar	BFG with 34% w/w of CO_2
Sink of Clean Gas	P = 1.5 bar T = 45 C	BFG after CO_2 absorption
Make-up Water	T = 50 C	Adds water to the buffer tank to account for the losses.
Reboiler Steam Side	Q = 155 MW	Modeled as a heat source
Sink of CO_2	P= 1.8 bar	The compression train is left out of the model.

As it was mentioned above, the model has been tuned in order to obtain an agreement as good as possible between the steady-state model performance and the behavior predicted by the dynamic model, following the method presented in Montañés et al. [39]. The tuning itself consists of making sensitivity analysis of several uncertain parameters of the model until the desired agreement was

achieved. The agreement was checked by matching the temperature profiles of absorber and stripper, lean/rich loadings and absorption and desorption rates. The results of this comparison is shown in section 5.2. The mentioned uncertain parameters include enhancement factors related to the mass transfer presented in Equation 7. In this model the enhancement factor has been tuned in both columns through a pre-multiplying factor $C_{ef,}$ which ended up being 0.25 for the absorber and 0.9 for the stripper.

5.2. VERIFICATION WITH THE STEADY-STATE MODEL

The next step is the verification of the dynamic model. Ideally, a validation would be done with dynamic or steady data from a real pilot or industrial plant. However, due to the lack of real data related to the CO_2 capture process of a Blast Furnace Gas, a verification will be done with the steady-state model developed in Aspen. Important to mention that the GLC models used have been validated by Montañés et al. [42] and [38] but using steady-state and transient data from Technology Center Mongstad, a demonstration scale capture plant, working with flue gas from a natural gas fired power plant.

In order to verify the validity of the model in all the span of operating conditions, 3 different steady-state cases (presented in section 4.1 and 4.2) have been simulated in Aspen: a) the maximum heat design point, b) the minimum heat design point and c) a 50% drop in BFG going into the capture plant. The results of the simulations of the three steady-state cases are shown in Table 9, where the comparison with the results obtained in the dynamic model is also shown. In order to keep track of the errors between the models, the absolute percentage error (*AP*) has been calculated as it is shown in Equation 12, where x_{dm} is the variable in the dynamic model and x_{sm} is the variable in the steady-state model:

$$AP(\%) = 100 \left| \frac{x_{dm} - x_{sm}}{x_{sm}} \right| \quad (12)$$

Table 9. Dynamic Model verification with steady-state data taken from Aspen Plus model. AP: Absolute Percentage Error

155 MW			
Process Variable	**Data Aspen Plus**	**Dymola Simulation**	**AP (%)**
Rich Loading	0.540	0.549	1.667
Lean Loading	0.320	0.334	4.375
CO_2 in the Clean Gas (kg/s)	4.800	4.850	1.042
Stripper bottom temperature (°C)	120.0	119.34	0.550
30 MW			
Process Variable	**Data Aspen Plus**	**Dymola Simulation**	**AP (%)**
Rich Loading	0.620	0.610	1.613
Lean Loading	0.320	0.290	9.375
CO_2 in the Clean Gas (kg/s)	36.520	36.680	0.438
Stripper bottom temperature (°C)	120.0	117.0	2.500
BFG Reduction in 50%			
Process Variable	**Data Aspen Plus**	**Dymola Simulation**	**AP (%)**
Rich Loading	0.550	0.510	7.273
Lean Loading	0.320	0.290	9.375
CO_2 in the Clean Gas (kg/s)	2.320	2.016	13.103
Stripper bottom temperature (°C)	120.0	119.0	0.833

The deviations observed between both models can be caused from the fact that a physical model is always a simplifications of reality. On top of that, the steady-state model developed in Aspen has its own deviations from reality, which makes the validation less accurate. However, it can be seen that the dynamic model accomplishes the desired degree of validity in most of the variables in every operating point. For the case with maximum heat, all the absolute errors are kept within reasonable limits. The same occurs for the minimum heat case, although the lean loading presents a higher error. The reason behind it is that the steady-state model performance losses accuracy when working at such low amount of heat, also empowered by the fact that the available amount of data from pilot plants at such condition is scarce. Some analysis have been done regarding the deviations from reality of different models at different conditions [52], where it can be observed that Aspen models differ highly from reality in some cases. Regarding the off-design case with the variation in blast furnace gas, there are some variations in terms of rich and lean loading, being the biggest error the capture rate (seen in the amount of carbon dioxide leaving in the clean gas). However, even though the mass flow presents a relatively high error, when it comes to calculate the capture rate the error is acceptable (Dymola model presents a capture rate of 91% instead of 90%). Further results of the verification are shown in Appendix C.

6. Results and Discussion

This chapter presents and discusses in detail all the results obtained in this thesis. At first, the results from the plant variations analysis are shown, which leads to the study of the transient response of the capture plant. Based on the dynamic simulation results, a control strategy has been implemented and analyzed. Finally, the chapter includes a performance comparison between steady and dynamic modes of operation.

6.1. Analysis of Variations and Transient Events

This first section covers the results of the transient events identified within the plant data considered in section 4.4. The results are shown for the three variables discussed also in chapter 4: available heat in the steam cycle, available heat in the flare and blast furnace gas.

Regarding the available heat in the steam cycle, Table 10 and Table 11 show the results of the analysis the two parts of the year considered, i.e., when the average available heat in the steam is 0 MW (2350 hours in winter) seen in the results as Period 1 and when the average available heat is 110 MW (1160 hours in summer), seen in the results as Period 2. Important to notice that the first period only has increase in heat while the second one includes both increases and drops. Figure 15 shows the plotted computed value for the entire year considered.

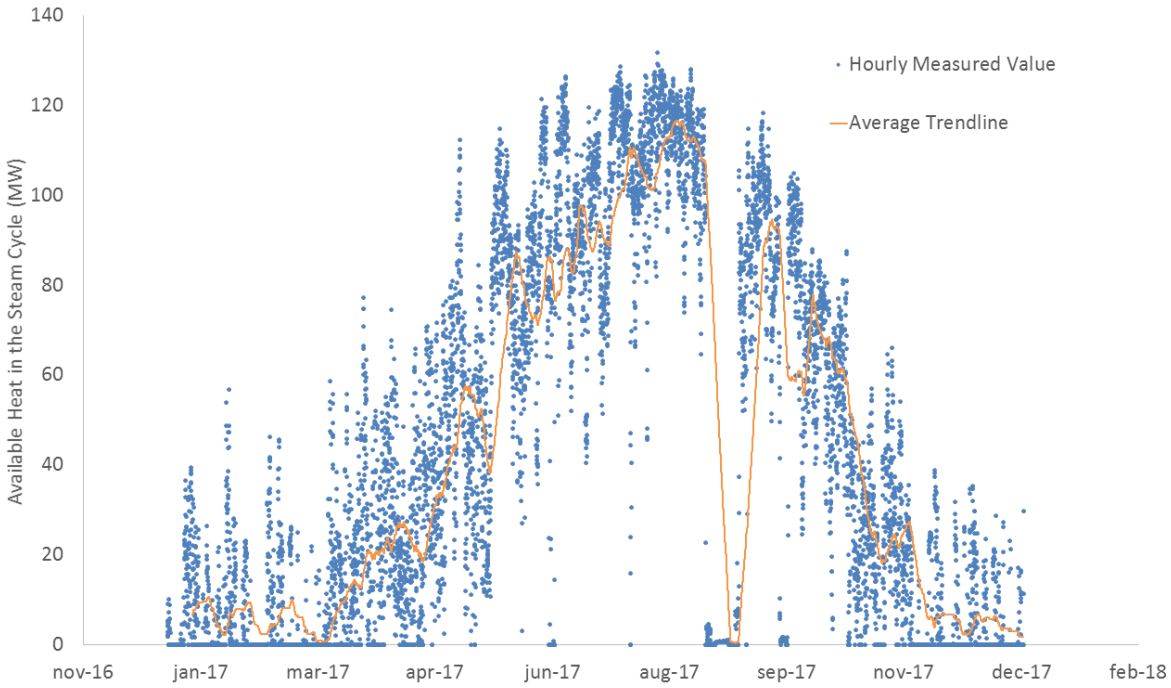

Figure 15. Lulekraft annual available heat in 2017. Y-axis is in MW while the X-axis represents the months. The drop during August/September represents the outage due to maintenance

Table 10. Variations in Available Heat in the steam cycle of Lulekraft for Period 1, i.e. 2350 hours in winter. Table shows for how many hours the available steam goes above or below certain values and with what frequency.

Period 1 : 2350h		**Average Available Heat: 0 MW**					
10-20 MW for	**Freq**	**20-30 MW for**	**Freq**	**30-40 MW for**	**Freq**	**40 MW for**	**Freq**
2h	14	2h	13	2h	4	2h	5
3h	10	3h	9	3h	6	3h	4
4h	8	4h	7	4h	4	4h	4
5h	12	5h	11	5h	9	5h	8
8h	17	8h	11	8h	10	8h	4
12h	18	12h	9	12h	1	12h	1
24h	1	24h	1	24h	0	24h	0
36h	1	36h	1	36h	1	36h	0

Table 11. Variations in Available Heat in the steam cycle of Lulekraft for Period 2, i.e. 1160 hours in summer. Table shows for how many hours the available steam goes above or below certain values and with what frequency.

Period 2 : 1160h		**Average Available Heat: 110 MW**			
120 MW for	**Freq**	**Less than 100 MW for**	**Freq**	**125 MW for**	**Freq**
2h	16	2h	11	2h	8
3h	6	3h	4	3h	3
4h	4	4h	5	4h	0
5h	7	5h	5	5h	4
8h	7	8h	2	8h	0
12h	1	12h	3	12h	0
24h	1	24h	2	24h	0
36h	0	36h	1	36h	0

Figure 16 shows the computed hourly available heat in the flare gases, while Table 12 and Table 13 summarize the main results of the analysis. The results show that a large amount of events occur throughout the year. The most common ones occur for two and three hours (both rises and drops of heat). It is also important to point out the large importance of the +30 MW events, with frequencies up to 40 (for 2 hours) and 27 (for 3 hours).

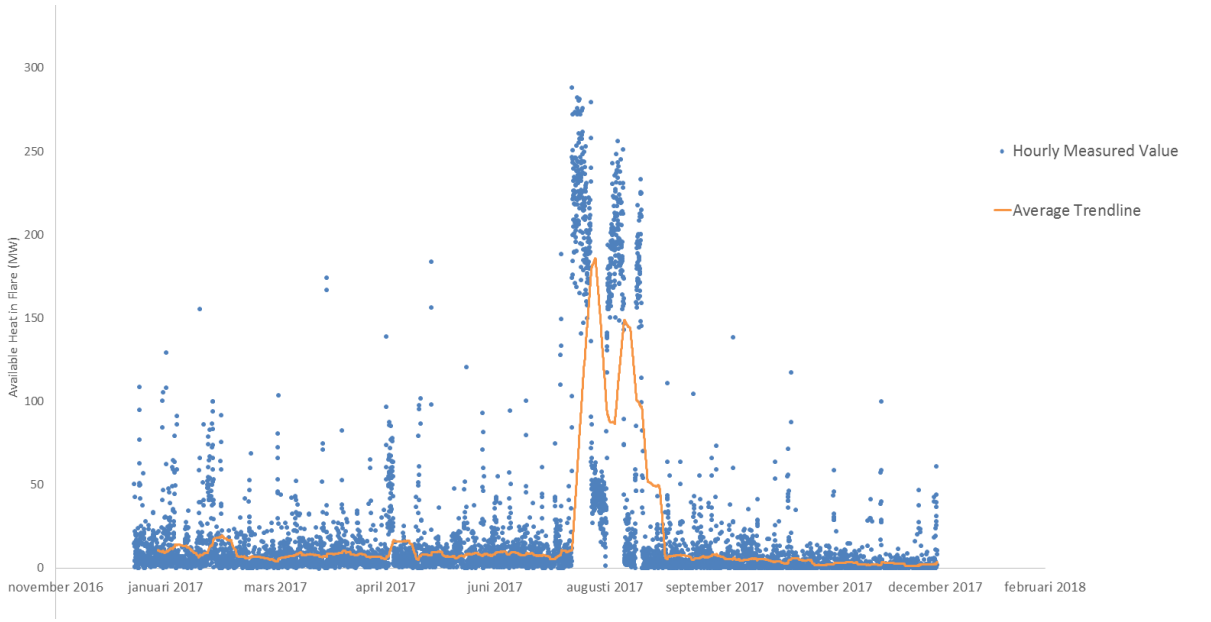

Figure 16. Available heat in the Flare Gas in SSAB Luleå Steel Mill in 2017.Y-axis is in MW while X-axis represents the months. Peak in August represents the shutdown of the power plant Lulekraft due to maintenance.

Table 12. Variations analysis in heat available in the flare gas. Table shows the increase in heat with respect to the average hourly heat, listing the magnitude of the increase as well as the frequency during the first part of the year -before shutdown of Lulekraft and second part of the year, i.e., after shutdown.

First Part of the year							
10-20 MW for	**Freq**	**20-30 MW for**	**Freq**	**30-40 MW for**	**Freq**	**>40 MW for**	**Freq**
2h	53	2h	29	2h	8	2h	24
3h	25	3h	15	3h	4	3h	22
5h	14	5h	8	5h	12	5h	11
8h	7	8h	4	8h	3	8h	3
12h	7	12h	3	12h	3	12h	1
16h	1	16h	1	16h	0	16h	0
30h	0	30h	1	30h	0	30h	0
50h	1	50h	0	50h	0	50h	0
Second Part of the year							
10-20 MW for	**Freq**	**20-30 MW for**	**Freq**	**30-40 MW for**	**Freq**	**>40 MW for**	**Freq**
2h	16	2h	13	2h	15	2h	16
3h	6	3h	13	3h	8	3h	5
5h	6	5h	6	5h	1	5h	3
8h	5	8h	2	8h	3	8h	1
12h	1	12h	0	12h	0	12h	0
16h	0	16h	0	16h	0	16h	0

Table 13. Variations analysis in heat at the flare gas. Table shows the decrease in heat with respect to the average hourly power, listing the magnitude of the decrease as well as the frequency during the first part of the year -before shutdown of Lulekraft and second part of the year – after shutdown.

First Part of the Year	
Less than 5 MW for	**Frequency**
2h	165
3h	179
5h	112
8h	36
12h	10
16h	6
30h	1
50h	0
Second Part of the Year	
Less than 5 MW for	**Frequency**
2h	45
3h	60
5h	57
8h	38
12h	31
16h	28
30h	10
50h	2

Table 14. 10% Drop in Blast Furnace Gas during the first and second part of the year (before and after power plant shutdown). Table shows for how long the event happens and with what frequency.

10% Drop			
First Part of the year		**Second part of the year**	
Decrease for	**Frequency**	**Decrease for**	**Frequency**
2h	5	2h	2
3h	5	3h	1
5h	0	5h	1
8h	0	8h	2
12h	1	12h	0
16h	4	16h	1
30h	0	30h	1
50h	2	50h	1

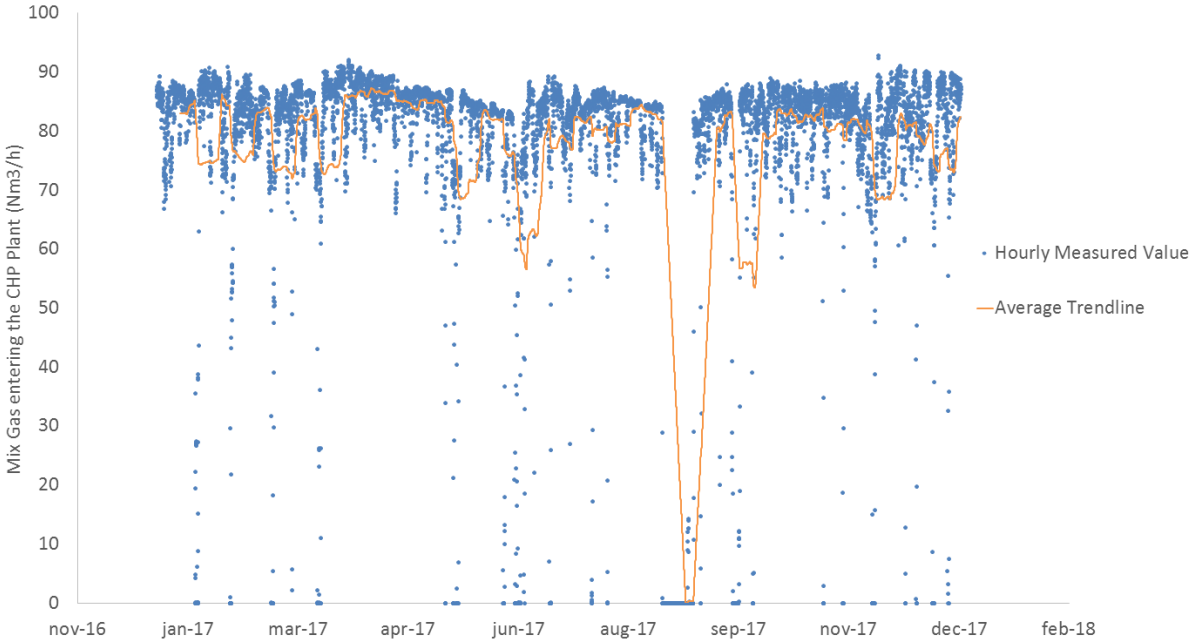

Figure 17. Mixed gas volumetric flow entering the Power Plant in 2017. Y-axis is in Nm³/h while the X-axis represents the months. The drop during August/September represents the outage for maintenance

Table 15. 20% Drop in Blast Furnace Gas during the first and second part of the year (before and after power plant shutdown). Table shows for how long the event happens and with what frequency.

20% Drop			
First Part of the year		**Second part of the year**	
Decrease for	**Frequency**	**Decrease for**	**Frequency**
2h	2	2h	3
3h	2	3h	1
5h	0	5h	1
8h	2	8h	2
12h	1	12h	1
16h	3	16h	1
30h	3	30h	1
50h	0	50h	0

Table 16. Drop to 0 m³/h volumetric flow in Blast Furnace Gas during the first and second part of the year (before and after power plant shutdown). Table shows for how long the event happens and with what frequency.

Drop to 0			
First Part of the year		**Second part of the year**	
Decrease for	**Frequency**	**Decrease for**	**Frequency**
2h	6	2h	1
3h	4	3h	2
5h	3	5h	2
8h	2	8h	1
12h	3	12h	0
16h	2	16h	2
30h	0	30h	0
50h	0	50h	1

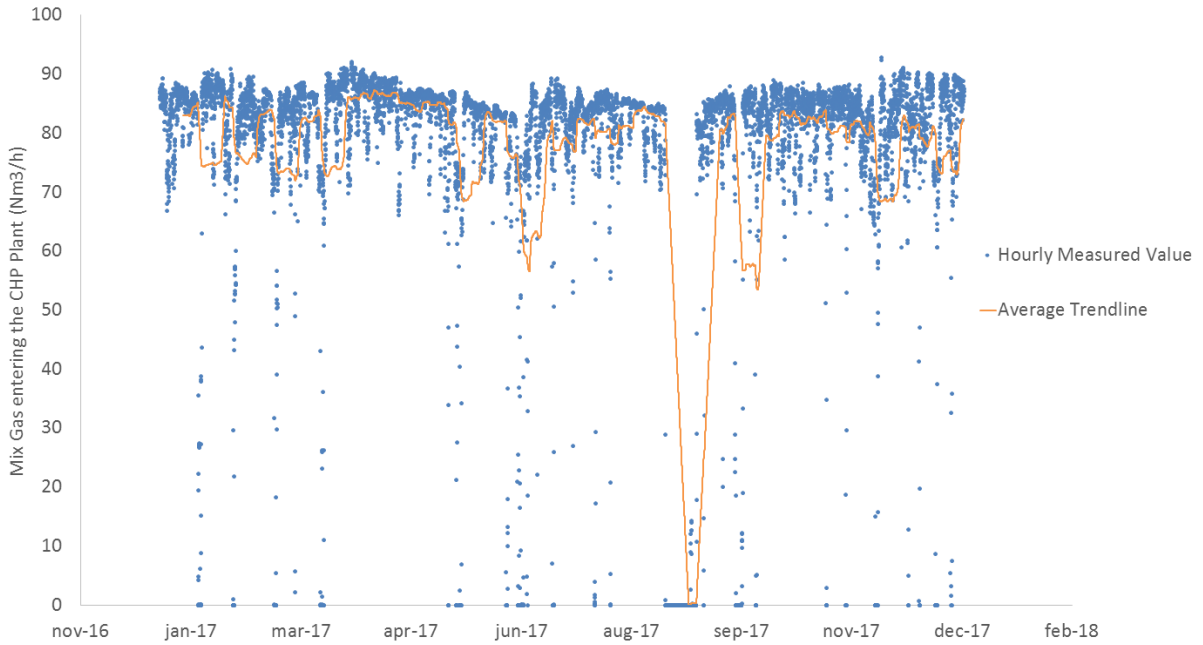

Figure 17. Mixed gas volumetric flow entering the Power Plant in 2017. Y-axis is in Nm3/h while the X-axis represents the months. The drop during August/September represents the outage for maintenance

Table 15 and Table 16 show the results of the analysis. The results show that variations in heat represent the most frequent disturbances, occurring more than 50 times per year (see Table 12 and Table 13). Even though variations in the gas are not very frequent (frequency never exceeds 10 times per period), it can be seen that the most extreme case, the drop to zero flow, is the most common event.

6.2. Off-Design Steady-State Performance Optimization

Figure 18 shows the results of the optimization study performed with the dynamic model in order to find the optimum operation points under off-design conditions, for both the case of 30 MW and the intermedium case of 100 MW. The blue line is the measured capture rate tracked when the steps in solvent flow rate were applied, while the red line is calculated from the final steady-state values reached.

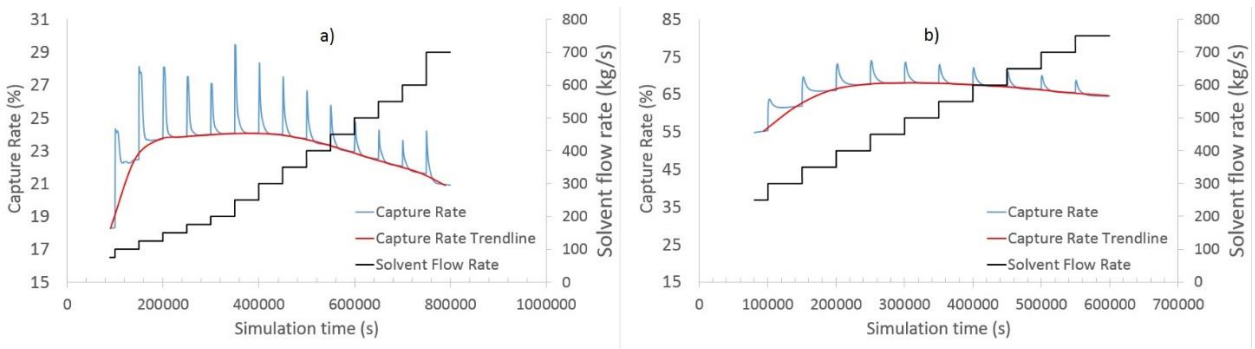

Figure 18. Optimization results for a) case B, i.e., 30 MW in the reboiler and b) case C, i.e. 100 MW. Black line shows the solvent flow rate steps and blue line the measured capture rate. Red line represents the capture rate trendline

It can be seen that the capture rate experiences a flat optimum in both cases, which means that there is a range of solvent flow rates that maximize the capture performance. This is extremely interesting from a dynamic perspective, since a small change in solvent flow rate will have a big impact in the dynamic performance of the plant, as it will be seen in further sections of the chapter. For all the simulations performed in this thesis, the solvent flow rate that maximizes the capture rate was chosen, without taking into account the flat optimum potential in the selection. In relation to this, it is also important to have in mind that lower solvent flow rates lead to maldistribution in the absorber column since the risk of underwetting is higher and the mass transfer efficiency is lowered. Table 17 summarizes the optimum values for both cases, which have been assumed to represent the steady-state conditions of case B and C in absence of disturbances.

Table 17. Steady-State operation points for cases B and C, obtained from the off-design optimization analysis. L_{abs}: Lean Loading (mol/mol), R_{str}: Rich Loading (mol/mol), T_{SB}: Temperature in the Stripper Bottom (°C).

Case	Solvent Flow Rate (kg/s)	Other Parameters
B	250	L_{abs} = 0.414 R_{str} = 0.604 T_{SB} = 110
C	450	L_{abs} = 0.237 R_{str} = 0.554 T_{SB} = 125

6.3. Open Loop Responses to Step Changes

6.3.1. Scenario 1 – Gas flow variations

Table 18 shows the stabilization time of the main process variables under different step changes in blast furnace gas entering the absorber, for the three cases considered. Figure 19 shows the dynamic response of the process variables in case A, while the cases B and C are plotted in figures shown in Appendix D. The graphs showing the responses for the drop to 0 are also shown in Appendix D due to the large magnitude of the steps.

Table 18. Response of the main process variables to different steps decrease in blast furnace gas for the cases studied. Stabilization times (hour) are shown. L_{abs}: Lean Loading, R_{str}: Rich Loading, T_{str}: Temperature in the Stripper Bottom, C_{abs}. Capture Rate in the absorber and P_{CO2}: CO_2 produced in the stripper. In the drop to 0 case, the capture rate is measured as absorbed for numerical reasons (*).

	Variable	10% Drop	20% Drop	Drop to 0
Case A – 155 MW	L_{abs}	2.34	3.38	5.97
	R_{str}	1.47	2.67	3.90
	T_{str}	2.16	2.93	5.49
	C_{abs}	0.58	0.15	0.10*
	P_{CO2}	0.36	2.5	2.01
Case B – 30 MW	L_{abs}	4.63	5.20	9.30
	R_{str}	3.23	3.27	8.40
	T_{str}	3.56	3.59	10.58
	C_{abs}	3.13	4.48	0.13*
	P_{CO2}	3.01	4.23	8.93
Case C – 100 MW	L_{abs}	1.65	2.20	4.24
	R_{str}	1.97	1.54	2.65
	T_{str}	1.67	1.78	8.40
	C_{abs}	1.27	1.13	0.11*
	P_{CO2}	0.85	0.88	2.12

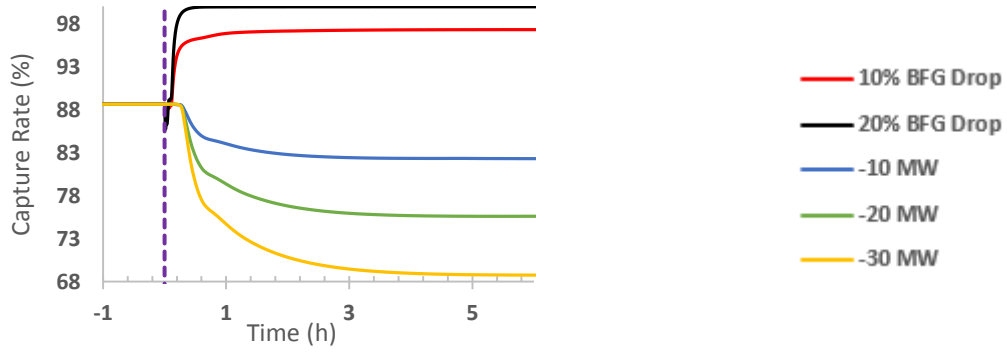

a) Capture Rate

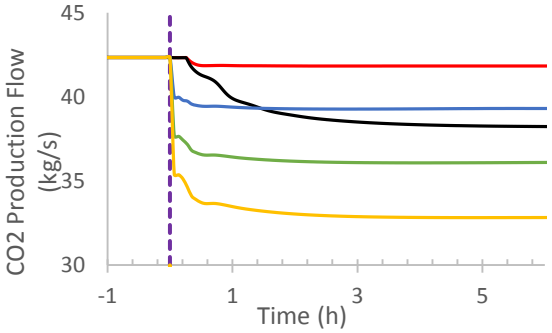

b) CO_2 Production Flow

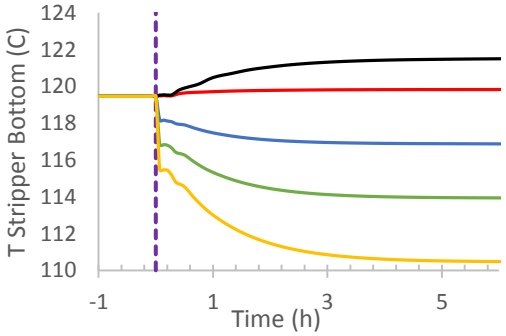

c) Temperature in the Stripper Bottom

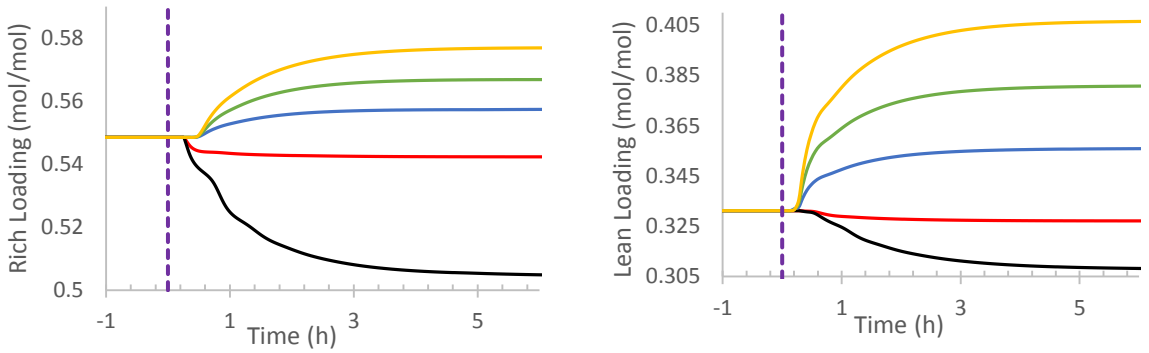

d) Rich Loading e) Lean Loading

Figure 19. Transient responses of the main process variables to different step changes in both gas and reboiler. The initial steady-state corresponds to case A with 155 MW in the reboiler. The steps were introduced in t=0, marked with the vertical purple line.

The capture rate C_{abs} in Table 18 stabilizes relatively fast in case A (less than an hour) for all the steps applied, while the stabilizing time t_s is around one hour for case C. However, when a drop in gas occurs in the low heat case B, where the plant is extremely far from design conditions, it can be seen that the capture rate C_{abs} requires stabilization times up to 3 to 4 hours, which can be explained by the low solvent flow rate circulating (low L/G), which makes the plant slower. The capture rate stabilizes faster for a 20% drop than for 10%, except case B, due to a larger first drop produced when the step is generated (called inverse response), so it takes more time to come back to stable values.

The CO_2 produced P_{CO2} stabilizes faster in the 10% drop than in the 20% for all the cases. It is important to point out that Table 18 shows that its stabilization time is faster than C_{abs}, partially caused by the small relative change. This also shows the different dynamic performance of the absorber and stripper columns. The dead time observed in P_{CO2} is caused by the residence time and to the solvent hold-ups in the different volumes of the cold side of the process, i.e., from absorber outlet to stripper inlet. This difference in dead times can also be seen in the CO_2 loadings, with lean loading L_{abs} showing larger stabilization times than rich loading R_{str}, which is also explained by the location of the buffer tank, placed at the inlet of the absorber.

Regarding the drop to zero, all the stabilization times get largely increased except the CO_2 absorbed (the capture rate makes no sense to be measured in this case), which drops to zero almost instantaneously when the step is introduced. The most interesting aspect that can be observed from the results is the fact that CO_2 keeps being produced for some hours even though there is no gas entering the process. The reason is the large amount of CO_2 stored in the solvent, which has high loadings regardless the case. In case B, not only the lean loading is the highest of the three cases, around 0.41, but also the solvent flow rate is the lowest. Both reasons explain that the plant is producing CO_2 for even a longer time than the other cases, with a t_s of 8.93h. Due to the large stabilization times observed, it is important to have in mind the actual duration of these events. As shown in section 6.1, the most frequent drop-to-zero events occur for 2h and 12h. Figure 20 shows the results of simulating these events in case B, since it represents the slowest and most extreme case.

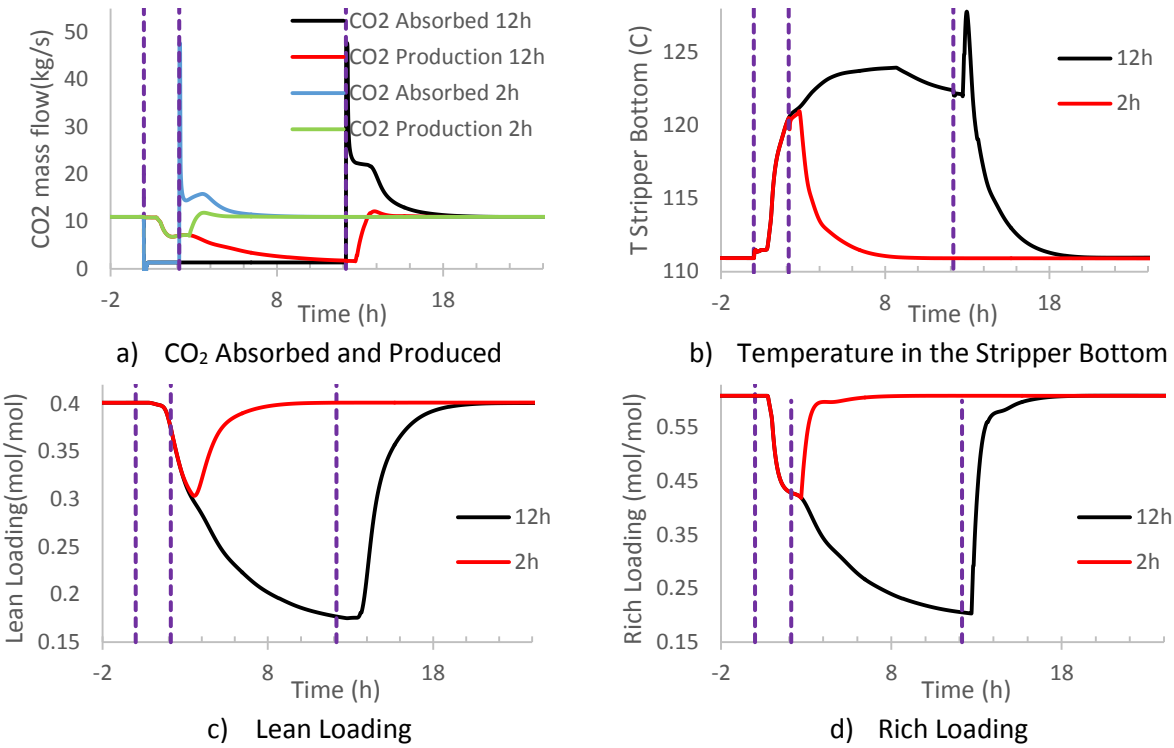

Figure 20. Transient responses of the main process variables under drops to zero in blast furnace gas flow for 2 and 12 hours. The initial steady-state corresponds to case B with 30 MW in the reboiler. The drop was introduced in t=0, marked with vertical purple line.

Figure 20a shows one more time the different response between absorbed and produced CO_2, due to, as explained before, the CO_2 stored in the system. Also, when the gas drops to zero, the absorption drops automatically while the production remains for some time, before experiencing any decrease. When the gas flow returns to normal values, the production reaches steady-state faster than the absorption, which shows the high non-linearity of the process. This feature is also seen in the solvent loading responses, being the response for both the lean (Figure 20c) and rich (Figure 20d) loading slower when the flow goes down than when it increases. Another important aspect is that rich and lean loading tend to reach the same steady-state in absence of gas, since there is no CO_2 to strip or capture.

This extreme situation with absence of gas while the rest of the plant keeps running has been studied by de Koeijer et al. [53] in the CO_2 Technology Center Mongstad as an equipment failure case. Results show similar trends for the main process variables, where the CO_2 production flow remained above zero for several hours, presenting faster ramp-up than down. There are some constraints that need to be taken into account when dealing with these circumstances. Due to the extreme characteristics of the disturbance, this situation can also be seen as a short-term shutdown followed by a hot start-up, so the same constraints can be applied. The general criteria for start-up is defined in [54], being the main factors the temperature in the reboiler, which must remain under 125°C in order to prevent degradation issues, and the solvent flow rate has to remain within certain values.

Leaving the reboiler and solvent recirculation untouched is not the only strategy to face the absence of gas. A shutdown of the heat and complete shutdown of the plant is also an option, which would save heat and plant operational costs. However, in the case studied the heat utilized is an excess from the steel mill and the power plant. Therefore, keeping the stripper working while producing CO_2 stored in the solvent will always be a better option than a total shutdown, not only from a production

perspective but also in order to keep the plant hot, taking into account the process constraints defined above.

An important discussion that arises when the gas flow drops to zero is the fact that it might lead the compressor beyond its surge limit, something that should be in all cases avoided, since anti-surge mode of compressors decreases highly the compressor efficiency, as it was discussed by Walters et al. [55]. Since there are also large variations of produced CO_2 flow rate during summer and winter operation, a solution could be that a parallel train of compressors is used instead of only one, so they can be turned off and down according to the capture unit requirements.

6.3.2. Scenario 2 – Reboiler duty variations

Table 19 shows the stabilization time of the main process variables under different step changes in heat available in the reboiler, for the three cases considered. Figure 19 shows the dynamic response of the process variables in case A, while the cases B and C are plotted in figures shown in Appendix D.

Table 19. Response of the main process variables to different steps increasing and decreasing heat in the reboiler for the cases studied. Stabilization times (hour) are shown

	Variable	-10 MW	-20 MW	-30 MW	+10 MW	+20 MW	+30 MW
Case A – 155 MW	L_{abs}	1.83	1.97	2.11	-	-	-
	R_{str}	2.03	2.15	2.45	-	-	-
	T_{str}	1.74	1.89	2.08	-	-	-
	C_{abs}	1.78	1.89	2.05	-	-	-
	P_{CO2}	0.25	0.28	0.3	-	-	-
Case B – 30 MW	L_{abs}	-	-	-	3.44	3.13	2.83
	R_{str}	-	-	-	6.08	4.94	4.91
	T_{str}	-	-	-	1.54	0.93	0.72
	C_{abs}	-	-	-	3.60	3.60	3.12
	P_{CO2}	-	-	-	0.93	0.81	1.16
Case C – 100 MW	L_{abs}	2.14	2.25	2.29	1.69	1.31	1.10
	R_{str}	2.43	2.43	2.54	2.15	1.92	1.76
	T_{str}	1.44	1.61	1.75	1.03	0.42	0.09
	C_{abs}	2.21	2.38	2.46	2.00	1.72	1.31
	P_{CO2}	1.22	0.01	0.01	0.01	1.35	1.37

Case C is the most representative case in order to compare the effect of increasing and decreasing the heat load in the reboiler since Case A and B represent cases with maximum and minimum heat constraint, respectively. The capture rate C_{abs} raises when the heat is increased, due to a decrease in the lean loading L_{abs}, and the opposite occurs when the heat is decreased. It can also be seen that the response is faster when the heat is increased than decreased, which shows one more time the non-linear behavior of the process, and it is observed in many other thermal processes. When the heat is decreased, the response is faster for lower step changes, presenting opposite response when the heat load increases: the plant responses faster for larger changes.

In all the cases simulated, the stabilization time of L_{abs} is lower than R_{str}, due to the recycle loop, resident times and hold-up, since the reboiler changes affect first the lean leaving the stripper. Similar behavior can be observed for the CO_2 production P_{CO2}, whose response is a lot faster compared to C_{abs}, since this stream is physically closer to the reboiler. For most of the variables the stabilization time is slower when the plant is operated at lower heat loads, due to lower circulating flow rate and higher residence times. The only variable independent of the case is the temperature in the stripper bottom.

Finally, it is important to add that the same behavior observed in Table 19 for Case C can be seen in case A and B: for drops in heat, the plant is faster when the disturbance is small (case A) while for a raise in heat the plant reaches steady-state faster for large disturbances (case B).

6.4. CONTROL STRATEGY PROPOSAL

This section covers the definition a control strategy and the results from testing two different algorithms via dynamic simulations. The performance of the plant is compared to the no-controlled results and a discussion about the implications and limitations of the control is added.

The definition of a control strategy starts by defining a control objective. In the case study that this thesis focus at, the CO_2 produced in the stripper is the variable that needs to be maximized, since both the flue gas flow rate and the reboiler duty are given as disturbances to the capture plant, fixed upstream in the steel mill or power plant processes. The supervisory control layer defined in section 4.6 has therefore one degree of freedom: the set point of solvent flow rate. Several studies in literature [56] suggest that keeping the temperature in the bottom of the stripper constant maximizes the plant performance. This means that modifying the solvent flow rate and keeping the temperature constant when disturbances occur can bring the production of CO_2 to a closer point to the optimum than it would be without any control.

This analysis proposes two different control algorithms to implement and compare: feedback (FB) control and feedforward (FF) control. In reality the second algorithm is a modification of the first one (both are the same strategy), since both work by changing the same manipulated variable (MV), the solvent flow rate, in order to control the same variable (CV), the stripper bottom temperature. Likewise the regulatory control, all the controllers have been tuned with the SIMC tuning rules [40]. The FF control is implemented with a ramp of 90s, moving the MV from the initial steady-state value to the expected steady-state after the disturbance.

In order to define a set point for the controller, i.e. a fixed temperature that maximizes the CO_2 production P_{CO2} under the disturbances included in the analysis, a parametric study is performed. The effect of the stripper bottom temperature on P_{CO2} for each of the disturbances is analyzed, setting a ceiling value of 125°C to prevent solvent degradation issues. Table 20 shows the selected temperature for cases with 30 and 110 MW respectively.

Table 20. Optimum stripper bottom temperature to keep constant under disturbances for the winter and summer cases

Case	Optimum Temperature
30 MW in the reboiler	122°C
110 MW in the reboiler	125°C

Figure 21 shows the simulated time trajectories with the two control algorithms in a case with 110 MW (set point of 125°C) heat under three different disturbances: a) a drop in heat of 30 MW, b) an increase of heat of 30 MW and c) a drop to 0 Nm^3/s in gas entering the absorber. Figure 21 also shows the response of P_{CO2} for the drop to zero case.

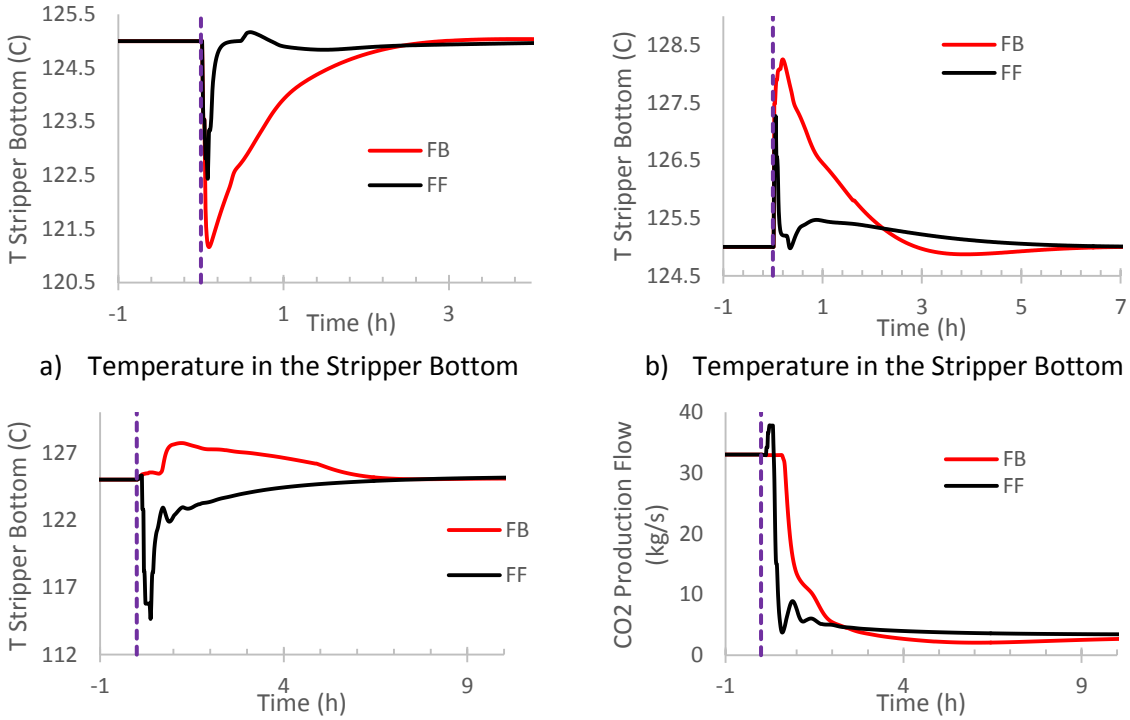

Figure 21. Transient response of the controlled variable (Stripper bottom temperature) with Feedback (FB) and Feedforward (FF) control, for step changes of a) -30 MW, b)+30 MW and c) drop to cero in gas. d) Response of the produced CO_2 when gas drops

It can be seen that for the three disturbances analyzed feedforward (FF) control is faster than feedback (FB), since the variable "knows" the steady-state it has to reach beforehand. This faster response of FF compared to FB relies on the disturbances being easy to measure and discretize. However, in a real plant there are many other disturbances affecting the control variable, and therefore feedback control is also needed in order to correct the error. Figure 21d shows that in the case of drop to zero in blast furnace gas flow, it might be convenient to choose the slowest control strategy in order to maximize P_{CO2} in the step down, since the step up will always be faster. Another interesting aspect to consider is that when more heat is available, generating a disturbance in the reboiler duty, the temperature in the stripper bottom exceeds the constraint of 125°C. In the case of FF control it happens only for a few minutes, while in case of feedback it stays above the limit for some hours. Depending on how flexible the constraint is, this should be taken into account when deciding the temperature set point, since it might be needed to be decreased from the optimum point in order to avoid these peaks over the limit, which is known as back-off control.

Figure 22 shows the comparison with a non-controlled simulation, showing the differences in steady-state values of P_{abs} after the disturbance. For the comparison, feedback control was chosen, since in terms of steady-state values it does not matter which strategy is simulated (both FB and FF reach the same final value). It can be seen that for both disturbances of +30 MW and -30 MW the plant reaches higher P_{abs}, which proves the effective performance of the control strategies.

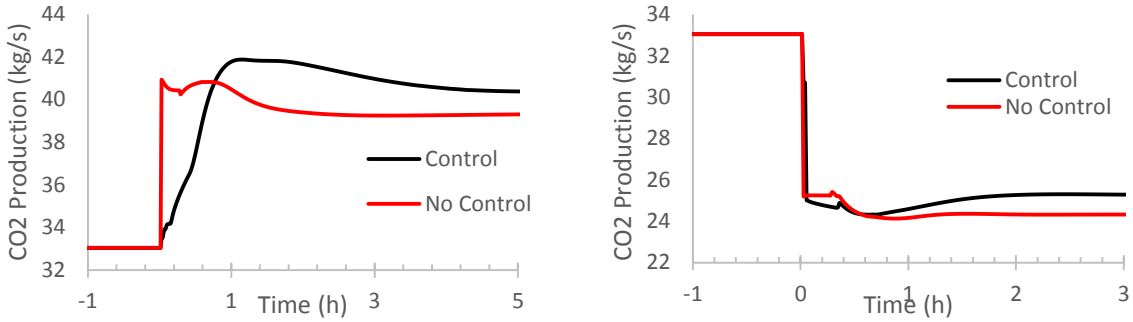

a) CO_2 Production Flow b) CO_2 Production Flow

Figure 22. Comparison between the CO_2 production in the non-controlled case and with feedback control, for a) +30MW step and b) -30 MW step.

6.5. Comparing Steady-State and Dynamic Simulations

This section focuses on the comparison between the performance of the capture plant under the assumption of running steady-state and considering disturbances and dynamics. Simulations of longer periods of time have been run, and potential values of actual CO_2 produced are calculated and compared.

With the aim of comparing the steady-state assumption with the dynamic-state performance as accurate as possible, the produced CO_2 over longer periods of time has been calculated. In order to capture the performance during the two most extreme cases over the year, simulations have been run for 2 weeks in summer and 2 weeks in winter. By using the data analysis shown in section 6.1, the average available heat for the 2 periods considered is calculated, being 110 MW for the summer weeks and 23 MW for the winter weeks. As it is explained in section 4.2.2, it is assumed in this study that the capture plant as a minimum value of heat of 30 MW. Therefore, the average values for the two week periods considered are 110 MW and 30 MW respectively. As it is explained below, disturbances have been considered in some of the cases included in the comparison, based in results shown in section 6.1.

Four cases have been included in the comparison, which are defined below, following a similar approach than the one used by Montañés et al. [38]:

- Steady-state plant: The CO_2 produced in both the summer and winter period is calculated from the steady-state Aspen model, considering the average heat value over the entire period and neglecting the disturbances in both heat and gas (even though the heat average is calculated from hourly data so it includes the disturbances in the calculated value).
- Ideal static plant: Disturbances are included in the calculation, but this case considers the plant to have instantaneous response to these disturbances, being capable to reach the new steady-state values as soon as they occur. This case is useful in order to analyze the effect the inertia of the process has over its performance. The CO_2 produced value has been calculated from steady-state final values in Dymola, accounting for all the disturbances and their duration.
- Dynamic plant: In this case not only disturbances are included, but also the real performance of the plant in open-loop, i.e., no control strategy implemented. The dynamic model developed in Chapter 5 has been used. The calculated value of produced CO_2 is computed by integrating the P_{CO2} trajectory, from the initial time t_0 to the final time t_f as shown in Equation 13.

$$CO2_{Produced} = \int_{t_0}^{t_f} P_{CO2}(t)dt \qquad (13)$$

- Dynamic controlled plant: The feedback control strategy discussed in section 6.4 has been implemented on top of the dynamic plant, utilizing again the dynamic model to obtain results. The accumulated CO_2 produced has been calculated like in the dynamic plant, by using Equation 13.

Figure 23 shows the plotted trajectory of P_{CO2} over the entire two-week periods simulated for the first and third cases, while the rest of cases, as well as the disturbances trajectories. It can be observed in Figure 23 that the capture plant frequently deviates from the steady-state value, which confirms the importance of taking disturbances of the steel mill and the adjacent power plant into consideration and not to neglect them. Several large drops in produced CO_2 are observed in both periods, caused by drops to zero in blast furnace gas flow. The rest of smaller variations are caused by disturbances in the reboiler available heat, produced upstream in both the flare and the excess heat from the steam cycle. It can also be observed that there are less variations in winter, due to the fact that it has been assumed a minimum heat level of 30 MW, so only increase of heat over that value have been considered.

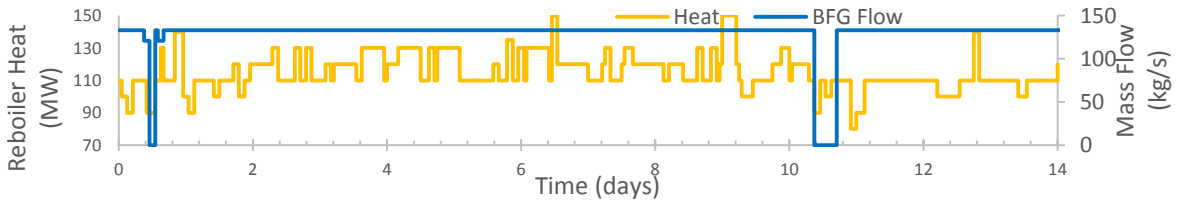

a) Heat and Gas variations over two weeks in summer

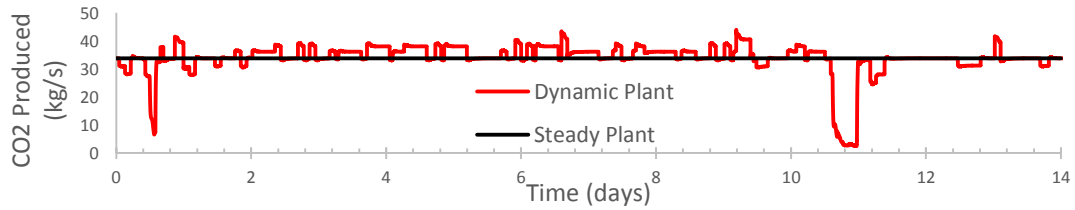

b) CO_2 produced summer case

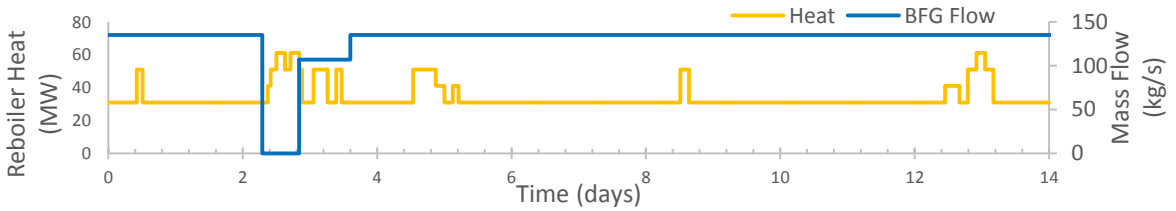

c) Heat and Gas variations over two weeks in winter

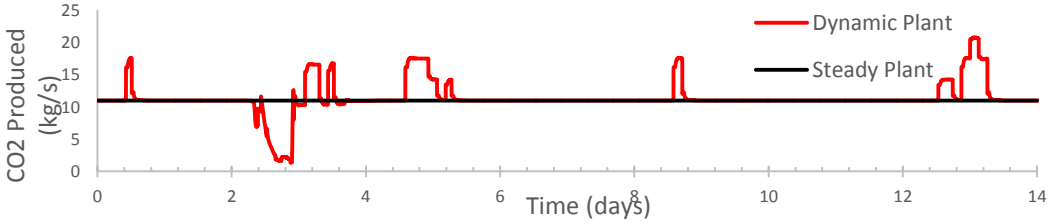

d) CO_2 produced winter case

Figure 23. Transient Response of the CO_2 production during two weeks simulations in b) summer and d) winter. Black line represents the capture under the assumption of a steady-state plant. Figures a) and c) show the transient events registered and simulated during the two periods considered.

Table 21. Calculated CO_2 production over summer and period under different cases. Results in thousands of ton

Period/Case	Steady-State [kton]	Ideal Static [kton]	Dynamic [kton]	Dynamic Controlled [kton]
Summer	40.86	41.13	41.85	42.35
Winter	13.30	14.00	13.63	13.94

Table 21 shows the results (in thousands of tons) from the CO_2 produced calculation for all the cases included in the comparison. Therein, it can be seen in Table 21 that, in line with the results discussed in section 6.4, the controlled case captures more than the non-controlled, for both summer and winter, which confirms the effectiveness of adding a control strategy. In the summer weeks, the steady-state assumption gives the worst results of CO_2 produced, which means that it is worth to let the plant go up and down whenever the disturbances appear. The reason behind this is that when a disturbance makes the production increase, the plant reaches the new steady-state faster than when decreasing (see section 6.3) the production. On top of this, when a step down occurs, the CO_2 production keeps producing more than expected due to the stored CO_2 in the solvent (see again 6.3). This is why Table 21 shows a larger value for the dynamic plant than for the ideal static in summer. However, in the winter period, since only increases in heat have been considered, the ideal static plant represents the maximum value, reaching the new production value faster than any other case.

Another interesting aspect that arises from these results is that the plant performs much better the closer it is to the design point, which is another reason for the higher value of CO_2 produced in the dynamic case compared to the steady-state and ideal static cases. Allowing the plant to reach values up to 155 MW of reboiler heat for some periods of time, increases largely the performance of the plant compared to keeping it performing in 110 MW, which is 35 MW below the design point. This brings up the discussion of how the design point should be chosen when sizing the plant. In this case it was decided to size it for the maximum amount of heat available, but it might be desired to low that value towards a point closer to the average, even though some of the heat would have to be non-used during some peaking periods.

6.5.1. Effect of Solvent Inventory

The solvent inventory in the system is an arbitrary decision. How much liquid is stored in the buffer tank is chosen based on pilot plant experience and seasonal variations, but it is not trivial to find an optimum. In this work, the size of the lean solvent buffer tank and therefore the amount of liquid in the system was designed to be the higher volume in the plant, based on pilot plant data [57]. However, this value is crucial in the dynamic results, since the residence time in the buffer tank is directly dependent on the amount of liquid. Therefore, an extra simulation was carried out in order to check the influence of the solvent inventory. The two summer week's period simulated in section 6.5 was simulated again with control implemented and having the amount of solvent within the tank increased. Table 22 shows the results of the simulation, where the volume of the tank can also be seen.

Table 22. CO_2 produced over two weeks in summer with control for the original process and the modified process. Table also shows the tank volume in m^3 for each case

Process	Tank Volume [m^3]	CO_2 produced [kton]
Original Process	502.7	42.35
Modified Process	1005.3	41.33

Table 22 shows that the CO_2 produced over the two weeks is decreased with increased solvent inventory, which is caused by the fact that the process reacts slower when disturbances occur. Due to the aspects discussed in section 6.3, the CO_2 capture performance gets increased when the plant is closer to the design point. Therefore, from a capture point of view, it is beneficial that the plant reaches the new steady-state as soon as possible when the heat is increased. However, it is important to mention that the modified process represents an interesting option in order to smooth the CO_2 production flow. If the variations in flow are an issue for the downstream compression, it might be interesting to reconsider the solvent inventory as a way to minimize them.

7. CONCLUSIONS

This thesis presents a study of the dynamic behavior of a post-combustion CO_2 capture plant integrated in a steel mill. The model developed in this thesis gives a deep understanding of the transient behavior of the process, while the verification of the dynamic model with the steady-state model shows that it has a good capability of predicting the steady-state performance of the capture plant.

The mapping of the operation of the reference steel mill carried out in this work shows a large number of transient events on daily basis. Some of the most important variables for the capture plant, such as the available heat and the flow of gas to be treated, may have considerable transients on an hourly scale. The analysis highlights the potential in designing the process and the control to consider these fluctuations. For the decentralized control structure, a closed-loop controller of solvent flow rate to set the temperature in the stripper improves the performance (stabilization time and capture efficiency at steady state) of the plant in all the cases considered.

The optimization performed for the intermedium and low reboiler duty cases shows that a flat optimum is found. For a given plant design operated at different times of the year, several L/G values give a capture rate close to the optimum value for maximized CO_2 production. This has a beneficial impact when designing the capture plant, since other aspects such as dynamic performance can be considered while maintaining an optimum capture rate.

The highlighted results of the dynamic simulations are listed below:

- The capture unit can handle the disturbances generated by the steel mill and CHP plant.
- The open-loop analysis shows the large differences in stabilization time depending on which time of the year is considered, i.e., depending on the solvent flow rate. Changes in desired solvent flow rate is a result of trying to maximize CO_2 produced when less heat is available. Generally, the plant responds more slowly at lower operating loads (winter), caused by the increase in residence time.
- The open-loop analysis also shows that the plant responds faster when the reboiler duty is increased than when it is decreased. Furthermore, the analysis shows that the CO_2 absorbed and the CO_2 produced present different responses, being faster the latest one when it comes to reboiler duty variations, but generally faster the first one when the disturbances occur in the gas flow.
- The increase in CO_2 production when taking into account disturbances in the operation, compared to the steady operation with the average heat.

The evaluation of the decentralized control structure shows that adding a closed-loop controller in the only degree of freedom existing in this plant –solvent flow rate- can control the temperature in the stripper, improving the CO_2 produced in all the cases considered. With the control loop implemented, the plant shows faster stabilization times and higher capture efficiencies in all the steady-states reached.

Finally, this work also shows the crucial role of the solvent inventory in the system. Since this is partially an arbitrary decision, it must be done carefully, taking into account that the larger the amount of liquid is, the slower the plant will handle disturbances and therefore the lower the CO_2 production will be. On the other hand, a slower plant could smooth out the CO_2 production flow entering the compressor, which could have a beneficial effect overall.

7.1. FUTURE WORK

The development of this thesis has led to new questions to answer. There are several aspects that can be further investigated, which would improve the understanding of the dynamic behavior of post-combustion CO_2 capture plants. The main concepts to be covered by future works are listed below:

- A more detailed variations study is needed in order to improve the understanding of the transient events occurring in the steel mill. More accurate data would be needed, so the disturbances could be analyzed from a minute's perspective rather than hours. By doing this, the assumption of step changes would be verified or discarded, and more realistic disturbances could be simulated.
- The design point chosen to size the capture plant is something that has a crucial impact on the results shown in this thesis. It would be interesting to perform a sensitivity analysis on the sizing and investigate the effect of the change, so an optimum point could be found.
- The variations in reboiler heat duty and gas flow will have an impact on gas concentration and flow leaving the absorber. Since this gas is burnt downstream in the CHP plant, it would be necessary to analyze how this variations affect the combustion.
- To be able to fully compare the steady-state assumption with the real case, periods longer than two weeks should be simulated, and extent the study to every month of the year, not only the two extreme cases.
- It could be seen in this thesis that the set point of the controller changes depending on the conditions (not the same in summer than in winter). Therefore, a real-time optimization of this set point would play a beneficial role when controlling the plant. This could be analyzed in optimization studies and predictive control simulations.

8. REFERENCES

[1] D. Q. Stocker, T.F., *IPCC 2013: CLIMATE CHANGE 2013 - The Physical Science Basis, Contribution of Working Group I to the Fifth Assessment Report of the Intergovernmental Panel on Climate Change*. Cambirdge University Press, 2013.

[2] IEA, *Prospects for CO_2 Capture and Storage*, vol. 1995, no. August 2005. OECD Publishing, 2004.

[3] WorldSteel, "Steel Statistical Yearbook 2010," Beijing, 2010.

[4] R. Remus, S. Roudier, M. a. Aguado Monsonet, and L. D. Sancho, *Best Available Techniques (BAT) Reference Document for Iron and Steel Production*, vol. BREF-IS. Luxembourg, 2013.

[5] ULCOS, "Ulcos," 2018. [Online]. Available: http://ulcos.org/en/index.php. [Accessed: 01-Feb-2018].

[6] "Global CCS." [Online]. Available: https://www.globalccsinstitute.com/projects/large-scale-ccs-projects. [Accessed: 25-May-2018].

[7] E. Tsupari, J. Kärki, A. Arasto, and E. Pisilä, "Post-combustion capture of CO_2 at an integrated steel mill - Part II: Economic feasibility," *Int. J. Greenh. Gas Control*, vol. 16, pp. 278–286, 2013.

[8] R. Montañés and L. O. Nord, "Dynamic Simulations of the Post-combustion CO_2 Capture System of a Combined Cycle Power Plant," in *12th International Modelica Conference*, 2017, pp. 111–119.

[9] S. Ó. Gardarsdóttir, F. Normann, K. Andersson, K. Prölss, S. Emilsdóttir, and F. Johnsson, "Post-combustion CO_2 capture applied to a state-of-the-art coal-fired power plant-The influence of dynamic process conditions," *Int. J. Greenh. Gas Control*, vol. 33, pp. 51–62, 2015.

[10] R. M. Montañés, M. Korpås, L. O. Nord, and S. Jaehnert, "Identifying operational requirements for flexible CCS power plant in future energy systems," *Energy Procedia*, vol. 86, pp. 22–31, 2016.

[11] H. Hummel and R. Canapa, "Steel Roadmap EU 2050," 2013.

[12] EUROFER, "EUROFER," 2018. [Online]. Available: http://eurofer.org/. [Accessed: 01-Apr-2018].

[13] J. Allwood, "Sustainable materials – with both eyes open," 2012.

[14] "Lulea - SSAB." [Online]. Available: https://www.ssab.se/ssab/om-ssab/production-sites-in-sweden/lulea. [Accessed: 20-Aug-2003].

[15] R. Skagestad *et al.*, "CO2stCap - Cutting Cost of CO_2 Capture in Process Industry," *Energy Procedia*, vol. 114, pp. 6303–6315, 2017.

[16] Lulekraft, "Lulekraft." [Online]. Available: http://lulekraft.se/. [Accessed: 05-Mar-2018].

[17] SSAB, "Ssab Annual Report 2016 Toward Industry-Leading Profitability Contents," 2016.

[18] M. Biermann, "Webinar: Cutting Cost of CO_2 Capture in Process Industry (CO2stCap) Project overview & first results for partial CO_2 capture at integrated steelworks," 2017. [Online]. Available: http://www.globalccsinstitute.com/insights/authors/WebinarOrganiser/2017/11/24/webinar-

cutting-cost-co2-capture-process-industry-co2stcap-project-overview-first-results-partial-co2-capture-integrated-steelworks?author=MTc1OTM%3D. [Accessed: 07-Apr-2018].

[19] "Nord Pool," *Spot day-ahead electricity market*. [Online]. Available: http://www.nordpoolspot.com/Market-data1/Elspot/Area-Prices/DK/Hourly/?view=table. [Accessed: 04-Mar-2018].

[20] M. Wang, A. Lawal, P. Stephenson, J. Sidders, and C. Ramshaw, "Post-combustion CO_2 capture with chemical absorption: a state-of-the-art review," *Chem. Eng. Res. Des.*, vol. 89, no. 9, pp. 1609–1624, 2011.

[21] G. Pellegrini, R. Strube, and G. Manfrida, "Comparative study of chemical absorbents in postcombustion CO_2 capture," *Energy*, vol. 35, no. 2, pp. 851–857, 2010.

[22] Y. Yang and R. Zhai, "MEA-based CO2 Capture Technology and its Application in Power Plants," *Paths to Sustain. Energy*, vol. 6, no. 24, pp. 499–510, 2010.

[23] IEA Greenhouse Gas R&D Programme (IEAGHG), "Partial Capture of CO_2," 2009.

[24] R. K. Ross Taylor, "Multicomponen mass transfer." New York, 1993.

[25] E. Y. Kenig, R. Schneider, and A. Górak, "Reactive absorption: Optimal process design via optimal modelling," *Chem. Eng. Sci.*, vol. 56, no. 2, pp. 343–350, 2001.

[26] Modelon AB, "CAPTURE WITH AMINE SOLUTIONS," 2018. [Online]. Available: http://www.modelon.com/fileadmin/user_upload/Industries/Energy_Process/CCS/PostCombustionCapture_flyer.pdf.

[27] Modelon AB, "Modelon Home," 2018. [Online]. Available: http://www.modelon.com/. [Accessed: 05-Mar-2018].

[28] "SSAB," 2018. [Online]. Available: https://www.ssab.com/company/about-ssab. [Accessed: 04-Apr-2018].

[29] M. Thern, K. Jordal, and M. Genrup, "Temporary CO_2 capture shut down: Implications on low pressure steam turbine design and efficiency," *Energy Procedia*, vol. 51, pp. 14–23, 2013.

[30] M. Lucquiaud, H. Chalmers, and J. Gibbins, "Capture-ready supercritical coal-fired power plants and flexible post-combustion CO_2 capture," *Energy Procedia*, vol. 1, no. 1, pp. 1411–1418, 2009.

[31] S. Linnenberg, U. Liebenthal, J. Oexmann, and A. Kather, "Derivation of power loss factors to evaluate the impact of post-combustion CO_2 capture processes on steam power plant performance," *Energy Procedia*, vol. 4, pp. 1385–1394, 2011.

[32] R. M. Montañés, S. GarÐarsdóttir, F. Normann, F. Johnsson, and L. O. Nord, "Demonstrating load-change transient performance of a commercial-scale natural gas combined cycle power plant with post-combustion CO_2 capture," *Int. J. Greenh. Gas Control*, vol. 63, no. May, pp. 158–174, 2017.

[33] Mathworks, "AspenTech Asset Optimization Software - Asset Performance Management, Process Engineering for Chemicals, Energy and Engineering & Construction." [Online]. Available: https://www.aspentech.com/. [Accessed: 08-Mar-2018].

[34] Z. Amrollahi, I. S. Ertesvåg, and O. Bolland, "Optimized process configurations of post-combustion CO_2 capture for natural-gas-fired power plant — Exergy analysis," *Int. J. Greenh. Gas Control*, vol. 5, pp. 1393–1405, 2011.

[35] K. Prölß, H. Tummescheit, S. Velut, and J. Åkesson, "Dynamic model of a post-combustion

absorption unit for use in a non-linear model predictive control scheme," *Energy Procedia*, vol. 4, no. 2010, pp. 2620–2627, 2011.

[36] E. Gjernes *et al.*, "Results from 30 wt% MEA Performance Testing at the CO_2 Technology Centre Mongstad," *Energy Procedia*, vol. 114, pp. 1146–1157, 2017.

[37] The Mathworks Inc., "MATLAB - MathWorks," *Www.Mathworks.Com/Products/Matlab*, 2016. [Online]. Available: http://www.mathworks.com/products/matlab/. [Accessed: 20-Mar-2018].

[38] R. Montañés, N. Flø, and L. Nord, "Dynamic Process Model Validation and Control of the Amine Plant at CO_2 Technology Centre Mongstad," *Energies*, vol. 10, no. 10, p. 1527, 2017.

[39] E. M. B. Aske and S. Skogestad, "Consistent inventory control," *Ind. Eng. Chem. Res.*, vol. 48, no. 24, pp. 10892–10902, 2009.

[40] S. Skogestad and C. Grimholt, "The SIMC method for smooth PID controller tuning," *Adv. Ind. Control*, no. 9781447124245, pp. 147–175, 2012.

[41] Modelica Association, "Modelica and the Modelica Association — Modelica Association," 1996. [Online]. Available: https://modelica.org/. [Accessed: 27-Jan-2018].

[42] R. M. Montañés, N. E. Flø, R. Dutta, L. O. Nord, and O. Bolland, "Dynamic Process Model Development and Validation with Transient Plant Data Collected from an MEA Test Campaign at the CO_2 Technology Center Mongstad," *Energy Procedia*, vol. 114, pp. 1538–1550, 2017.

[43] J. Åkesson *et al.*, "Models of a post-combustion absorption unit for simulation , optimiza- tion and non-linear model predictive control schemes," in *8th Modelica Conference*, 2011, pp. 64–74.

[44] H. Dang and G. T. Rochelle, "CO_2 Absorption Rate and Solubility in Monoethanolamine/Piperazine/Water," *Sep. Sci. Technol.*, vol. 38, no. 2, pp. 337–357, 2003.

[45] W. Böttinger, "NMR-spektroskopische Untersuchung der Reaktivabsorption von Kohlendioxid in wässrigen Aminlösungen," University of Stuttgart, Stuttgart, Germany, 2005.

[46] K. Onda, H. Takeuchi, and Y. Okumoto, "Mass transfer coefficients between gas and liquid phases in packed columns," *J. Chem. Eng. Japan*, vol. 1, no. 1, pp. 56–62, 1968.

[47] G. F. Versteeg and W. P. M. van Swaaij, "On the kinetics between CO_2 and alkanolamines both in aqueous and non-aqueous solutions-II. Tertiary amines," *Chem. Eng. Sci.*, vol. 43, no. 3, pp. 587–591, 1988.

[48] J. van Holst, G. F. Versteeg, D. W. F. Brilman, and J. A. Hogendoorn, "Kinetic study of CO_2 with various amino acid salts in aqueous solution," *Chem. Eng. Sci.*, vol. 64, no. 1, pp. 59–68, 2009.

[49] R. Stockfleth and G. Brunner, "Holdup, pressure drop, and flooding in packed countercurrent columns for the gas extraction," *Ind. Eng. Chem. Res.*, vol. 40, no. 1, pp. 347–356, 2001.

[50] R. M. Montañés, N. E. Flø, and L. O. Nord, "Experimental results of transient testing at the amine plant at Technology Centre Mongstad: Open-loop responses and performance of decentralized control structures for load changes," *Int. J. Greenh. Gas Control*, vol. 73, no. January, pp. 42–59, 2018.

[51] M. Dreillard, P. Broutin, P. Briot, T. Huard, and A. Lettat, "Application of the DMXTM CO_2 Capture Process in Steel Industry," *Energy Procedia*, vol. 114, no. November 2016, pp. 2573–2589, 2017.

[52] B. Omell, A. S. Chinen, J. C. Morgan, D. Bhattacharyya, C. David, and N. Energy, "Rigorous Model Development of a MEA-based CO_2 Capture System and Validation with Pilot Plant Data

Across Multiple Scales," in *TCCS-9*, 2017.

[53] G. M. De Koeijer, K. I. Aasen, and E. Steinseth Hamborg, "Scale-up and Transient Operation of CO_2 Capture Plants at CO_2 Technology Centre Mongstad," in *Abu Dhabi International Petroleum Exhibition and Conference*, 2014.

[54] T. Marx-Schubach and G. Schmitz, "Optimizing the start-up process of post-combustion capture plants by varying the solvent flow rate," in *12th International Modelica Conference*, 2017, pp. 121–130.

[55] M. S. Walters, T. F. Edgar, and G. T. Rochelle, "Regulatory Control of Amine Scrubbing for CO_2 Capture from Power Plants," *Ind. Eng. Chem. Res.*, vol. 55, no. 16, pp. 4646–4657, 2016.

[56] M. Panahi and S. Skogestad, "Economically efficient operation of CO_2 capturing process part I: Self-optimizing procedure for selecting the best controlled variables," *Chem. Eng. Process. Process Intensif.*, vol. 50, no. 3, pp. 247–253, 2011.

[57] N. E. Flø, *Nina Enaasen Flø Post-combustion absorption-based CO_2 capture : modeling , validation and analysis of process dynamics*. PhD Doctoral Thesis, 2015.

A. APPENDIX A – REFERENCE PLANT DATA

This appendix shows the most relevant variables of the reference plant through the year considered (2017). All the graphs are in hourly basis and the orange line represents the daily average trendline. In all the figures there is a drop to 0 in between august and September which shows the power plant temporary shutdown due to maintenance.

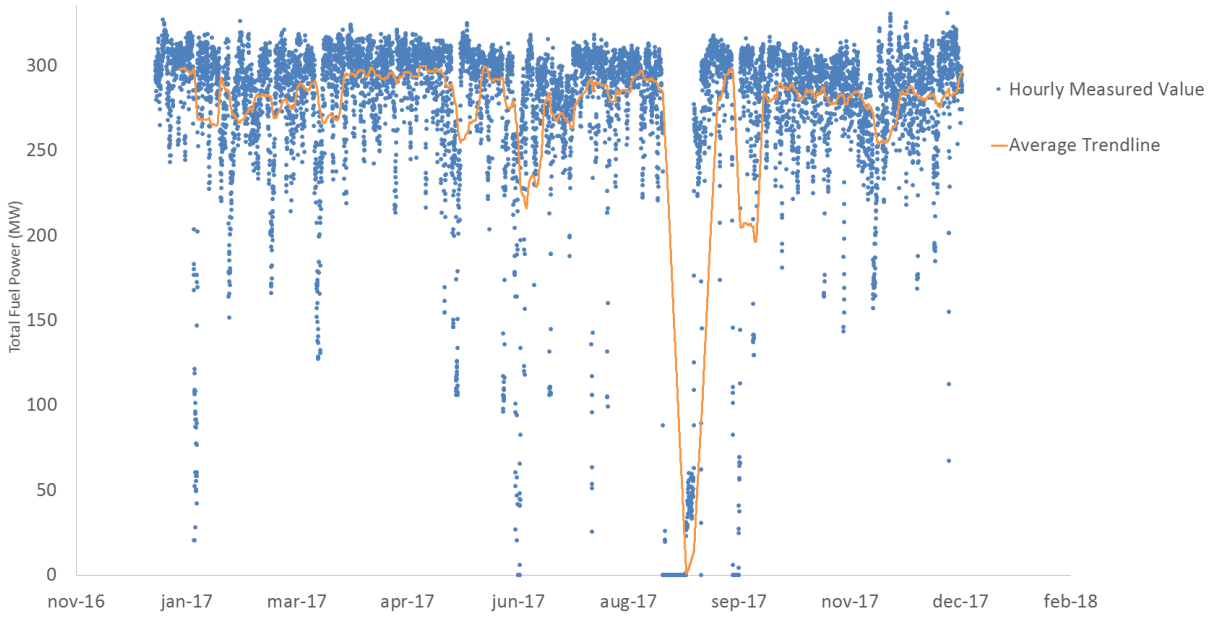

FIG A-a. Total fuel power hourly data over the year 2017. The orange line shows the average daily trendline. The drop between August and September is due to the maintenance shutdown of the power plant.

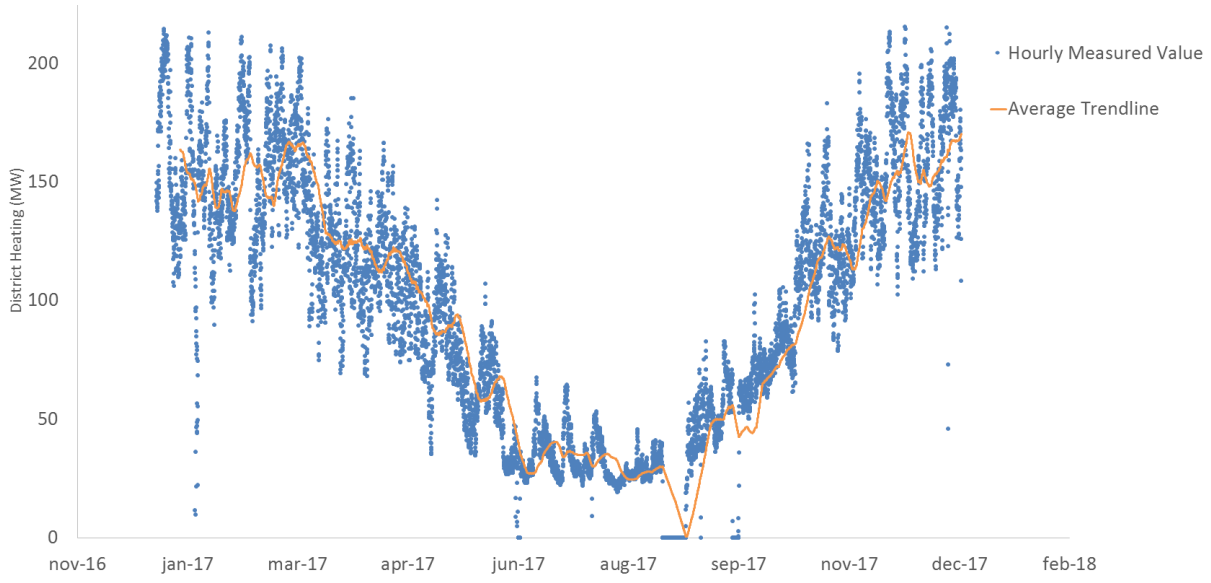

FIG A-b. District Heating hourly data over the year 2017. The orange line shows the average daily trendline. The drop between August and September is due to the maintenance shutdown of the power plant.

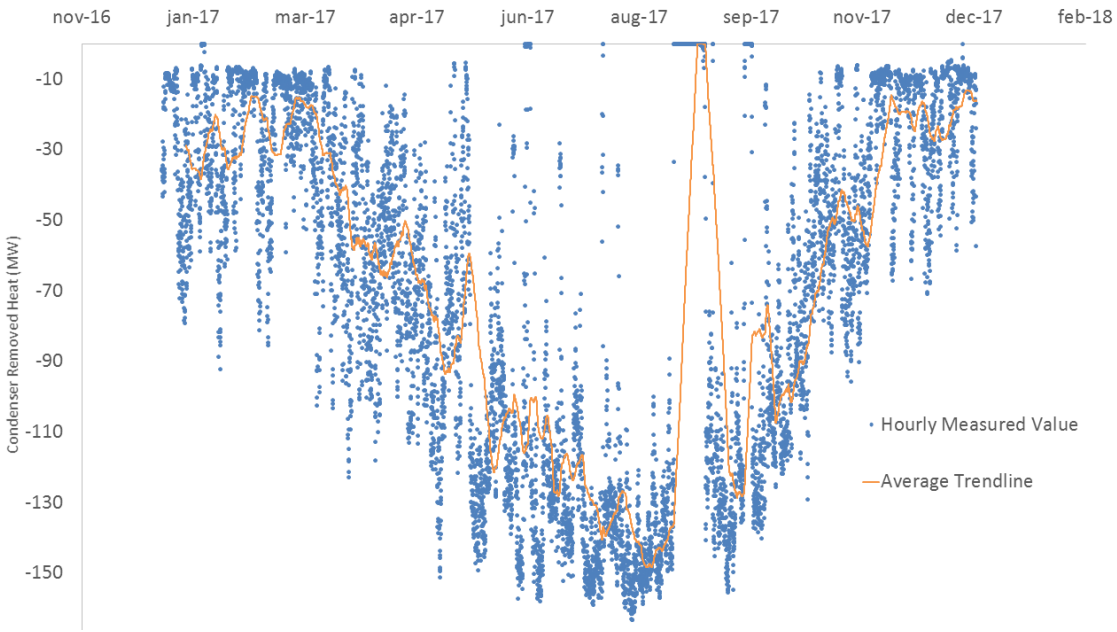

FIG A-c. Heat removed in the condenser hourly data over the year 2017. The orange line shows the average daily trendline. The drop between August and September is due to the maintenance shutdown of the power plant.

B. APPENDIX B – DATA ANALYSIS METHOD

This appendix focuses on the algorithm developed in Matlab used to identify and quantify the variations occurring in the steel mill reference plant. The code is shown below, followed by the explanation of how it works.

```
AvHeat

for n = 1:1000

 if AvHeat(n)<90
        AvHeat(n)=1;
    end
end;
B = AvHeat.';
x =3; %// number of consecutive matches
match = 1; %// match to be used
out = strfind(['1' num2str(B==match,'%1d')],['1' repmat('1',1,x)]);
```

In the attached code, AvHeat represents the variable with the data that wants to be analyzed, which in this particular case it would be Available Heat in the steam cycle, which is a vector with 1000 values for instance (that correspond to summer period, for example). The “if” statement sets the disturbance that wants to be analyzed. In this particular case, it would be that the amount of available heat drops below 90 MW. Whenever that happens, that position of the array will be marked with a 1. After converting the column array into a row, the value of x sets the duration of the disturbance. The function strfind will calculate how many times the available heat has a value of 1 for at least 3 straight hours. In other words, it will tell the user how many times (frequency) and when the available heat is lower than 90 MW. If the out variable is saved (which contains all the positions where a 3 hours or more disturbance occur), and the code is run for all the different durations (4h, 5h, 6h, 7h, etc.), the disturbances can easily be grouped and sorted depending on their durations.

C. Appendix C – Verification of the Model

The temperature inside the columns is also an important process variable to analyze since it defines the phase equilibrium at liquid and gas-liquid interface by affecting other thermophysical properties, i.e. most properties calculations are temperature dependent. Therefore, another step within the model validation is to compare both models in terms of temperature profiles of both absorber and stripper, for each of the operating points. In FIG C-a, FIG C-b, FIG C-c, FIG C-d, FIG C-e and FIG C-f the temperatures along the columns have been plotted. In the X-axis the different stages through the column (going from top to down), while in the Y-axis the temperatures can be found.

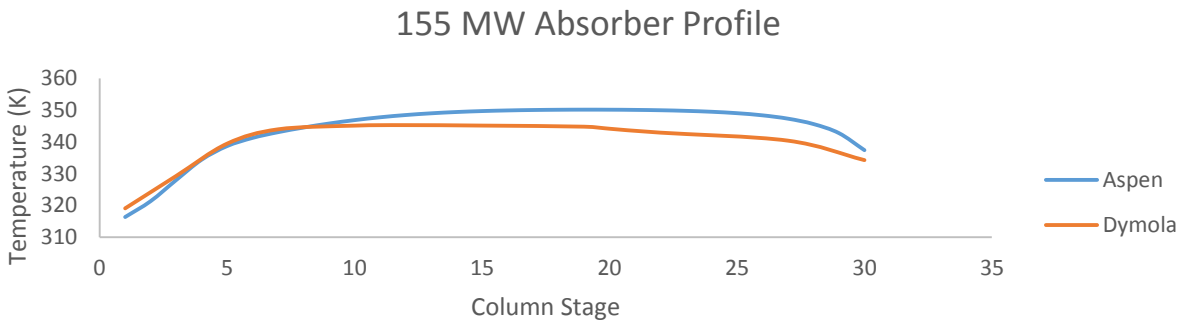

FIG C-a. Absorber Temperature Profile 155 MW Operating Point

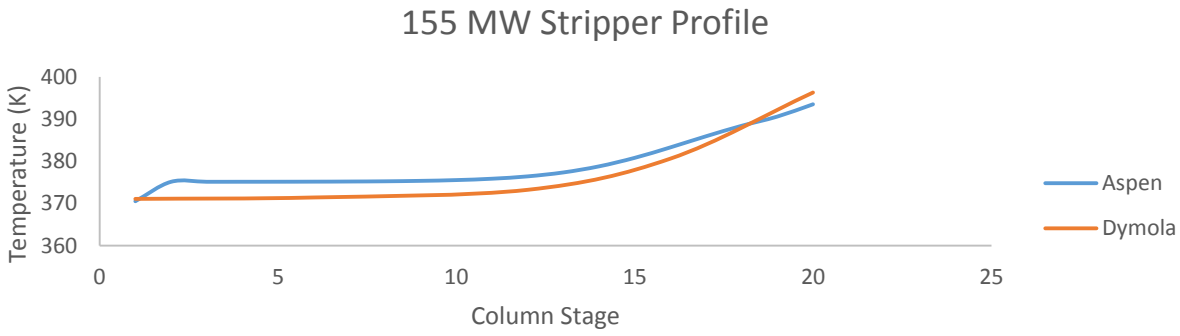

FIG C-b. Stripper Temperature Profile 155 MW Operating Point

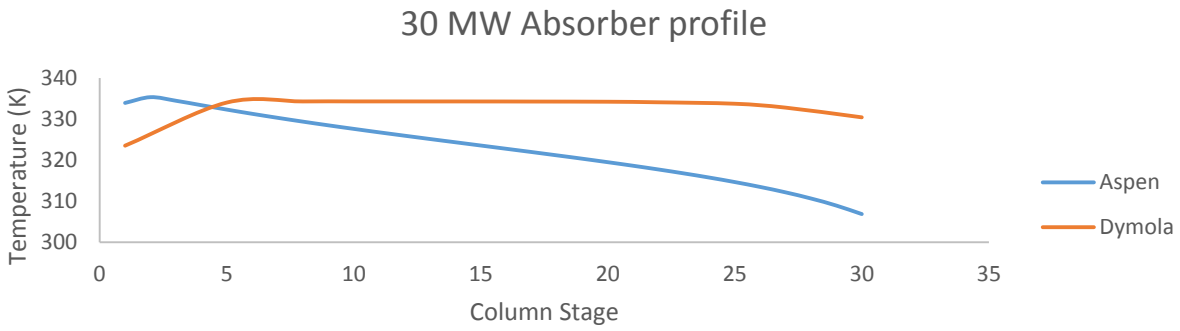

FIG C-c. Absorber Temperature Profile 30 MW Operating Point

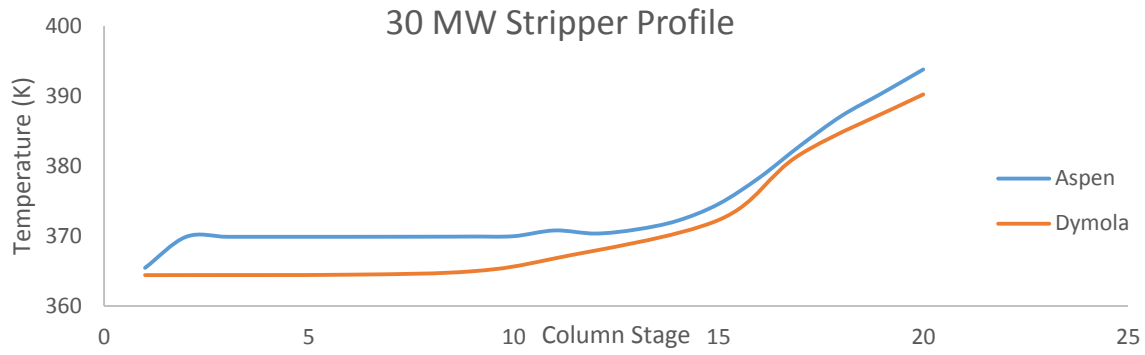

FIG C-d. . Stripper Temperature Profile 30 MW Operating Point

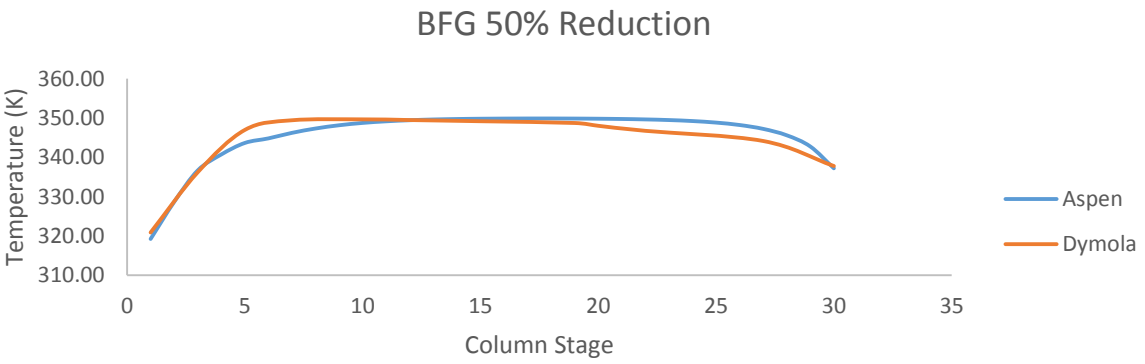

FIG C-e. Absorber Temperature Profile BFG Drop Operating Point

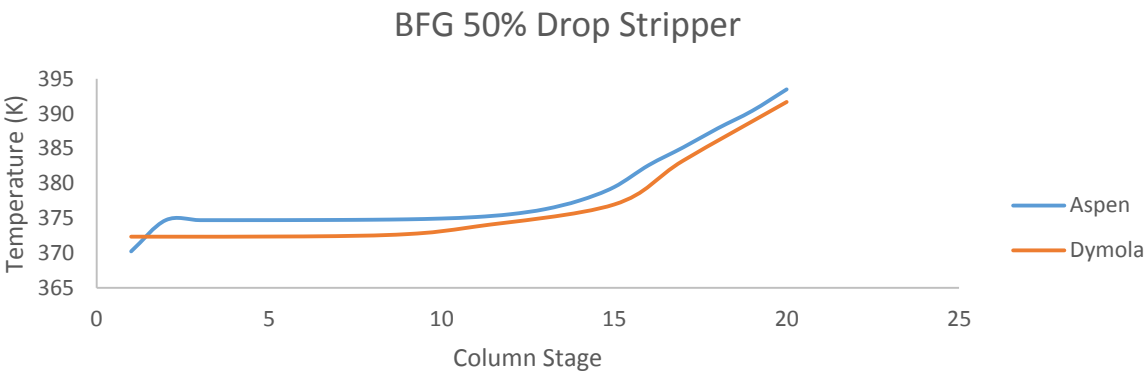

FIG C-f. Stripper Temperature Profile BFG Drop Operating Point

In FIG C-a and FIG C-b it can be seen that the dynamic process provides very similar temperature profiles in both absorber and stripper for the two models compared. The main difference in performance is found at the top of the stripper, where the Aspen model presents a drop in temperature while the dynamic model remains constant. The reason is that in the steady state model

the feed of liquid in the stripper is placed in the second stage, while in the Dymola model is located on the very top of the column. This deviation can be seen in the stripper profiles of all three points analyzed.

FIG C-c and FIG C-d show that the point with 30 MW available at the reboiler have a large deviation in the absorber temperature profile, while the stripper presents a better correlation between the two models. The reason behind it is again the same deviation observed in literature [52], where the Aspen model accuracy drastically drops at such low heat available.

Finally, regarding the blast furnace gas drop in flow, FIG C-e and FIG C-f show that the dynamic model columns match the Aspen model, with a really well correlated temperature profile for both absorber and stripper.

To conclude, it is stated that the dynamic model developed in this work can sufficiently predict the performance of the steady state model developed in Aspen, presenting higher discrepancies in off-design cases with low heat in the reboiler.

D. APPENDIX D – OPEN LOOP RESPONSE

This appendix comprises all the results of the open loop simulations that were not shown in the main sections of the report. The results have been grouped in Scenario 1 and Scenario 2, while each of them contains results from cases A, B and C.

D.1. SCENARIO 1

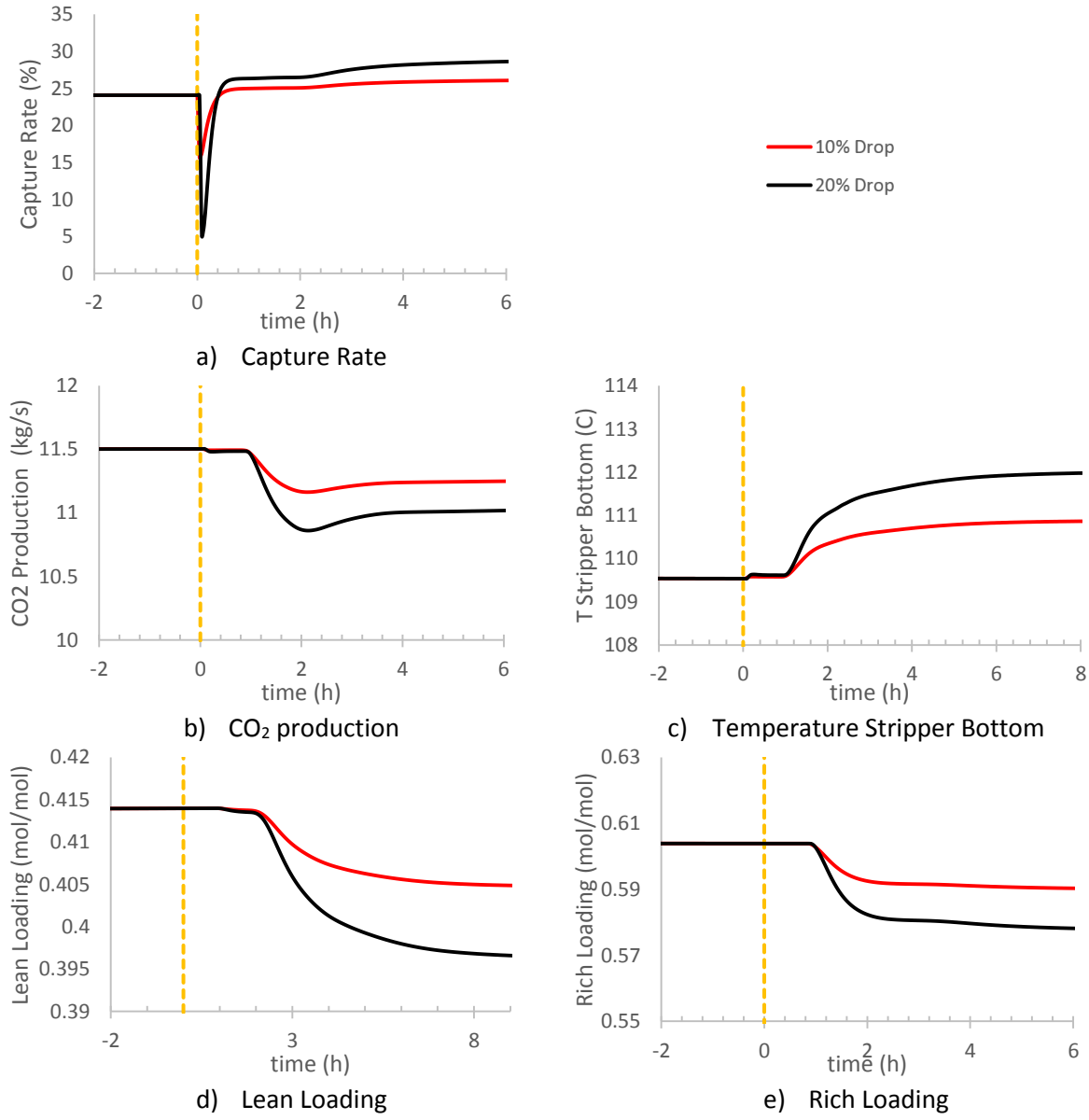

FIG -D-a. Case B Open Loop responses of the main process variables for 10% and 20% drop in BFG flow

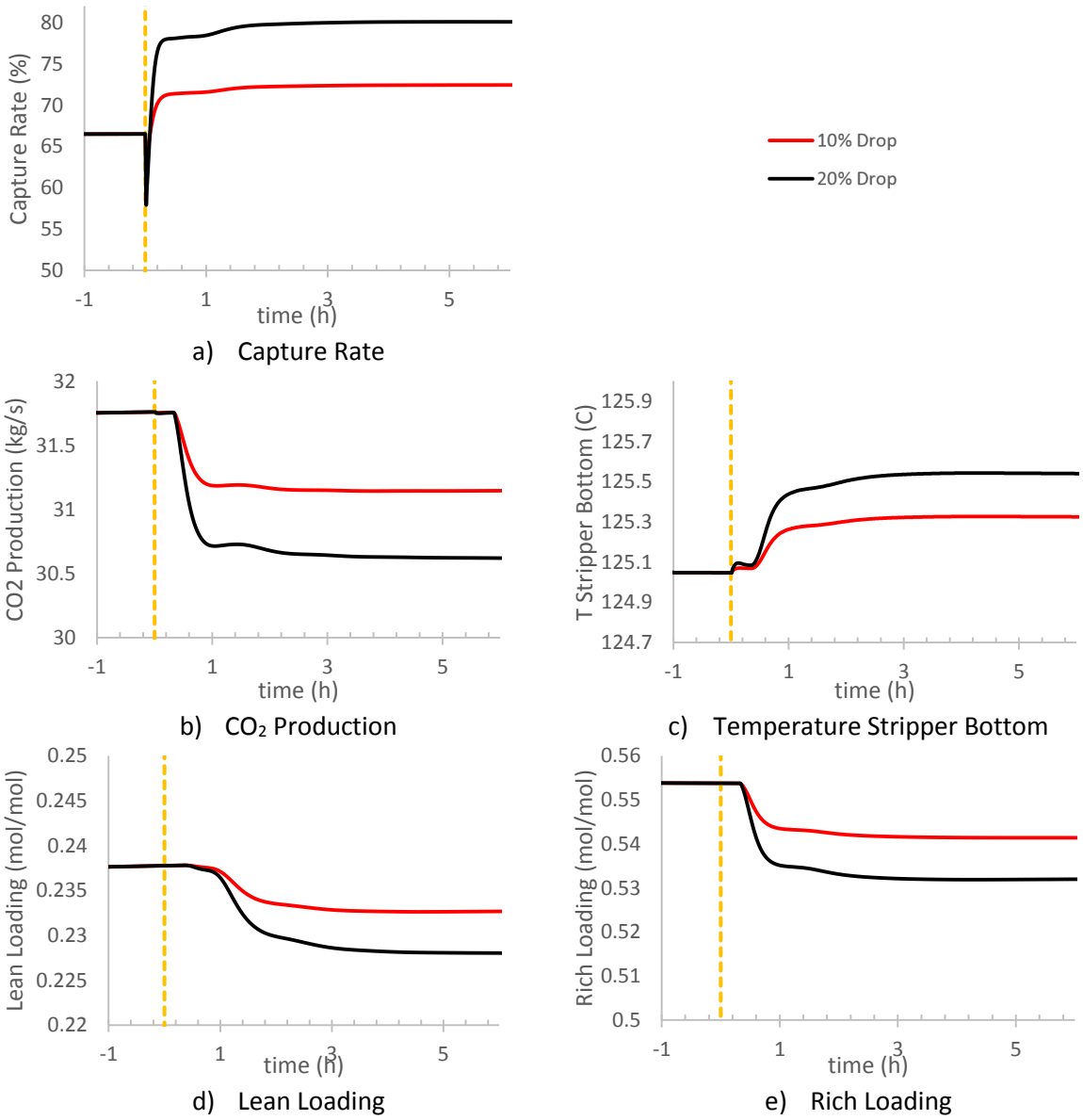

FIG D-b. Case C Open Loop responses of the main process variables for 10% and 20% drop in BFG flow

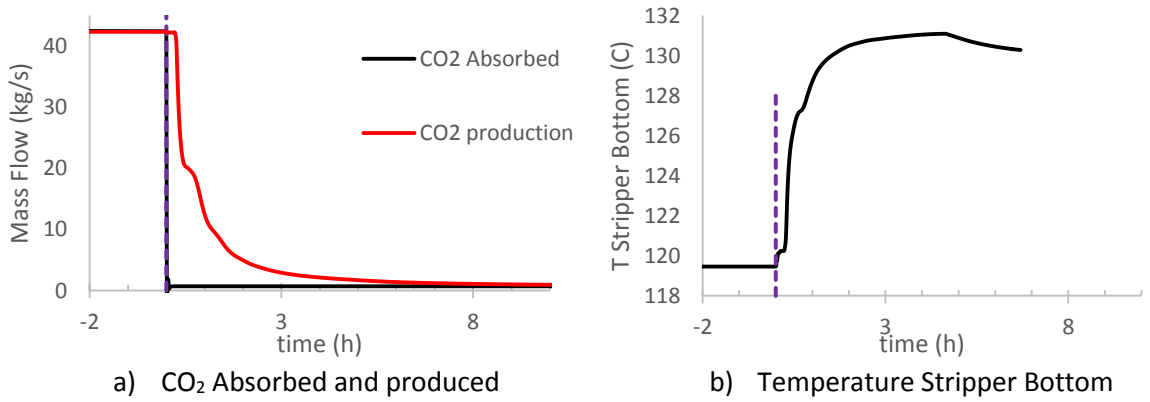

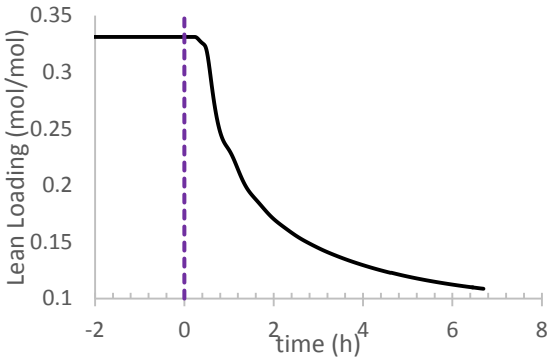

c) Lean Loading

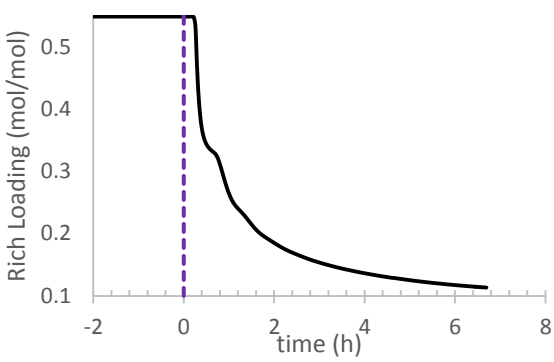

d) Rich Loading

FIG D-c. Case A Open Loop responses of the main process variables for drop to 0 in BFG

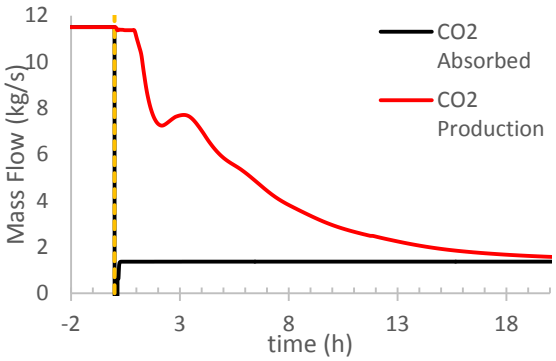

a) CO_2 Absorbed and Produced

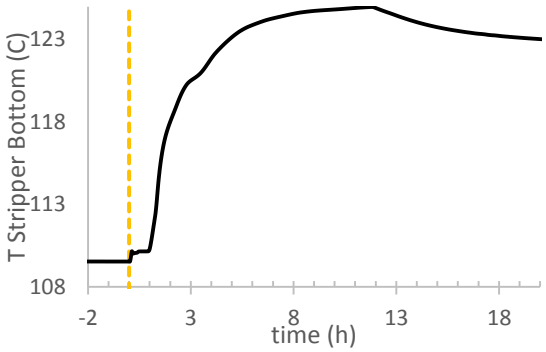

b) Temperature Stripper Bottom

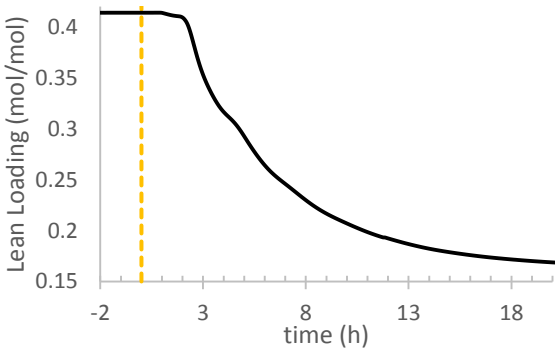

c) Lean Loading

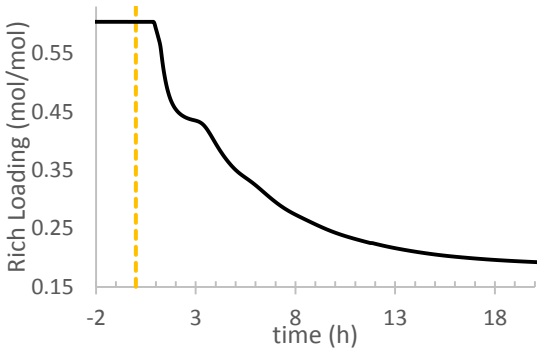

d) Rich Loading

FIG D-d. Case B Open Loop responses of the main process variables for drop to 0 in BFG

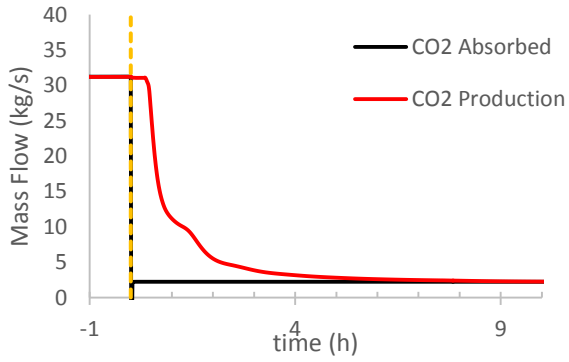

a) CO_2 Absorbed and Produced

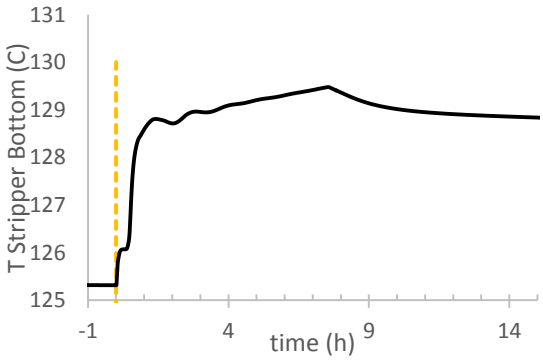

b) Temperature Stripper Bottom

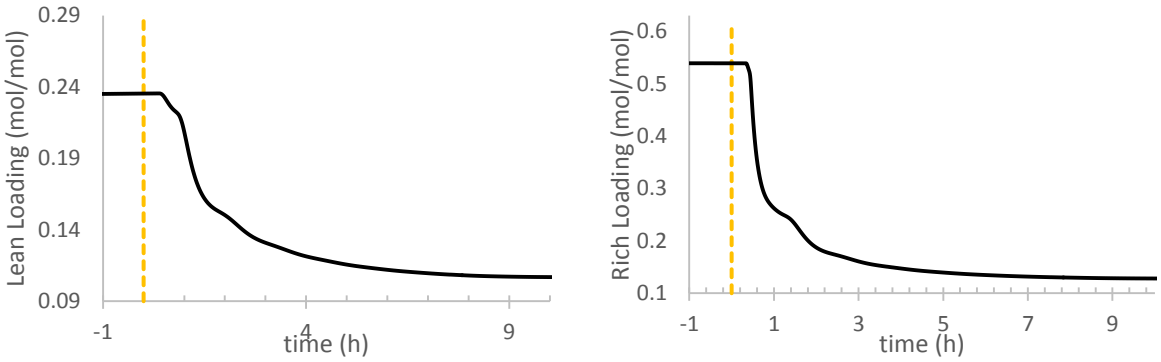

c) Lean Loading d) Rich Loading

FIG D-e. Case C Open Loop responses of the main process variables for drop to 0 in BFG

D.2. SCENARIO 2

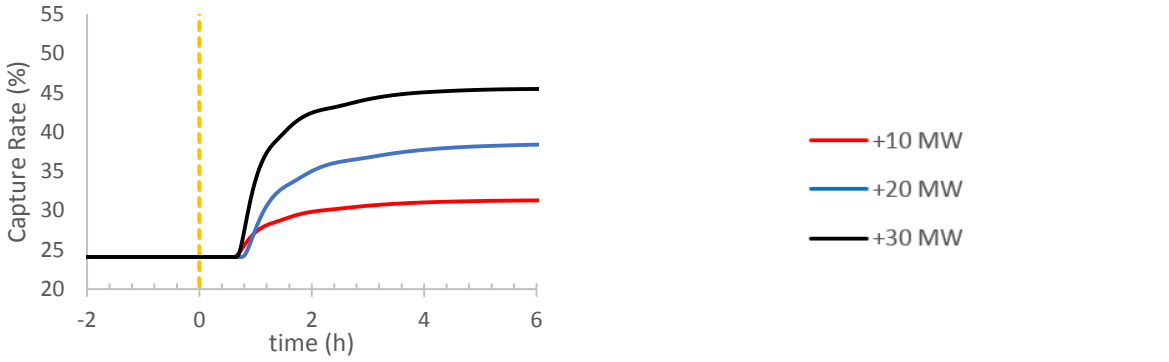

a) Capture Rate

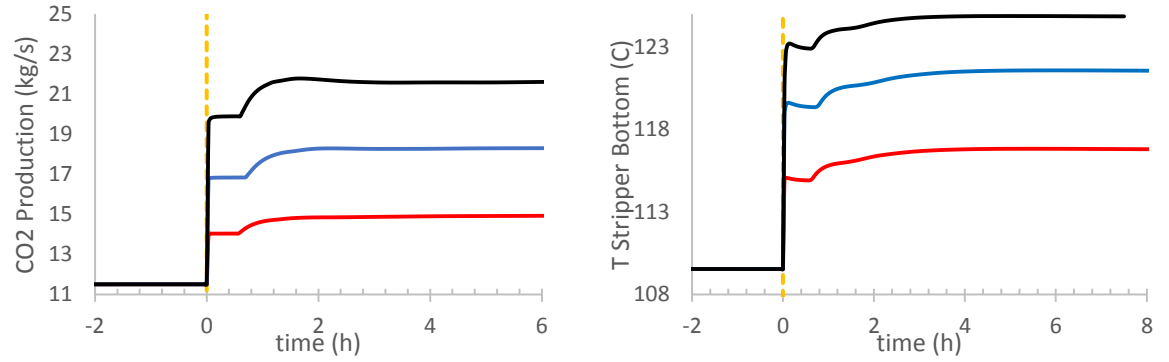

b) CO_2 production c) Temperature Stripper Bottom

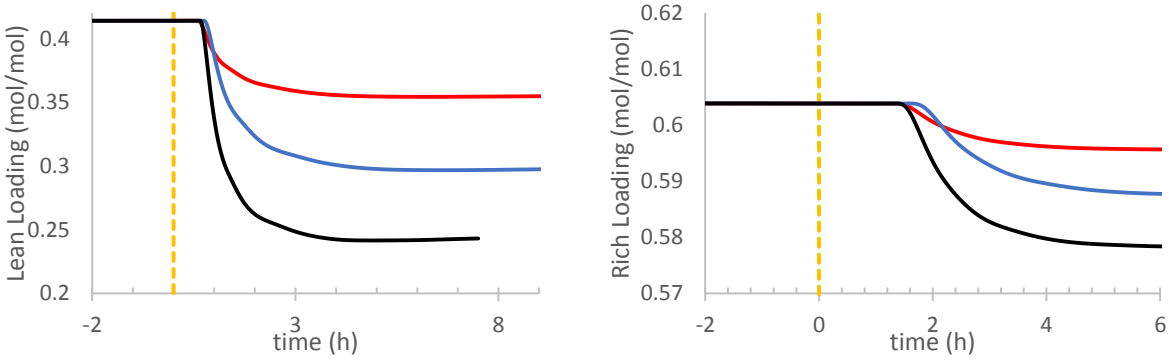

d) Lean Loading e) Rich Loading

FIG D-f. Case B Open Loop responses of the main process variables for +10, +20 and +30MW increase of reboiler duty

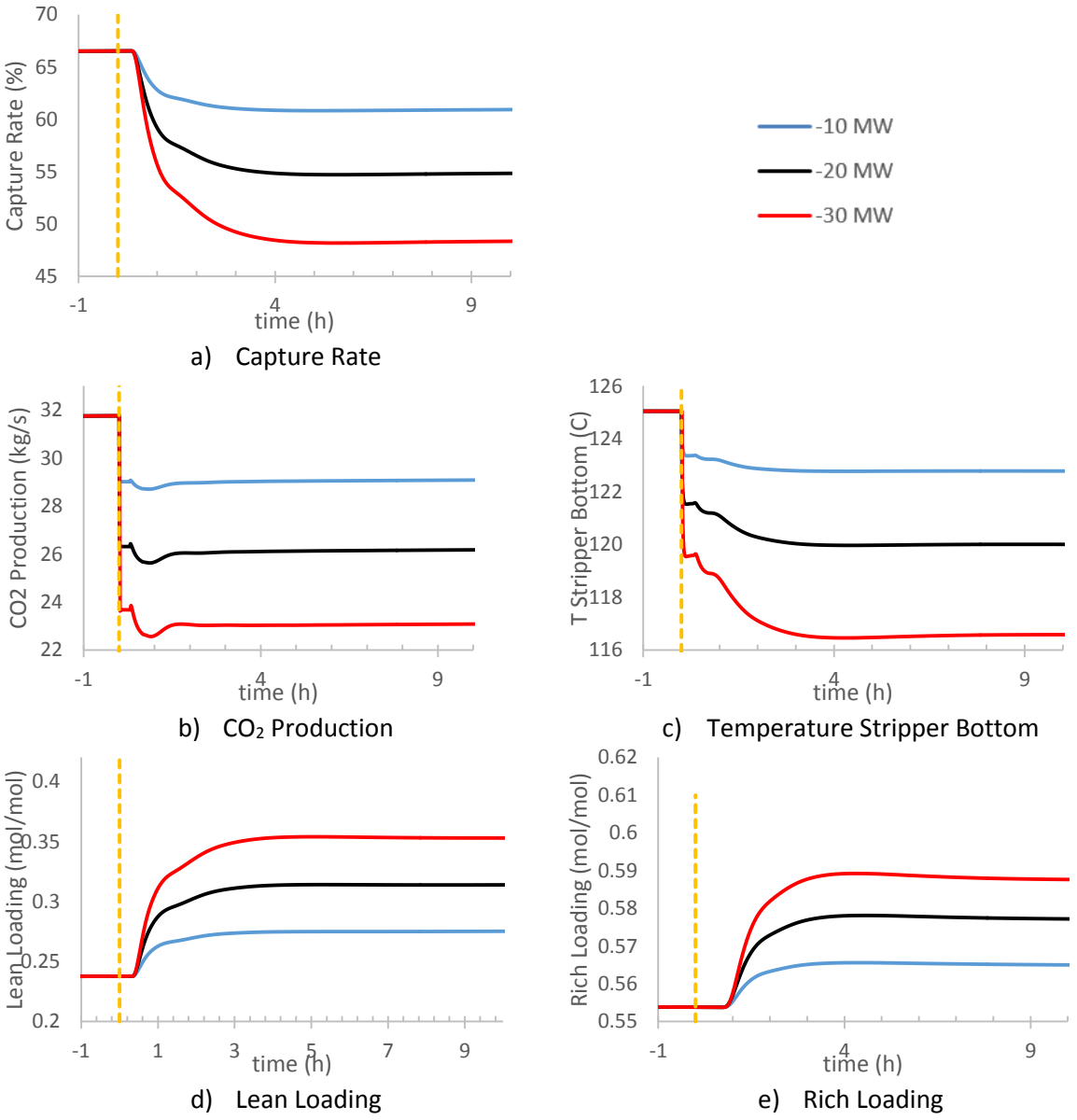

a) Capture Rate

b) CO_2 Production

c) Temperature Stripper Bottom

d) Lean Loading

e) Rich Loading

FIG D-g. Case C Open Loop responses of the main process variables for -10, -20 and -30MW decrease of reboiler duty

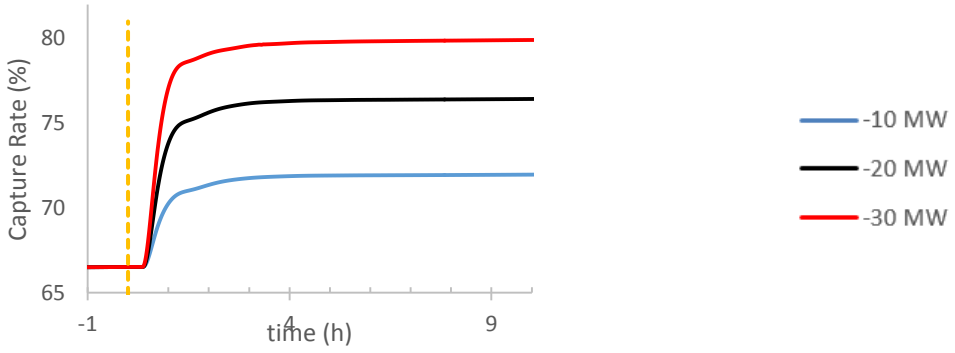

a) Capture Rate

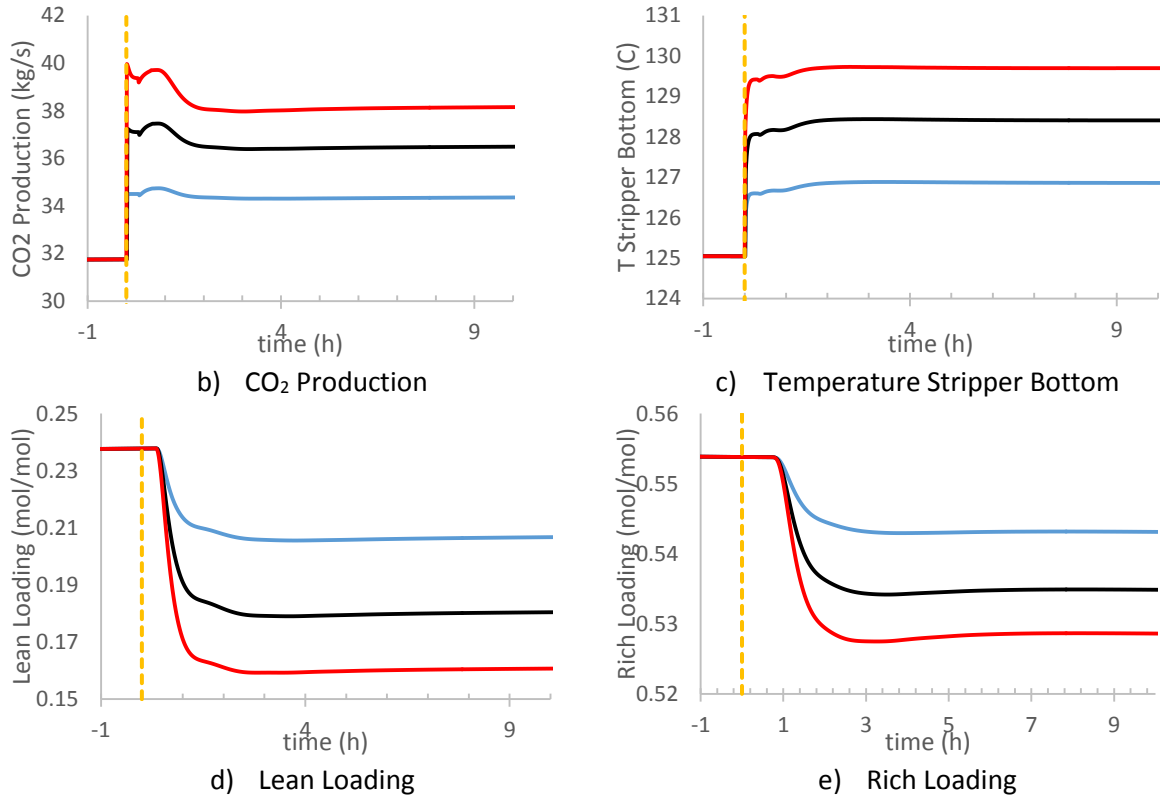

b) CO_2 Production

c) Temperature Stripper Bottom

d) Lean Loading

e) Rich Loading

FIG D-h. Case C Open Loop responses of the main process variables for +10, +20 and +30MW increase of reboiler duty